MAX-PLANCK-INSTITUT
FÜR METEOROLOGIE

Snowball Earth aftermath: Ocean dynamics and carbon cycling under extreme greenhouse conditions

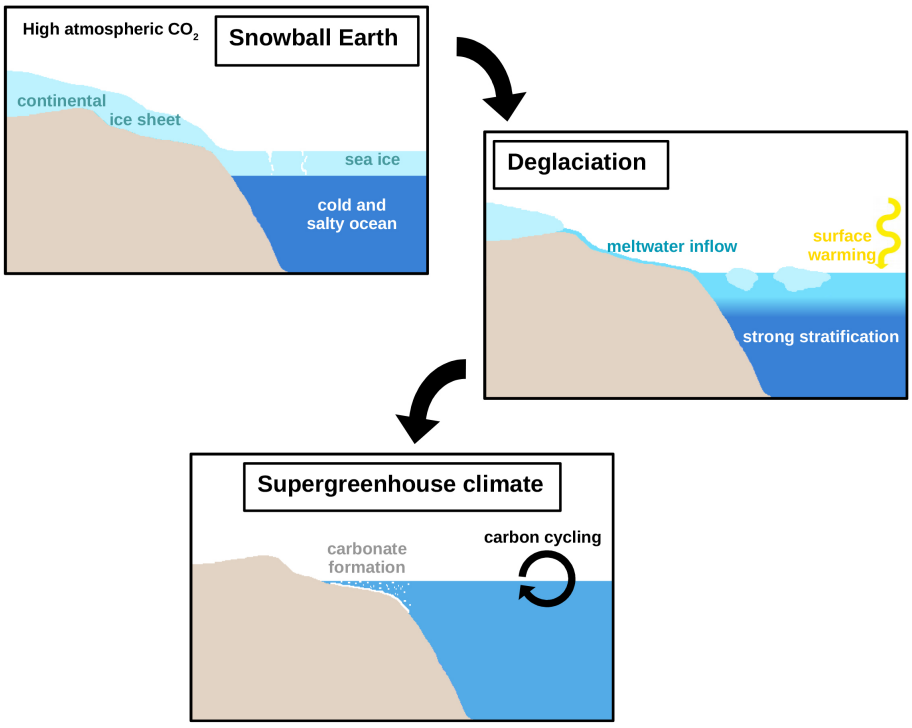

Lennart Ramme

Hamburg 2023

Berichte zur Erdsystemforschung 265
Reports on Earth System Science 2023

Hinweis

Die Berichte zur Erdsystemforschung werden vom Max-Planck-Institut für Meteorologie in Hamburg in unregelmäßiger Abfolge herausgegeben.

Sie enthalten wissenschaftliche und technische Beiträge, inklusive Dissertationen.

Die Beiträge geben nicht notwendigerweise die Auffassung des Instituts wieder.

Die "Berichte zur Erdsystemforschung" führen die vorherigen Reihen "Reports" und "Examensarbeiten" weiter.

Anschrift / Address

Max-Planck-Institut für Meteorologie
Bundesstrasse 53
20146 Hamburg
Deutschland

Tel./Phone: +49 (0)40 4 11 73 - 0
Fax: +49 (0)40 4 11 73 - 298

name.surname@mpimet.mpg.de
www.mpimet.mpg.de

Notice

The Reports on Earth System Science are published by the Max Planck Institute for Meteorology in Hamburg. They appear in irregular intervals.

They contain scientific and technical contributions, including PhD theses.

The Reports do not necessarily reflect the opinion of the Institute.

The "Reports on Earth System Science" continue the former "Reports" and "Examensarbeiten" of the Max Planck Institute.

Layout

Bettina Diallo and Norbert P. Noreiks
Communication

Copyright

Snowball Earth aftermath: Ocean dynamics and carbon cycling under extreme greenhouse conditions

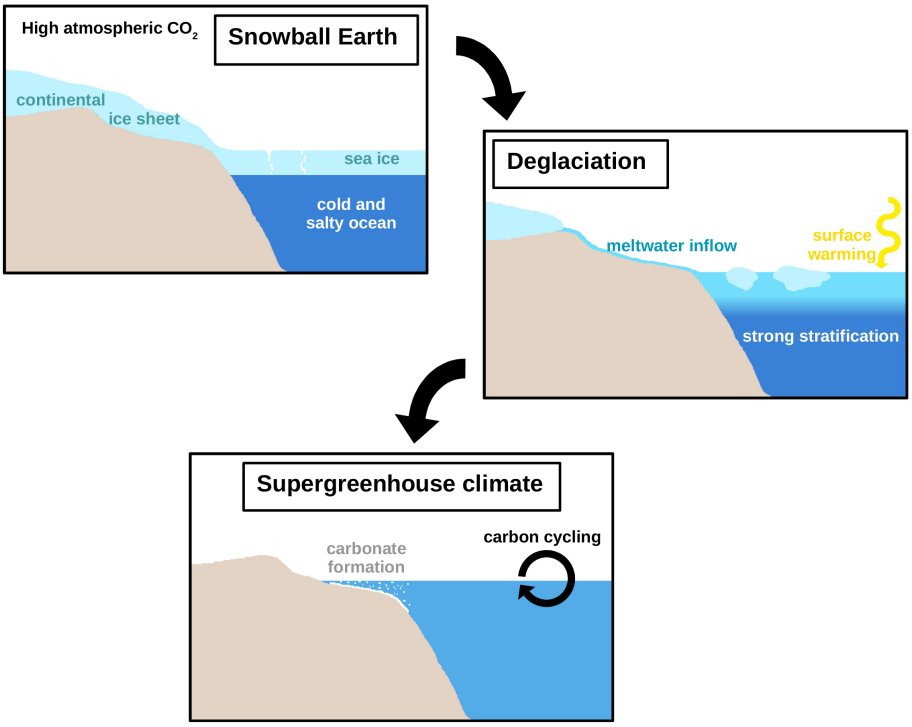

Lennart Ramme

Hamburg 2023

Lennart Ramme
aus Gifhorn, Deutschland

Max-Planck-Institut für Meteorologie
The International Max Planck Research School on Earth System Modelling
(IMPRS-ESM)
Bundesstrasse 53
20146 Hamburg

Tag der Disputation: 27. Februar 2023

Folgende Gutachter empfehlen die Annahme der Dissertation:
Prof. Dr. Jochem Marotzke
Dr. Tatiana Ilyina

Vorsitzender des Promotionsausschusses:
Prof. Dr. Hermann Held

Dekan der MIN-Fakultät:
Prof. Dr.-Ing. Norbert Ritter

Titelgrafik von Lennart Ramme: *The snowball Earth aftermath*

Berichte zur Erdsystemforschung / Max-Planck-Institut für Meteorologie 265
Reports on Earth System Science / Max Planck Institute for Meteorology 2023

ISSN 1614-1199 - doi: 10.17617/2.3505247

I dedicate this thesis to my family
for their continuous support.

This document was typeset using the typographical look-and-feel `classicthesis`
developed by André Miede and Ivo Pletikosić.

ABSTRACT

In this thesis, I study the dynamics of the ocean and the carbon cycle in the aftermath of the Marinoan snowball Earth (635 million years ago). The snowball Earth describes a state of the Earth's climate with global or near-global ice cover. When it deglaciates under elevated atmospheric CO_2 concentrations, the surface temperatures increase with a rapidity unrivaled in Earth's past and a very warm supergreenhouse climate develops. These extreme conditions have influenced the major transformations of the late Neoproterozoic Era, such as the oxygenation of the atmosphere to modern-like levels and the first widespread appearance of complex multicellular life. But in order to understand how these transformations are linked with the evolution of the Earth system, first the climatic boundary conditions need to be better constrained. I study the climate after the Marinoan snowball Earth using a comprehensive Earth system model, whereby I focus on the ocean's influence on the carbon cycle and the evolution of the supergreenhouse climate.

One of the main features of the ocean circulation in the snowball Earth aftermath is the stratification that develops as a consequence of the freshwater inflow during the deglaciation. I show that this stratification breaks up within just a few thousand years, which is substantially shorter than the previous best estimate of fifty thousand years. The break-up is largely driven by a strong circumpolar current, which develops in the northern hemisphere in the absence of continents that could block the flow. The fast destratification highlights that the deep ocean heat and carbon reservoirs have become well connected to the surface carbon cycle and the climate system on a time scale of less than ten thousand years after the Marinoan snowball Earth.

I demonstrate that three different processes can lead to an oceanic uptake of CO_2 in the first few thousand years of the snowball Earth aftermath: 1. the diluting effect of the meltwater inflow, 2. the biological carbon pump and 3. the carbon uptake of a depleted sub-snowball ocean. Conversely, the warming of the ocean leads to outgassing of CO_2 in various ways. However, the individual importance of these processes is highly dependent on the uncertain ocean chemistry at the start of the deglaciation. Both a rapid decline of the supergreenhouse climate and its long-term intensification are possible scenarios. Nevertheless, my results indicate that the supergreenhouse climate could have been moderate, exhibiting global mean surface temperatures of just around 30°C and large temperate regions. In conclusion, my findings provide an improved description of the climate and the ocean state in the aftermath of the Marinoan snowball Earth. Thereby, they provide helpful boundary conditions for future studies on the enigmatic biological and geological evolution during that time.

ZUSAMMENFASSUNG

In dieser Arbeit untersuche ich die Dynamik des Ozeans und des Kohlenstoffkreislaufs nach der Marinoischen Schneeball Erde (vor 635 Millionen Jahren). Die Schneeball Erde beschreibt einen Zustand des Erdklimas mit globaler oder nahezu globaler Eisbedeckung. Wenn eine Schneeball Erde aufgrund einer sehr hohen atmosphärischen CO_2 Konzentration abschmilzt, erwärmt sich die Erdoberfläche mit einer in der Erdgeschichte sonst unerreichten Geschwindigkeit und es entwickelt sich ein sehr warmes Supertreibhausklima. Diese extremen Bedingungen beeinflussten die großen Transformationen des späten Neoproterozoikums, wie den Anstieg der atmosphärischen Sauerstoffkonzentration auf ein Niveau ähnlich wie das heutige, oder die erste weite Verbreitung von komplexen, mehrzelligen Lebensformen. Aber um zu verstehen wie diese Transformationen mit der Entwicklung des Erdsystems verbunden sind, müssen zunächst die klimatischen Randbedingungen genauer beschrieben werden. Ich untersuche das damalige Klima mit einem umfassenden Erdsystemmodell, wobei ich mich auf den Einfluss des Ozeans auf den Kohlenstoffkreislauf und die Entwicklung des Supertreibhausklimas fokussiere.

Eine der Haupteigenschaften der Ozeanzirkulation nach einer Schneeball Erde ist die starke Schichtung, die sich infolge eines Eintrages von Frischwasser während des Abschmelzens entwickelt. Ich zeige, dass diese Schichtung innerhalb weniger tausend Jahre aufgebrochen wird, was deutlich kürzer ist als die bisherige Schätzung von fünfzigtausend Jahren. Der Hauptfaktor für das schnelle Aufbrechen der Schichtung ist ein starker Zirkumpolarstrom, der sich in der nördlichen Hemisphäre entwickelt, wo keine Kontinente die Strömung blockieren. Das schnelle Aufbrechen der Schichtung hebt hervor, dass die Wärme- und Kohlenstoffreservoire des tiefen Ozeans innerhalb von weniger als zehntausend Jahren gut mit dem oberflächennahen Ozean verbunden waren.

In meiner Arbeit demonstriere ich, dass innerhalb weniger tausend Jahre nach einer Schneeball Erde drei verschiedene Prozesse zu einer Aufnahme von CO_2 durch den Ozean führen können: 1. der verdünnende Effekt des Eintrages von Schmelzwasser in den Ozean, 2. die biologische Kohlenstoffpumpe und 3. die Aufnahme von Kohlenstoff durch einen Ozean, der mit niedrigem Kohlenstoffgehalt aus der Schneeball Erde kommt. Umgekehrt führt die Erwärmung des Ozeans über verschiedene Wege zu einem Ausgasen von CO_2 in die Atmosphäre. Allerdings ist die individuelle Bedeutung der einzelnen Prozesse stark abhängig von der unbestimmten chemischen Zusammensetzung des Ozeans beim Start des Abschmelzvorganges. Tatsächlich sind sowohl eine schnelle Abschwächung als auch eine langfristige Verstärkung des Supertreibhausklimas möglich. Nichtsdestotrotz weisen meine Ergebnisse darauf hin, dass das Supertreibhausklima moderat gewesen sein könnte, mit einer globalen Mitteltemperatur von 30°C und großen gemäßigten Regionen. Zusammenfassend stellen meine Ergebnisse eine verbesserte Beschreibung des Klimas und des Ozeanzustandes nach der Marinoischen Schneeball Erde dar. Dadurch bieten sie hilfreiche Rahmenbedingungen für zukünftige Studien über die noch unentschlüsselten biologischen und geologischen Entwicklungen der damaligen Zeit.

PUBLICATIONS RELATED TO THIS DISSERTATION

Ramme, L. and Marotzke, J.: Climate and ocean circulation in the aftermath of a Marinoan snowball Earth, *Clim. Past*, 18, 759–774, https://doi.org/10.5194/cp-18-759-2022, 2022.

Ramme, L., Ilyina, T. and Marotzke, J.: Assessment of the carbon cycle evolution after a snowball Earth, *in preparation*

ICON: the final frontier. These are the voyages of my PhD.
Its 4-year mission: to explore strange old climates.
To seek out new bugs and new model crashes.
To boldly go where no one has gone before!

Slightly modified quote from Patrick Steward a.k.a. Jean-Luc Picard

ACKNOWLEDGMENTS

After about 4000 manually submitted simulations on two supercomputers, approximately 250,000-300,000 simulated years with ICON and numerous models crashes (I am not going to count those), I can say that the four non-simulated years of my PhD were quite a journey and that I have learned a lot. I would not have gotten to this point without the help of many people.

Special thanks go to Jochem for providing guidance and advice where I needed it, but also for giving me the opportunity and freedom to pursue my own ideas. In the same way, I want to express my gratitude to Tatiana for making the HAMOCC group a second home for me in the institute and for seeding the idea of the (rather pathetic) quote above. I would also like to thank Matthias for his availability as panel chair and for making the panel meetings something to look forward to. All in all, I could not have asked for a better supervision throughout my PhD.

Learning to work with an Earth system model is not possible without the help of others, and I would have done much worse without the consultation of Stephan Lorenz, Helmuth Haak and Rene Redler, who always had at least some idea about which screw I could turn or button I should press. I want to further thank the IMPRS Office for dealing so efficiently with all administrative questions. I am very happy to have been able to conduct my research in such a supportive and inspiring atmosphere that is created by the people of the ocean department and the MPI for Meteorology in general.

I am grateful for my fellow PhD students and good friends that accompanied me over the last four years, and without whom this time would have been much harder. I especially thank Arjun and David for the great times we shared in Hamburg and for providing helpful feedback for the unifying essay. I thank Arjun also for being a good flatmate with a sense of humour that is actually not that questionable. I want to further thank Dan for being a great office-mate and partner for discussions about alkalinity and biogeochemistry throughout my entire PhD. And lastly, thank you Karina for being on my side and giving me something to look forward to during the last months of writing this thesis.

Where would I have been without the support of my family? I thank my parents for their encouragement and trust that have motivated me to always do my best. I thank my grandmother and my sisters for always being there. My visits home have been a continuous source of energy and have carried me to the finish line.

CONTENTS

I Unifying Essay

1 Introduction 3
1.1 Two global glaciations in the Neoproterozoic . . . 3
1.2 Why do we study past climates like the snowball Earth aftermath? . . 5
1.3 The snowball Earth theory . . . 6
1.3.1 Snowball Earth initiation . . . 7
1.3.2 Snowball Earth deglaciation . . . 7
1.3.3 Supergreenhouse climate . . . 8
1.3.4 The cap dolostone problem . . . 9
1.4 Modeling the snowball Earth aftermath . . . 10
1.4.1 Remaining uncertainties . . . 10
1.4.2 Transient dynamics in the snowball Earth aftermath . . . 11
1.5 Research questions . . . 12
2 Ocean dynamics and the climate after a snowball Earth 15
2.1 Rapid break-up of the stratification . . . 15
2.2 Consequences of the fast destratification . . . 17
2.3 Temperatures in the supergreenhouse climate . . . 18
3 Carbon cycle dynamics after a snowball Earth 21
3.1 Air-sea CO_2 exchange after a snowball Earth . . . 22
3.1.1 The potential effect of a non-permeable snowball sea-ice cover 22
3.1.2 Tracer dilution through meltwater inflow . . . 23
3.1.3 An efficient biological carbon pump? . . . 25
3.1.4 Ocean warming drives outgassing of CO_2 . . . 26
3.2 Duration of the supergreenhouse climate . . . 28
4 Conclusions and outlook 31
4.1 On the value of paleo studies for climate modeling . . . 31
4.2 Filling the gap - Answers to the research questions . . . 32
4.3 The snowball Earth context and outlook . . . 34

II Appendices

A Climate and ocean circulation in the aftermath of a Marinoan snowball Earth 39
A.1 Introduction . . . 42
A.2 Methods . . . 43
A.2.1 Model . . . 43
A.2.2 Marinoan setup . . . 44
A.3 Experimental design . . . 45
A.4 Control climate and snowball period . . . 47
A.5 Temporal evolution of climate and ocean circulation in the snowball Earth aftermath . . . 50
A.6 Supergreenhouse climate . . . 54
A.7 Discussion . . . 56
A.7.1 Impact of CO_2-scenarios . . . 56

A.7.2 Conditions after the Marinoan snowball Earth 57
A.7.3 Ocean destratification and vertical mixing 59
A.8 Conclusions 61
A.9 Appendix: Impact of model errors on the simulations 62
B Assessment of the carbon cycle evolution after a snowball Earth 63
B.1 Introduction 66
B.2 Simulating the carbon cycle dynamics after a snowball Earth 67
B.3 Ocean carbon uptake during deglaciation 69
B.4 Ocean warming, circulation changes and the biological carbon pump 72
B.5 Warming-induced inorganic precipitation of carbonates 74
B.6 A possible mechanism for the rapid formation of Marinoan cap dolostones 77
B.7 What is the fate of atmospheric CO_2 in the snowball Earth aftermath? 78
B.8 Methods 79
B.8.1 ICON-ESM model description 79
B.8.2 Simulation design 80
B.8.3 Carbonate chemistry model 81
B.9 Supporting information 82
B.9.1 List of experiments 82
B.9.2 Supplementary figures and tables 84

Bibliography 87

Part I

UNIFYING ESSAY

1 INTRODUCTION

The paleoclimate record is the basis for how we understand the potential range and rate of climate change. [...] The study of past climates continues to reveal key insights into Earth's response to increased concentrations of greenhouse gases.

Tierney et al. (2020)

The concentration of atmospheric greenhouse gases and the color of the Earth are the two major factors that control the climate of our planet. The color of the Earth, i.e. its albedo, determines how much of the solar radiation is transformed into heat (Stephens et al., 2015). A higher albedo means that more solar radiation is reflected back to space, hence the climate becomes cooler. Atmospheric greenhouse gases absorb the Earth's thermal radiation and send some of it back to the surface (Mitchell, 1989). A higher concentration of greenhouse gases therefore means that more energy is trapped in the lower atmosphere, which increases the surface temperature of the Earth. We experience the drastic impact of even small perturbations to this system in light of the current climate change. An increase in the concentration of the greenhouse gas carbon dioxide (CO_2) of roughly 50% compared to pre-industrial levels has already led to a global warming of more than one degree Celsius (Gulev et al., 2021), with severe consequences for ecosystems and humanity (IPCC, 2022).

The dynamical system that is controlled by these two factors can be well captured with relatively simple energy-balance models (Budyko, 1969; Sellers, 1969). These models not only predicted the warming effect of anthropogenic CO_2 emissions already in the 1960s, but they also indicated that the Earth could freeze over completely through a "self-developed feedback" (Budyko, 1969), once the sea ice reaches a critical latitude. This fully glaciated climate state was later termed "snowball Earth" (Kirschvink, 1992). In a snowball Earth, the bright surface of sea ice, glaciers and snow reflects most of the incoming solar radiation back into space. It can therefore only be ended when enormous amounts of greenhouse gases, primarily CO_2, accumulate in the atmosphere (Caldeira and Kasting, 1992; Hoffman et al., 1998). The dramatic change in climate, ocean circulation and the carbon cycle that follows the termination of the pan-glacial state, that is, the snowball Earth aftermath, is the overarching subject of this thesis.

1.1 TWO GLOBAL GLACIATIONS IN THE NEOPROTEROZOIC

Glacial deposits provide a reference to the climate at the time of their deposition, as they must have been formed by glaciers in cold environments (Stephenson et al., 1988). Similarly, carbonate sediments are indicative of a warm climate and commonly associated with tropical waters (Opdyke and Wilkinson, 1990; Ziegler et al., 1984). Over several decades, a growing bulk of evidence showed that glacial deposits

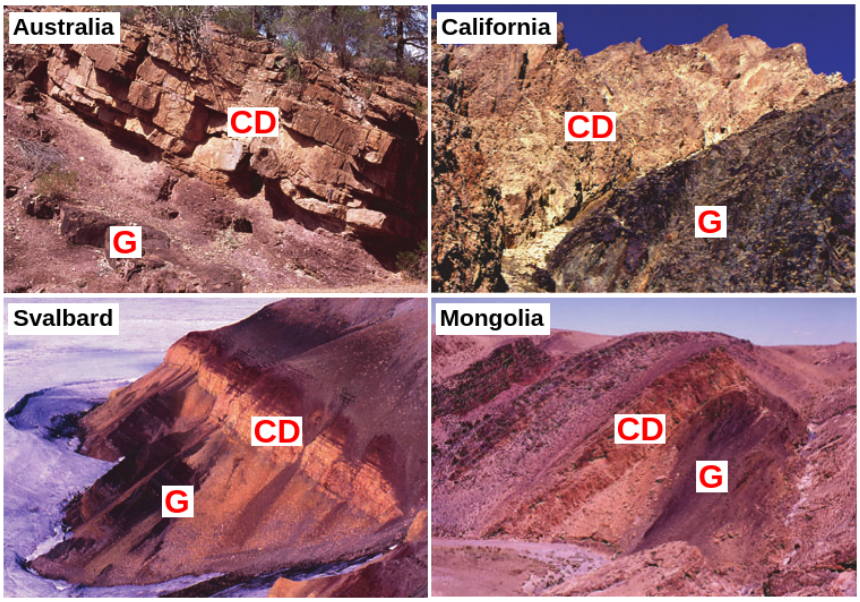

Figure 1.1: Photographs of glacial deposits from four different continents that are overlain by carbonate units and that date back to the same time period within the late Neoproterozoic. Pictures are from Hoffman (2011, adapted, with permission). The letter "G" in the pictures denotes the glacial deposits and "CD" stands for a specific form of rapidly accumulated carbonates that is typically found in geological sequences from the Marinoan snowball Earth (cap dolostones, see Section 1.3.4 and Hoffman, 2011).

were formed almost globally in the late Precambrian (Harland, 1964; Hambrey and Harland, 1981; Hoffman et al., 1998). However, these glacial deposits are often directly overlain by carbonates (Roberts, 1976; Kennedy, 1996; Hoffman et al., 1998; Hoffman, 2011, Fig. 1.1). This represents a paradox, as the widespread appearance of glacial deposits indicates a very cold climate, which is at odds with the deposition of carbonates in warm waters. In 1992, Kirschvink proposed the hypothesis of a Neoproterozoic ($1000 - 540$ million years ago, Ma) snowball Earth to solve this problem. A snowball Earth not only explains globally distributed glacial deposits, but it also provides a mechanism for the formation of carbonates directly on top of the glacial deposits. Once a snowball Earth deglaciates, the elevated greenhouse gas concentration rapidly drives the Earth into a hot supergreenhouse climate, where carbonate rocks are readily formed (Hoffman et al., 1998; Higgins and Schrag, 2003). The snowball Earth hypothesis was later refined and supported through numerous geological, biological and climate modelling studies (see Hoffman et al., 2017, for a recent overview and a detailed description of the snowball Earth state). By now, it is largely accepted that there were at least two periods of global or near-global glaciation during the Neoproterozoic, the "Sturtian" ($717 - 659$ Ma) and the "Marinoan" ($645 \pm 5 - 635$ Ma) snowball Earth (Hoffman et al., 2017).

The two snowball Earth periods of the Neoproterozoic fall into a time of major transformations within the Earth system (Fig. 1.2). The break-up of the supercontinent Rodinia started prior to the Sturtian snowball Earth (Li et al., 2013) and probably contributed to the occurrence of the snowball Earth periods, as I discuss later. The first forms of multicellular life developed at the latest during the non-glacial inter-

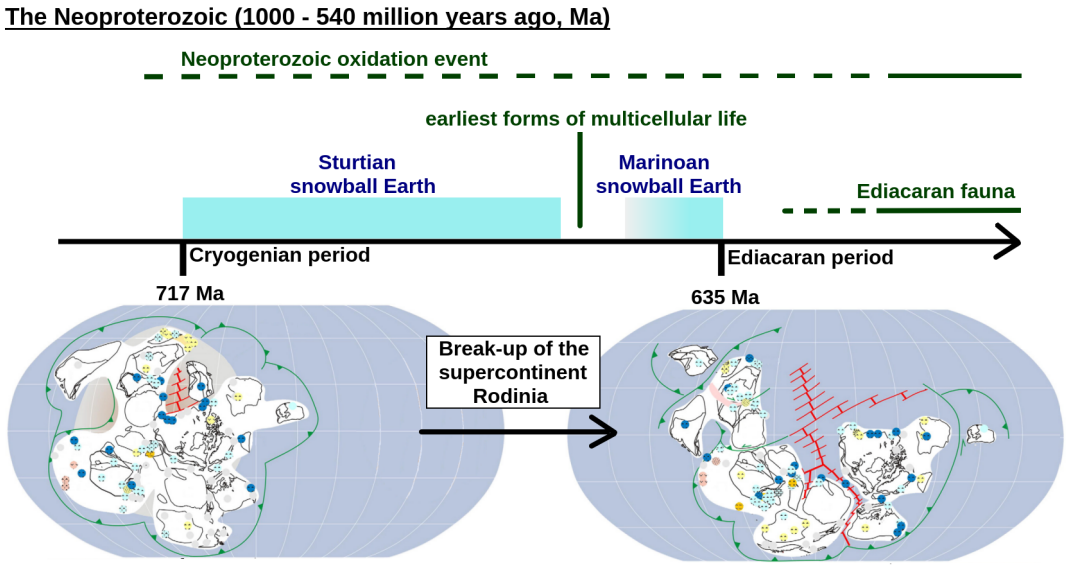

Figure 1.2: Overview of the major transformations during the Neoproterozoic and timeline of the two snowball Earth events. The dashed part of the lines indicates uncertainties in the timing of the Neoproterozoic oxidation event and the appearance of the Ediacaran fauna. The two maps are taken from Li et al. (2013, modified). The small colored dots in the maps refer to data points of various types of sediments, and the green and red lines indicate hypothetical subduction zones and mid ocean ridges, respectively (Li et al., 2013).

lude between the Sturtian and the Marinoan snowball Earth (Love et al., 2009; Brocks and Butterfield, 2009; Brocks et al., 2017; Dohrmann and Wörheide, 2017; Turner, 2021). Eukaryotic life in the ocean was shifting from red to green algae within the Cryogenian period (717 – 635 Ma Knoll et al., 2007; Hoffman et al., 2017), and algae replaced bacteria as the dominant primary producers in the late Cryogenian (Brocks et al., 2017). After the Marinoan snowball Earth, a surge in eukaryotic diversity led to the development of the Ediacaran fauna, the first widespread appearance of multicellular life on Earth (Erwin et al., 2011; Erwin, 2015; Droser and Gehling, 2015). Tightly connected to the evolution of life is the oxygenation of the atmosphere to modern-like levels, known as the Neoproterozoic oxygenation event (Och and Shields-Zhou, 2012; Lyons et al., 2014). All these biological and chemical transformations were influenced by the climatic excursions associated with the snowball Earth episodes. This brings us to the motivation of studies on the snowball Earth and its aftermath.

1.2 WHY DO WE STUDY PAST CLIMATES LIKE THE SNOWBALL EARTH AFTERMATH?

> *[Research on snowball Earth climate dynamics is conducted] not only to assist geology and geobiology but also to pursue potential applications for study of exoplanets, to gain insight from intermodel comparison, and to stimulate fresh perspectives on the Anthropocene.*
>
> Hoffman et al. (2017)

This quote from Hoffman et al. (2017) and the quote from Tierney et al. (2020) at the start of this chapter illustrate the broader value of paleo studies and research on the snowball Earth. Here, I elaborate on the specific insight that can be gained from studying the aftermath of a snowball Earth.

The dramatic excursions of the climate that are associated with a snowball Earth and its termination are potentially threatening for early forms of life (Hoffman et al., 1998; Moczydłowska, 2008; Griffiths et al., 2022). In particular, the rapid transition into a hot greenhouse climate after a snowball Earth is a major burden for biota that previously adapted to the freezing conditions of a snowball Earth lasting for millions of years (Brocks and Butterfield, 2009; Love et al., 2009; Erwin, 2015). Understanding how these climatic excursions are linked with the major transformations of life that occurred during that time, on the one hand, informs us about the response of simple forms of life to a rapidly changing climate in the future. On the other hand, we gain invaluable insight about how the evolution of life could perform under the extreme conditions that may be found on other planets inside or outside of our solar system (Rothschild and Mancinelli, 2001). In order to understand the linkage between climate, chemical conditions and life during the snowball Earth aftermath, it is imperative to first reconstruct what the climate and the biogeochemical conditions during that time were.

The snowball Earth aftermath also represents a period of intense global warming and enhanced atmospheric greenhouse conditions, which is, in principle, comparable to anthropogenic climate change. Of course, compared to other greenhouse periods in the Earth's past, like the Paleocene-Eocene thermal maximum (PETM, see e.g. McInerney and Wing, 2011), the parallels to modern global warming are small. For example, the continental configuration is radically different, the temperature increase in the snowball Earth aftermath is substantially larger, and the warming is not contemporaneous with the increase of atmospheric greenhouse gases. But modern climate change is extreme as well, and the warming after the termination of a snowball Earth may be one of a few - if not the only - case in Earth's geological past, where the temperature increase outpaces current global warming. Especially the question of whether and how the ocean takes up atmospheric CO_2 is eminent for the snowball Earth aftermath as well as for scenarios of future anthropogenic CO_2 emissions (Sabine and Tanhua, 2010). Studies of the snowball Earth aftermath, as an extreme case of rapid warming and high atmospheric CO_2 concentrations, can help to improve our understanding of the climate, as well as the dynamics of the ocean and the carbon cycle that also shape the response of the Earth system to anthropogenic climate change.

1.3 THE SNOWBALL EARTH THEORY

Now that we know why studies of the snowball Earth aftermath are useful, I describe in the following sections how the snowball Earth theory has developed. For the remainder of this thesis, I focus on the Marinoan snowball Earth, because the geological evidence for a rapid deglaciation and very high atmospheric CO_2 concentrations is strongest for this snowball Earth event (Hoffman et al., 2017). However, the mechanisms described here will inevitably also play a role for the Sturtian snowball Earth.

1.3.1 *Snowball Earth initiation*

The initiation of the snowball Earth episodes in the Neoproterozoic was closely related to the break-up of the supercontinent Rodinia in equatorial latitudes (Donnadieu et al., 2004; Hoffman et al., 2017). The break-up increased the length of coastlines and thereby also the area of humid regions on Earth. In warm and humid regions, continental weathering of silicate rocks is especially strong (Li et al., 2016). This weathering consumes CO_2 from the atmosphere, leading to a reduction of the atmospheric CO_2 concentration and a cooling of the climate (Dessert et al., 2001; Hartmann et al., 2014). Additionally, during the Cryogenian, the intensity of the sun was about 5-6% lower than today (Gough, 1981) and the albedo of the continents was higher, as a vegetational land cover had not yet developed (Puttick et al., 2018; Morris et al., 2018). Both factors support a cooler climate, making the planet more susceptible to snowball Earth inception. Many more processes are expected or at least hypothesized to have contributed to the initiation of a snowball Earth, and I refer the reader to the review papers of Pierrehumbert et al. (2011) and Hoffman et al. (2017) for a more detailed discussion of these processes.

Once the climate had cooled sufficiently, sea ice reached a critical latitude and the Earth froze over due to a runaway ice-albedo feedback (e.g. Voigt et al., 2011; Yang et al., 2012). The ice-albedo feedback describes the process by which a cooling of the planet increases the amount of sea ice, snow cover and continental glaciers, thereby increasing the albedo of the Earth's surface and cooling the climate even further (Budyko, 1969; Held and Suarez, 1974; Curry et al., 1995). It represents a positive feedback loop that acts also in the opposing scenario of a warming climate. The feedback becomes stronger the closer the sea-ice edge gets to the equator, because of the increasing importance of solar radiation in those latitudes. Beyond the critical latitude, counteracting processes cannot balance the further cooling induced by the ice-albedo feedback. The final transition into the snowball Earth is therefore extremely rapid (Marotzke and Botzet, 2007; Voigt and Marotzke, 2010; Voigt et al., 2011; Yang et al., 2012). Once a snowball Earth is established, the reduced efficiency of continental weathering in a cold climate and the continuous emission of CO_2 from volcanoes lead to an accumulation of CO_2 in the atmosphere (Hoffman et al., 1998; Le Hir et al., 2008c).

1.3.2 *Snowball Earth deglaciation*

Vast amounts of atmospheric CO_2 are required in order to overcome the strong reflection of sunlight by the glaciated surface and trigger snowball Earth deglaciation. Early modeling suggested that atmospheric CO_2 concentrations of substantially more than 10^5 parts per million (ppm) are required to melt a snowball Earth (Caldeira and Kasting, 1992; Pierrehumbert, 2005). However, these thresholds can be lowered significantly by the effects of clouds (Abbot et al., 2012), volcanic ash or dust (Le Hir et al., 2010; Abbot and Pierrehumbert, 2010; Vrese et al., 2021; Lan et al., 2022), and other processes impacting the radiative balance during a snowball Earth (Abbot et al., 2010; Wu et al., 2021; Edkins and Davies, 2021). The lower thresholds are more in line with geochemical proxy data, which indicate atmospheric CO_2 concentrations of $10^4 - 10^5$ ppm in the aftermath of the Marinoan snowball Earth (Kasemann et al.,

2005; Bao et al., 2008, 2009). Nevertheless, also the lower CO_2 concentrations cause a rapid deglaciation that is driven by the ice-albedo feedback (Caldeira and Kasting, 1992; Marotzke and Botzet, 2007; Myrow et al., 2018; Wu et al., 2021; Zhao et al., 2022). Even the continental ice sheets deglaciate within just 2 kiloyears (kyr, Hyde et al., 2000).

A stable oceanic stratification develops during the deglaciation in response to the inflow of meltwater to a snowball ocean of high salinity (Shields, 2005; Liu et al., 2014; Yang et al., 2017; Hoffman et al., 2017; Zhao et al., 2022). The stratification is enhanced through the warming of the surface layer under the strong greenhouse conditions (Yang et al., 2017). Yang et al. (2017) suggest that this stratification could have endured for around 50 kyr, but uncertainties about the time scale of destratification and the associated sea-level changes are large. However, these time scales are important for understanding the formation of a specific type of Marinoan carbonate rocks that is discussed later.

1.3.3 *Supergreenhouse climate*

The strong greenhouse conditions in the aftermath of a snowball Earth are often called the "supergreenhouse climate" (Higgins and Schrag, 2003; Le Hir et al., 2008b). The intensity of the supergreenhouse climate, i.e. the temperature at the Earth's surface, depends on the CO_2 concentration threshold at which the snowball Earth deglaciates. It is estimated that the global mean surface temperature was high at around 50°C (Le Hir et al., 2008b; Yang et al., 2017; Hoffman et al., 2017). The duration of these elevated greenhouse conditions is not constrained by geological data (Le Hir et al., 2008b), and mechanisms that affect the carbon cycle on a time scale of less than 10 kyr from the start of the deglaciation have so far not been discussed in the literature. However, the most common assumption is that the supergreenhouse climate weakened slowly as a consequence of intense continental weathering (Hoffman et al., 1998; Higgins and Schrag, 2003; Le Hir et al., 2008b; Fabre et al., 2011; Hoffman et al., 2017).

The hydrological cycle is intensified in the supergreenhouse climate, and the rain becomes acidic because of the high atmospheric CO_2 concentrations (Fabre et al., 2011). Additionally, the continental surface is covered by shattered rock and unweathered particles after the glacial retreat (Fabre and Berger, 2012). All of this means that continental weathering should have been extremely effective in reducing the atmospheric CO_2 concentration (Hoffman et al., 2017). Nevertheless, it could still have taken hundreds of thousands to millions of years until continental weathering brought the atmospheric CO_2 concentration back to more normal Neoproterozoic values (Higgins and Schrag, 2003; Le Hir et al., 2008b; Fabre et al., 2011).

The enhanced continental weathering in the supergreenhouse climate also implies a substantial flux of carbonate and other ions like Ca^{2+} and Mg^{2+} into the ocean (Higgins and Schrag, 2003; Le Hir et al., 2008b; Fabre and Berger, 2012). These fluxes are assumed to be the main contributor to the formation of the massive carbonate rocks, the so-called cap carbonates, that overlay the glacial deposits of the snowball Earth periods (Hoffman et al., 2017). However, the time scale of cap carbonate deposition is uncertain (Hoffman et al., 2017; Yu et al., 2020). Especially the formation of the distinctive Marinoan "cap dolostones" is an unresolved conundrum.

1.3.4 *The cap dolostone problem*

Dolostone (or dolomite) rocks are a specific form of carbonate sediments that mainly consist of the mineral dolomite $CaMg(CO_3)_2$ (Warren, 2000). Directly above many of the Marinoan glacial deposits, as part of the cap carbonate sequence, lies a massive layer of dolostones that is unique to the Marinoan snowball Earth (Hoffman, 2011). These "cap dolostones" are transgressive, which means that they were deposited during a period of sea-level rise (Hoffman et al., 2017). This occurred during the deglaciation, which lasted for just about 2 kyr (Hyde et al., 2000). But the sea-level changes could also be caused by glacio-isostatic adjustments or by ocean expansion through long-term warming, both presumably acting on time scales of up to $50 - 60$ kyr (Creveling and Mitrovica, 2014; Yang et al., 2017; Hoffman et al., 2017). Furthermore, the cap dolostones show sedimentary signs of rapid deposition (Allen and Hoffman, 2005; Hoffman and Macdonald, 2010; Hoffman, 2011), and geochemical proxy data reveal the influence of a freshwater layer during accumulation, indicating that the cap dolostones were deposited before the ocean destratified after the snowball Earth (Liu et al., 2014, 2018a; Wei et al., 2019; Ahm et al., 2019). In combination, these aspects point to a formation time scale of Marinoan cap dolostones of a few kyr and a maximum upper bound of $50 - 60$ kyr.

The origin of the vast amounts of Ca^{2+}, Mg^{2+} and carbonate that are required to form the massive carbonate rocks on these geologically short time scales is unclear (Yu et al., 2022). Calcifying organisms had not yet developed in the late Neoproterozoic (Knoll, 2003), so that the cap carbonates in general were formed through inorganic or microbially aided precipitation of carbonates from the water column at high seawater alkalinity[1] (Yu et al., 2020). As mentioned earlier, alkalinity is transported into the ocean by intense continental weathering during the supergreenhouse climate. However, Le Hir et al. (2008a) argue that continental weathering would take 20 kyr just to increase the seawater carbonate saturation state above a value of one, which is still far below the critical threshold for inorganic carbonate precipitation (Shaojun and Mucci, 1993; Pan et al., 2021). A possible solution is that shallow ridge volcanism increased the ocean alkalinity reservoir already during the snowball state (Gernon et al., 2016), but it was never quantified how dolomite rocks would accumulate in this scenario. Therefore, it is still unknown how the cap dolostones were formed in the aftermath of the Marinoan snowball Earth.

The formation of Marinoan cap dolostones is not only an interesting scientific problem in the quest to reconstruct the evolution of the Earth system. It also represents a test case for studies that aim to reproduce the climate and biogeochemical conditions during that time. Every proposed scenario for the evolution of the Earth system in the aftermath of the Marinoan snowball Earth must be reconcilable with a rapid formation of dolomite rocks.

1 Alkalinity is the excess of proton acceptors over donors in seawater. It largely determines the ocean's capacity to store carbon through its close relation with pH. See Middelburg et al. (2020) for a recent review.

1.4 MODELING THE SNOWBALL EARTH AFTERMATH

In this thesis, I investigate the evolution of the carbon cycle and the ocean circulation that together shape the climate in the aftermath of the Marinoan snowball Earth. I take a modeling approach, in which I use ICON-ESM (Jungclaus et al., 2022), a coupled atmosphere-ocean general circulation model incorporating the ocean biogeochemistry model HAMOCC (Ilyina et al., 2013). This is, by far, the most complex model used to study the Earth system during the snowball Earth aftermath (Higgins and Schrag, 2003; Le Hir et al., 2008a; Yang et al., 2017; Zhao et al., 2022). Here, I first describe the uncertainties that have to be taken into account when modeling the snowball Earth aftermath. Then I discuss how using ICON-ESM complements previous studies by resolving the transient evolution of the Earth system after the deglaciation.

1.4.1 *Remaining uncertainties*

Reconstructing a past state of the Earth becomes more difficult the further back in time the period of interest is, as the amount and reliability of geochemical and other proxy data decreases accordingly. Consequently, the uncertainties associated with the termination of the Marinoan snowball Earth 635 million years ago are large. The most important uncertainties when studying the dynamics of the ocean and the carbon cycle are listed below.

- Meltwater with a volume of $500 - 1500$ m of sea-level equivalent enters the ocean during the deglaciation (Tziperman et al., 2012; Abbot et al., 2013; Benn et al., 2015; Zhao et al., 2022). The uncertain amount of meltwater that actually forms the meltwater lid has a major impact on the destratification time scale (Yang et al., 2017).
- The atmospheric CO_2 concentration that triggered snowball Earth deglaciation is only loosely constrained to $10^4 - 10^5$ ppm (Kasemann et al., 2005; Bao et al., 2008, 2009).
- It is unclear whether the thick sea-ice cover still allowed for an efficient gas exchange between the ocean and the atmosphere during the snowball period (Le Hir et al., 2008c; Hoffman et al., 2017).
- The amount of alkalinity in the ocean, a major factor in the carbon cycle dynamics, is only constrained by the observation that large amounts of carbonates were formed in the snowball Earth aftermath.

These uncertainties cannot be reduced directly by modeling studies; only measurements from geochemical and other proxy data can do so. Instead, the uncertainties have to be acknowledged, when modeling the aftermath of a snowball Earth. What modeling approaches can do, however, is to present different scenarios that follow from the range of possible initial and boundary conditions. By representing processes using natural laws or parameterizations, models can then provide insight into the dynamical behavior of the system (McGuffie and Henderson-Sellers, 2005). This, in turn, may lead to predictions or consequences that are falsifiable through the

geological record, which can help to reduce the uncertainties regarding the snowball Earth aftermath indirectly. This is the approach that I take in this thesis.

1.4.2 *Transient dynamics in the snowball Earth aftermath*

The variety of processes acting on different time scales during the deglaciation of a snowball Earth make it difficult to capture the full evolution of the Earth system with a model. Chemical weathering or sedimentation processes in the snowball Earth aftermath dominate over periods of hundreds of thousands to millions of years (Higgins and Schrag, 2003; Le Hir et al., 2008b). The time scale of snowball deglaciation, ocean destratification and cap dolostone deposition is a few thousand years, possibly extending to several ten thousand years (Hyde et al., 2000; Zhao et al., 2022; Yang et al., 2017; Hoffman et al., 2017). But a representation of the dynamical processes that ultimately determine the climate and the ocean circulation requires resolving much shorter periods of time and incorporating also three-dimensional spatial features (McGuffie and Henderson-Sellers, 2005). Typically, a trade-off has to be made between model complexity and the considered time scale.

So far, no study has ever considered the three-dimensional ocean circulation or the transient carbon cycle dynamics that dominate on a time scale of < 10 kyr from the start of the deglaciation. Studies of the snowball Earth aftermath that included a carbon cycle considered only the long-term dynamics of chemical weathering processes without simulating the atmosphere or ocean circulation (Higgins and Schrag, 2003; Le Hir et al., 2008b; Le Hir et al., 2008a; Fabre et al., 2011; Fabre and Berger, 2012). Studies that simulated the climate neglected the impact of the dynamical ocean circulation (Le Hir et al., 2008b; Yang et al., 2017). In fact, the destratification time scale is the only aspect of the ocean in the snowball Earth aftermath that has been investigated in a study so far (Yang et al., 2017). However, even in that study the ocean is only represented by a one-dimensional mixing model. I fill this gap by using an Earth system model that can simulate the dynamics of the ocean and the carbon cycle on a time scale of several thousand years from the start of the deglaciation.

A range of previously neglected processes are accounted for by my modeling approach. Resolving the three-dimensional ocean circulation enables a more accurate representation of the destratification after a snowball Earth and an investigation of the evolution of circulation features like the meridional overturning circulation (MOC). The MOC of the ocean determines the exchange of heat, carbon and nutrients between the deep ocean and the surface (Schmittner, 2005; Marshall and Speer, 2012). Including the ocean circulation therefore also strongly influences the simulated climate (Winton, 2003), and it allows a study of carbon cycle processes that are affected by the ocean circulation.

The strength of the supergreenhouse climate is determined by the amount of CO_2 in the atmosphere, but the carbon reservoir of the ocean can be much larger than that of the atmosphere (Siegenthaler and Sarmiento, 1993). The CO_2 exchange between both reservoirs is determined by the difference between the atmospheric concentration of CO_2 and the partial pressure of CO_2 (pCO_2) in the surface ocean (Sarmiento, 2013). The pCO_2 of the ocean is strongly impacted by the chemical and physical transformations during the deglaciation and the transition into the

supergreenhouse climate. Therefore, the ocean plays a major role in setting the intensity of the supergreenhouse climate. Simple box models capture some of these transformations (Higgins and Schrag, 2003; Le Hir et al., 2008c; Le Hir et al., 2008a), but only an Earth system model properly resolves the spatio-temporal variations within the ocean that determine the distribution of carbon between the ocean and the atmosphere.

Lastly, the biology component of ICON-ESM enables a simulation of the biological carbon pump. The biological carbon pump is a well known process, by which phytoplankton and cyanobacteria affect the carbon cycle through their uptake of carbon during primary production (Sarmiento, 2013). It leads to a reduction of pCO_2 in the surface ocean, where primary production occurs, and to an increase of carbon in the deep ocean, where the organic matter is remineralized. At the time of the Marinoan snowball Earth, different types of primary producers had already evolved (Knoll et al., 2007). Therefore, the biological carbon pump might have played an important role in the carbon cycle dynamics during the snowball Earth aftermath. The efficiency of the biological carbon pump is dependent on the exchange of waters from the deep ocean with the surface and hence on the stratification that develops during the deglaciation of a snowball Earth (Appen et al., 2021). Therefore, only a model that resolves the ocean circulation can quantify the contribution of the biological carbon pump.

1.5 RESEARCH QUESTIONS

In the previous sections, I have described the modeling approach that I take. The added value of this approach has two components. On the one hand, I consider transient ocean and carbon cycle dynamics that have not been recognized in previous studies. On the other hand, I account for the large range of uncertainties that come with the conditions at the start of the deglaciation. Here, I define the specific questions that I address in this thesis.

I have mentioned on several occasions the importance of the time scale of ocean destratification after a snowball Earth. Ocean destratification determines the time scales of long-term ocean warming and cap dolostone deposition (Yang et al., 2017), as well as the mixing of nutrients from the deep ocean to the surface (Liu et al., 2014) and the efficiency of the biological carbon pump (Qin et al., 2022). My first research subject therefore addresses the following question:

RQ1. How and over which time scale does the ocean destratify after a snowball Earth?

The destratification time scale has already been quantified by Yang et al. (2017) to be $10 - 100$ kyr, with a best estimate of 50 kyr. However, the large uncertainty range is unsatisfying and their simplified modeling approach does not take into account the contribution of the dynamical ocean circulation.

Similarly, the intensity of the supergreenhouse climate was only investigated without considering the three-dimensional ocean circulation (Le Hir et al., 2008b; Yang et al., 2017). Additionally, the climatic conditions that could arise under atmospheric CO_2 concentrations that are at the lower end of the possible range have not been investigated in detail (Le Hir et al., 2008b). Therefore, my second research question is:

RQ2. What were the temperatures in the supergreenhouse climate?

The duration of the supergreenhouse climate is of similar importance as its intensity. In the last part of my thesis, I will take a closer look at the carbon cycle processes that could affect the atmospheric CO_2 concentration on a time scale of < 10 kyr from the start of the deglaciation. The overall question thereby is:

RQ3. How did the supergreenhouse climate evolve?

In order to answer this question, I will quantify the ocean's role in the carbon cycle. I specifically do not address the role of long-term weathering processes in modulating the atmospheric CO_2 concentration, as this has been done in great detail before (Higgins and Schrag, 2003; Le Hir et al., 2008b; Le Hir et al., 2008a; Fabre et al., 2011; Fabre and Berger, 2012). On the contrary, I make use of the fact that my modeling approach resolves the short-term processes of air-sea CO_2 exchange, hypothesizing that these processes can substantially alter the atmospheric concentration of CO_2.

2

OCEAN DYNAMICS AND THE CLIMATE AFTER A SNOWBALL EARTH

Let us start our investigation of the Earth system dynamics in the snowball Earth aftermath with a closer look at the physical characteristics of the ocean and the climate. We know that there will be an inflow of freshwater into the ocean and that the climate will warm quickly due to the strong ice-albedo feedback during the deglaciation of a snowball Earth. Here, I quantify how the freshwater stratification was broken up and how warm the supergreenhouse climate was. I use the general circulation model ICON-ESM with boundary conditions for the Marinoan snowball Earth (635 Ma). A detailed description of the model setup and references to the individual model components can be found in Appendix A. In these simulations, I prescribe the atmospheric CO_2 concentration and investigate the response of the ocean circulation and the climate to a predetermined evolution of the greenhouse conditions.

2.1 RAPID BREAK-UP OF THE STRATIFICATION

I find that the freshwater stratification after a snowball Earth is removed within roughly 2 kyr. This time scale is substantially shorter than the previous best estimate of 50 kyr (Yang et al., 2017), which used a comparable initial state but a radically different model. In the following, I describe the settings of my simulations, the mechanisms behind the fast destratification in ICON-ESM and why the stratification should indeed break up rapidly.

The strength of the freshwater stratification after a snowball Earth depends strongly on the amount of meltwater generated during the deglaciation, which is only loosely constrained, as discussed in section 1.4.1. Here, I study the response of the ocean circulation to an idealized freshwater stratification. In this scenario, I adapt the salinity field of the ocean to a simple two-layer case with a 1000 m thick surface layer of low salinity (5 psu) above a highly saline (46.7 psu) deep ocean (see Appendix A for a detailed description of the simulation design). This represents an intermediate amount of freshwater, when compared to the existing estimates (Tziperman et al., 2012; Abbot et al., 2013; Benn et al., 2015; Zhao et al., 2022), and the scenario is comparable to the one used in Yang et al. (2017). This approach is sufficient to determine the first-order response of the ocean circulation and the destratification time scale.

The evolution of the freshwater stratification can be investigated in terms of zonal averages of the salinity field (Fig. 2.1). The horizontal stratification of the salinity field becomes tilted quickly in the high latitudes, especially in the northern hemisphere. In the northern hemisphere, a strong circumpolar current exists, as there are no continents north of 51°N that could block the flow. Furthermore, the westerly winds that drive the circumpolar current are especially strong during the supergreenhouse climate and centered at high latitudes, where they can force the current particularly

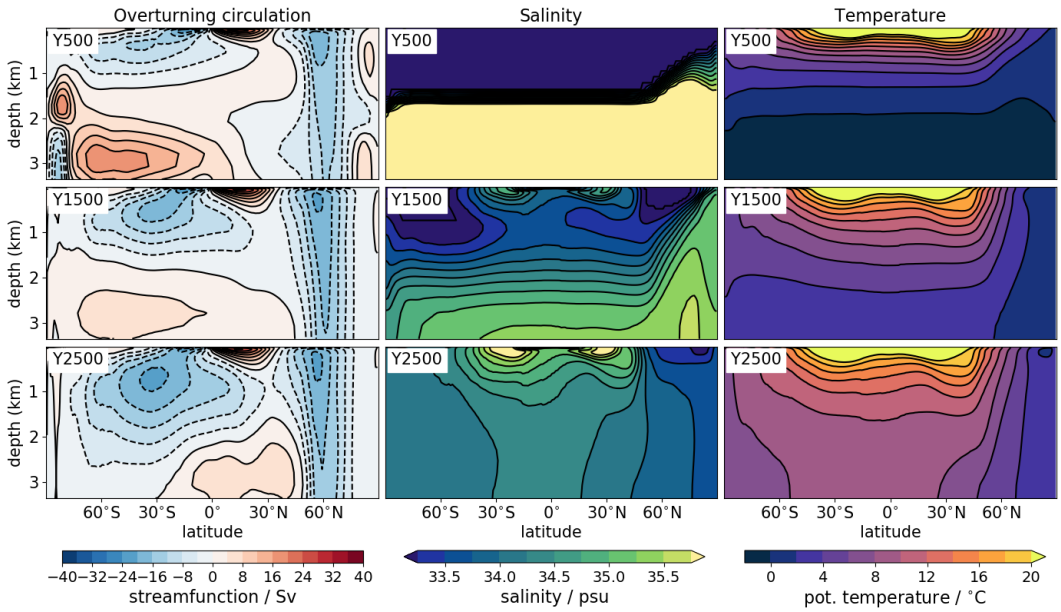

Figure 2.1: Zonally averaged meridional overturning circulation (MOC, left), salinity (middle) and potential temperature (right) at 500, 1500 and 2500 years since an idealized salinity field was prescribed. The data are from an ICON-ESM simulation with a constant atmospheric CO_2 concentration, and they are depicted by 30-year averages around the given timestamp. Positive MOC values represent a clockwise circulation. The strong initial freshwater stratification is mostly removed already after 1500 years and completely gone after 2500 years.

well. The circumpolar current initially incorporates a large vertical shear in the zonal velocity component. Through the thermal wind relationship (see e.g. Olbers et al., 2012, for a detailed explanation), this vertical shear within the current can be connected to the northward sloping isopycnals, which closely follow the isohalines during the early snowball Earth aftermath. The mixing along the sloped isopycnals supports the exchange of surface waters with the deeper ocean and therefore favors the destratification. Furthermore, the zonal profile of the westerly winds induces a surface divergence through Ekman transport, also leading to the upwelling of deeper waters. The fast break-up of the stratification after a snowball Earth is therefore a consequence of the dynamical ocean circulation. In particular, the Marinoan distribution of continents and the winds during the supergreenhouse climate induce a circumpolar current that acts as the main driver of the destratification.

Before moving on, we should discuss how uncertainties and the assumptions that were made here impact the finding of a fast destratification. First of all, the prescribed two-layer initial state is a highly idealized scenario. While it is an extreme case of a stratification, it neglects the continuous inflow of meltwater during the deglaciation of a snowball Earth. I conduct an additional simulation (termed "Exp. 4" in Appendix B), with a continuous freshwater input during the deglacial period. In this experiment, the MOC recovers shortly after the end of the freshwater input period, indicating that the stratification after a snowball Earth possibly persisted throughout the deglacial period, but not for much longer. A further experiment presented in Appendix A shows that even with significantly reduced parameterized vertical mixing the destratification time scale is prolonged only by some 500 years.

Lastly, differences in the continental setup and the ocean bathymetry would lead to changes in the circulation, which could weaken those components of the circulation that break up the stratification. However, the reconstructions are clear in that probably no continents were located north of 60°N (Li et al., 2013; Merdith et al., 2017). The existence of a circumpolar current that drives a major vertical exchange of waters is therefore likely. Based on the findings presented here and the discussed uncertainties, I argue that a surface freshwater layer resulting from the deglaciation of a snowball Earth will very likely be removed in less than 10 kyr, possibly in just around 2 kyr.

2.2 CONSEQUENCES OF THE FAST DESTRATIFICATION

The meridional overturning circulation (MOC) recovers together with the break-up of the stratification. The MOC of the ICON-ESM Marinoan setup is characterized by a large cell rotating counterclockwise in the southern hemisphere. We can see from the left column of Fig. 2.1 that the MOC is initially suppressed and shallow due to the stratification, but that it regains strength as the stratification is broken up. A comparison of different scenarios for the evolution of the atmospheric CO_2 concentration (see Appendix A), shows deviating pathways of the MOC recovery, depending on the amount of warming and the thermal component of the stratification. At the same time, the removal of the freshwater stratification occurs on almost identical time scales in those scenarios. This leads to the conclusion that the recovery of the MOC is a consequence of the general stratification and not a driver of the break-up of the freshwater component. It should be mentioned that the shape of the MOC is strongly dependent on the uncertain topographical features of the ocean, and not enough information exists to confidently assume a strong MOC in the snowball Earth aftermath. Nevertheless, the strong connection between MOC recovery and destratification highlights that the deep ocean was possibly well ventilated already a few thousand years after the start of the deglaciation.

The fast recovery of the MOC implies that nutrients, which were stored in the deep ocean during the snowball state, were brought back to the surface relatively soon after the deglaciation, presumably fueling primary production. On a similar time scale, the anoxic ocean waters that might have existed during the snowball state (Johnson et al., 2017; Shen et al., 2022), would come into contact with the atmosphere. The biological carbon pump is especially effective when the ocean stratification is strong. The findings of this chapter therefore also play a role in the carbon cycle dynamics after a snowball Earth, and I will come back to this in Chapter 3.

The rapid destratification also suggests that the warming of the deep ocean mostly occurred on a time scale of several thousand years from the start of deglaciation (right column of Fig. 2.1). Additionally, my simulations indicate that the associated thermal expansion of the ocean could have led to a sea-level rise of just 8 m, which is much less than the previous estimate of up to 50 m (Yang et al., 2017). On the one hand, this is a consequence of the lower atmospheric CO_2 concentration used in my study. On the other hand, this is because temperatures in the deep ocean are set more realistically in ICON-ESM by the cold waters that sink to the ocean bottom in deep water formation regions. My results suggest that ocean warming and the

associated sea-level rise could have been substantially weaker and developed on a much shorter time scale than previously expected (Yang et al., 2017).

The Marinoan cap dolostones were formed in the snowball Earth aftermath during a period of sea-level rise (Hoffman, 2011; Hoffman et al., 2017) and before the freshwater stratification was removed (Liu et al., 2014, 2018a; Wei et al., 2019; Ahm et al., 2019). Yang et al. (2017) argued that this could have happened on a time scale of 50 kyr, based on their findings of a slow destratification and a substantial long-term sea-level rise. I have shown here that the freshwater stratification cannot be sustained for long after the deglaciation and that the thermal expansion of the ocean cannot explain a major sea-level rise over a time scale of more than a few thousand years. My findings therefore indicate that the Marinoan cap dolostones were deposited in the first ten thousand years of the snowball Earth aftermath, possibly within just $2-3$ kyr from the start of the deglaciation. This gives us a helpful constraint when investigating the evolution of the supergreenhouse climate in Chapter 3.

2.3 TEMPERATURES IN THE SUPERGREENHOUSE CLIMATE

With an atmospheric CO_2 concentration of 1.5×10^4 ppm, ICON-ESM simulates a global mean surface temperature of around 30°C. This is substantially colder than the common assumption of global mean temperatures of around 50°C in the supergreenhouse climate (Yang et al., 2017; Hoffman et al., 2017). The main reason for the lower temperatures in my simulations is that I use an atmospheric CO_2 concentration that is at the lower end of the possible range ($10^4 - 10^5$ ppm, Kasemann et al., 2005; Bao et al., 2008, 2009). Le Hir et al. (2008b) already used an atmospheric general circulation model to study equilibrium climate states in the aftermath of a Marinoan snowball Earth at a range of different atmospheric CO_2 concentrations. They find global mean surface temperatures between roughly 30°C and 55°C for atmospheric CO_2 concentrations of $10^4 - 10^5$ ppm. How do my simulations with an atmosphere-ocean general circulation model compare to that?

The equilibrium climate sensitivity of my ICON-ESM Marinoan setup is +4.9°C per doubling of CO_2, which I calculate from a comparison of the above-mentioned supergreenhouse climate with a Marinoan "control climate" at 1.5×10^3 ppm. In a simple estimation, assuming a constant climate sensitivity, I calculate that global mean temperatures would be between 27°C and 43°C for atmospheric CO_2 concentrations between 10^4 and 10^5 ppm. Although such a simplified calculation should be considered with caution, my simulations generally point to lower temperatures in the supergreenhouse climate than previously assumed. I conclude that global mean temperatures of around 50°C are unlikely, given that they would require an atmospheric CO_2 concentration at the upper end of the possible range and a very high climate sensitivity that is on the order of +7°C per doubling of CO_2.

The simulations with ICON-ESM represent the first investigation of the climate in the snowball Earth aftermath that accounts for a three dimensional ocean circulation. Therefore, the simulated sea surface temperatures have a larger reliability than those of simulations with atmosphere-only general circulation models (Le Hir et al., 2008b; Yang et al., 2017). A notable finding of my simulations is that, with an atmospheric CO_2 concentration of 1.5×10^4 ppm, the annual mean temperatures near the north

pole are still below 10°C. This is because the strong circumpolar current prevents warm water masses from penetrating into higher latitudes. In summary, my results suggest that the temperatures in the supergreenhouse climate were probably not as threatening for early forms of life as previously assumed. This is because global mean temperatures might have generally been lower and because temperate regions would likely exist in the high latitudes, even at very high atmospheric CO_2 concentrations.

3

CARBON CYCLE DYNAMICS AFTER A SNOWBALL EARTH

Now that we know the basic characteristics of the ocean circulation and the climate, we can turn our attention to the dynamics of the carbon cycle. These dynamics determine the evolution of the supergreenhouse climate through changes in the concentration of CO_2 in the atmosphere. I start with a quantification of the major processes by which the ocean affects the carbon cycle (Fig. 3.1, top), before I integrate my findings in a discussion about the duration of the supergreenhouse climate. The processes I discuss here are known, and they are understood reasonably well for situations like the modern climate (or past climates like the PETM, e.g. Heinze and Ilyina, 2015; Ilyina and Heinze, 2019). However, the ocean's role in the carbon cycle has never been quantified for the snowball Earth aftermath.

At this point, it is helpful to introduce the basic variables of the ocean carbon cycle. As CO_2 enters the ocean, it reacts with seawater and is differentiated into aqueous CO_2 and carbonic acid (H_2CO_3), bicarbonate (HCO_3^-) and carbonate (CO_3^{2-}). The distribution between the different species is highly dependent on the pH of the ocean, and in the modern ocean most of the dissolved inorganic carbon (DIC) is stored in the form of bicarbonate (Zeebe and Wolf-Gladrow, 2001). The pH of the ocean, in turn, is strongly correlated to the total alkalinity of the ocean (just "alkalinity" from now on), which is the excess of proton acceptors over donors in seawater. The most important feature of alkalinity is that it has an overarching control on the amount of carbon that can be stored in the ocean (see Zeebe and Wolf-Gladrow, 2001; Middelburg et al., 2020, for more information). Being a function of DIC and alkalinity, the carbonate saturation state in seawater (Ω) is a helpful quantity to characterize whether carbonate rocks would be dissolved ($\Omega < 1$) or readily formed (very high Ω, Zeebe and Westbroek, 2003; Hood et al., 2022) in the ocean. Ultimately, the difference between the atmospheric CO_2 concentration and the partial pressure of CO_2 in the surface ocean (pCO_2) determines the exchange of carbon between the two reservoirs. The ocean's pCO_2 is a function of DIC and alkalinity, but also depends on temperature and salinity. The processes that are discussed in the next sections all influence the pCO_2 of the surface ocean in one way or another.

The magnitude of individual carbon cycle processes is highly dependent on the uncertain conditions at the start of the deglaciation, and I account for uncertainties in two major variables throughout the following text:

1. I consider atmospheric CO_2 concentrations between 10^4 and 10^5 ppm, which is the full uncertainty range of values in the aftermath of the Marinoan snowball Earth (Kasemann et al., 2005; Bao et al., 2008, 2009).

2. I consider ocean alkalinity in a wide range of $1 - 60$ mol m^{-3}. The lower bound represents a value that is unrealistically low (Higgins and Schrag, 2003; Le Hir et al., 2008a; Gernon et al., 2016), but its inclusion provides instructive insights. The upper bound of possible alkalinity is hardly constrained. I use 60 mol m^{-3}, because it is already a very high concentration, and no qualitatively different behavior is expected at even higher values.

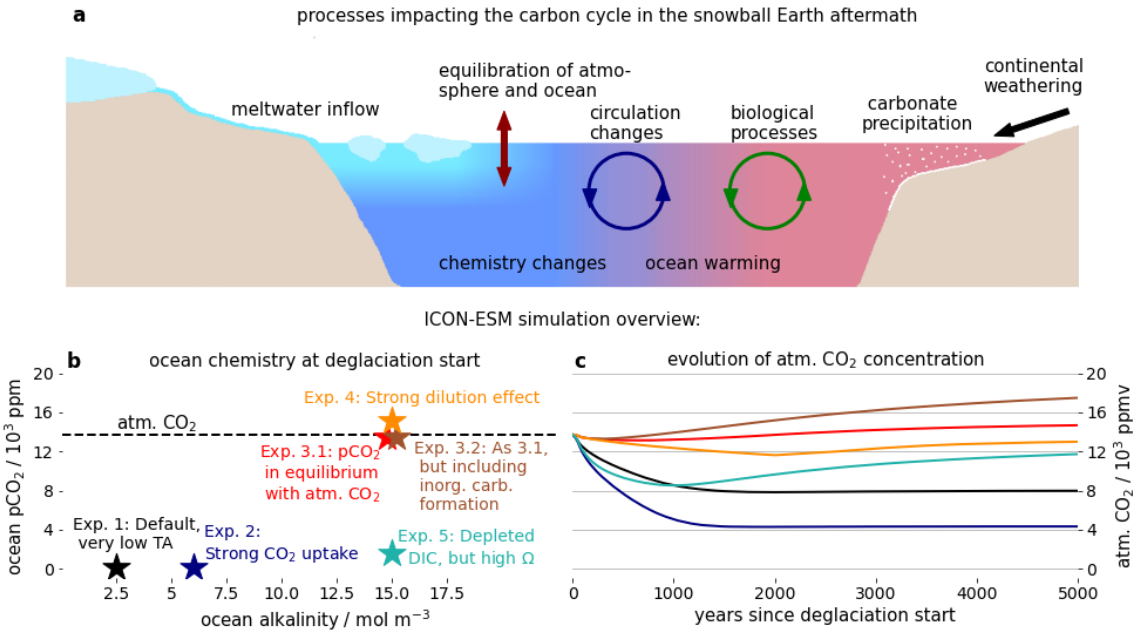

Figure 3.1: Air-sea CO_2 exchange after a snowball Earth and simulation overview. **a**, Illustration of the different processes that impact the air-sea CO_2-flux after a snowball Earth. **b**, Alkalinity and pCO_2 of the ocean at the start of the deglaciation for the different ICON-ESM simulations. **c**, Evolution of atm. CO_2 in the ICON-ESM simulations. More details on the experiment settings are found in Appendix B.

In contrast to the uncertain ice volume and deglaciation process discussed in the previous chapter, a simplified best-guess scenario for atmospheric CO_2 and ocean alkalinity is not sufficient to determine the first-order dynamics of the carbon cycle. As we shall see, very different scenarios for the evolution of the supergreenhouse climate are possible, depending on the uncertain conditions at the start of the deglaciation (Fig. 3.1, bottom).

3.1 AIR-SEA CO_2 EXCHANGE AFTER A SNOWBALL EARTH

3.1.1 *The potential effect of a non-permeable snowball sea-ice cover*

It is unclear whether the snowball Earth sea-ice cover was permeable for the exchange of CO_2. If the thick sea-ice cover during a snowball Earth prevented an efficient gas exchange between the atmosphere and the ocean, then the two carbon reservoirs were presumably out of equilibrium. While the atmospheric CO_2 concentration rose during the snowball period, it is unclear how the ocean pCO_2 was influenced by seafloor weathering processes and hydrothermal outgassing (Hoffman et al., 1998; Le Hir et al., 2008c). Negative feedbacks between increasing ocean pCO_2 and weathering processes (Le Hir et al., 2008a), as well as possible sources of alkalinity from extensive ridge volcanism during the snowball period (Gernon et al., 2016), make it possible that the sub-snowball ocean pCO_2 was lower than the atmospheric CO_2 concentration. I describe here the CO_2 uptake that results when a non-permeable sea-ice cover is broken up during the deglaciation, and an ocean with low pCO_2

comes into contact with a high pCO_2 atmosphere. The resulting oceanic uptake of CO_2 is what I call the "reservoir equilibration effect".

In order to quantify the isolated reservoir equilibration effect, I consider an idealized scenario of a snowball Earth state at high atmospheric CO_2 concentration, in which the sea-ice cover is suddenly permeable for the gas exchange of CO_2. The initial oceanic concentration of DIC is assumed to be very low, but still high enough in order to avoid $pCO_2 < 100$ ppm and unrealistically high carbonate saturation states. Carbon dioxide is then removed from the atmosphere and added to the ocean in the form of DIC until a new equilibrium between the partial pressures of CO_2 is reached. This simplified calculation is done with a box model that I developed specifically for this study, and I refer the reader to Appendix B for a detailed explanation.

I find that the reservoir equilibration effect can theoretically reduce the atmospheric CO_2 concentration by up to 80% (Fig. 3.2). The largest relative reduction in the atmospheric CO_2 concentration occurs when the initial atmospheric CO_2 concentration is low and the ocean alkalinity is in the range of $4 - 10$ mol m^{-3}. At lower alkalinity, the atmospheric carbon reservoir is of a comparable size or even larger than the ocean carbon reservoir. Hence, already small relative reductions in atmospheric CO_2 increase the ocean pCO_2 substantially and lead to a new equilibrium. In contrast to that, at high alkalinity, the large carbonate saturation states do not allow for a significant disequilibrium between the two reservoirs, and the relative reduction in atm. CO_2 through the reservoir equilibration effect is small as well. The magnitude of the effect, therefore, depends strongly on the combination of the initial concentrations of atmospheric CO_2 and ocean alkalinity.

These idealized calculations are backed up by a number of ICON-ESM simulations (see Fig. 3.1 and Appendix B), which exhibit reductions in the atmospheric CO_2 concentration that are comparable to the calculated CO_2 removal of the isolated effect. This shows that, despite the variety of additional processes included in ICON-ESM, the reservoir equilibration effect potentially dominates the evolution of the atmospheric CO_2 concentration after a snowball Earth. However, my calculations should be seen as the maximum possible reduction of atmospheric CO_2 through this effect. The mechanism could also draw down much less CO_2, or not come into play at all, if the disequilibrium between the atmosphere and the ocean was smaller. In the following sections, we will always assume an efficient gas exchange during the snowball Earth period, that is, we assume that the reservoir equilibration effect is not at work.

3.1.2 *Tracer dilution through meltwater inflow*

The dilution of the ocean by the inflow of meltwater reduces, among all other tracer concentrations, the concentration of DIC and hence the pCO_2 of the ocean. This will induce a flux of CO_2 from the atmosphere into the ocean and reduce the intensity of the supergreenhouse climate. In contrast to the reservoir equilibration effect, the dilution effect definitely occurred, as meltwater will have entered the ocean during the deglaciation, but uncertainties remain regarding the meltwater volume and its chemical composition.

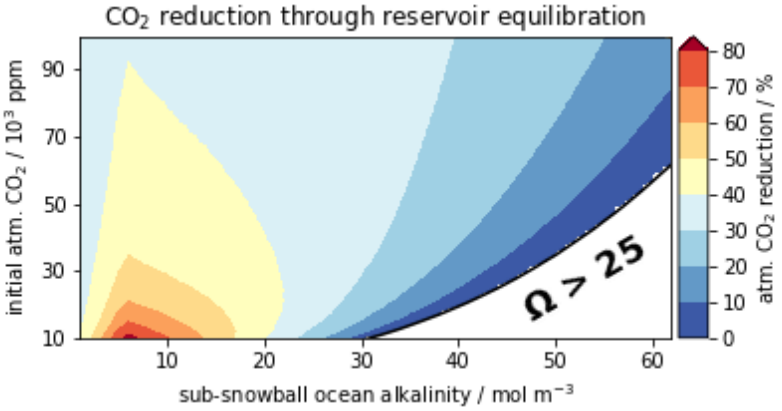

Figure 3.2: The reservoir equilibration effect. Relative reduction of the atmospheric CO_2 concentration in response to the isolated reservoir equilibration effect. A sub-snowball ocean with low pCO_2 is assumed to suddenly come into contact with a high pCO_2 atmosphere. In the white area, the calcium carbonate saturation state of the ocean (Ω) would be unrealistically high (see Appendix B).

In order to quantify the isolated effect of the dilution on the oceanic uptake of CO_2, I consider a similarly idealized scenario as for the reservoir equilibration effect: A chemically evolved ocean in a snowball Earth state is diluted through the inflow of 1000 m of pure freshwater, devoid of any biogeochemical tracers and salt. The ocean is assumed to be mixed instantaneously, causing carbon to be transferred from the atmosphere into the ocean until a new equilibrium is found between the two reservoirs. Again, this idealized calculation is done with a box model, which is described in Appendix B.

I find that the atmospheric CO_2 concentration is reduced by 10-15% in this scenario. The reduction is only weakly dependent on the initial ocean alkalinity and the atmospheric CO_2 concentration. About 30% of this reduction comes from the dilution of salinity from around 48 psu to a global mean value of 34.3, as the solubility of CO_2 is increased at lower salinity. The further uptake must then result from the dilution of the DIC concentration directly and from a shift in the carbonate chemistry that causes a rearrangement between the different carbonate species. Two of the ICON-ESM simulations differ only by a dilution effect that is comparable to the effect in the idealized calculations (Appendix B). These simulations show that the 10-15% reduction of atmospheric CO_2 that was estimated with the simplified box model also holds in the much more comprehensive setup of ICON-ESM.

Here, I have assumed that the deglacial waters are devoid of any biogeochemical tracers. However, some DIC and alkalinity are normally also present in sea ice, often with a ratio of alkalinity:DIC that is larger than one (Fransson et al., 2011; Grimm et al., 2016), and further alkalinity could come with the meltwater flushes from the continents (Fabre and Berger, 2012). Consequently, DIC in the ocean could easily be diluted stronger than alkalinity, which would lower the ocean's pCO_2 even further and cause an even stronger dilution effect than predicted here. Therefore, I conclude that my finding of a 10-15% reduction of the atmospheric CO_2 concentration is at the lower end of possible values. Nevertheless, it should be a good first-order estimate of the actual magnitude of the dilution effect during the deglaciation of a snowball Earth.

3.1.3 *An efficient biological carbon pump?*

During the snowball state, the ocean is well mixed and no vertical gradient of the DIC concentration exists (Ashkenazy et al., 2013). In the snowball Earth aftermath, the biological carbon pump will then reintroduce a vertical gradient, in which DIC increases with depth, and therefore remove DIC from the surface ocean and the atmosphere. Here, I introduce the relevance of the biological carbon pump in my ICON-ESM simulations, noting, however, that the biological evolution after the Marinoan snowball Earth might not be properly represented in the HAMOCC model. I come back to this at the end of this section.

I quantify the effect of the reappearing biological carbon pump with two ICON-ESM simulations. These simulations are identical except that in one of the simulations primary production is suppressed. After 1000 years from the start of the deglaciation, the atmospheric CO_2 concentration is 2000 ppm higher in the simulation with suppressed primary production than it is in the simulation where the biological carbon pump is active. The rate of primary production is independent of the ocean alkalinity and increases only slightly at higher temperatures in ICON-ESM. This indicates that the efficiency of the biological carbon pump is mostly independent of the uncertain atmospheric CO_2 concentration and ocean alkalinity at the start of the deglaciation. Therefore, the oceanic carbon uptake driven by the biological carbon pump will have its largest relative impact at lower initial atmospheric CO_2 concentrations.

The biological carbon pump leads to a reduction of atmospheric CO_2 until the downward transport of organic carbon is balanced by the upward mixing of carbon-enriched deep waters. This mechanism therefore depends on the ocean stratification, whereby a stronger stratification can support a larger deep-ocean carbon reservoir and lead to more uptake of CO_2. When the stratification breaks up, the increased upwelling of deep waters reintroduces carbon into the atmosphere. This delayed outgassing of CO_2 is visible in the simulations presented in Appendix B. It suggests that, because of the stratification, a part of the reduction of the atmospheric CO_2 concentration through the biological carbon pump is only temporary. After all, while a strong stratification increases the efficiency of the biological carbon pump, it also means that nutrients from the deep ocean are not easily accessible for primary production.

The availability of nutrients in the post-snowball ocean is one major source of uncertainty when quantifying the effect of the biological carbon pump on the global carbon cycle. It is further debatable whether the parameterization of biological activity in HAMOCC is appropriate for the organisms of the late Neoproterozoic. The fact that primary production recovers rapidly in the ICON-ESM simulations might be unrealistic, as it is questionable whether those biota that adapted to a snowball Earth state could indeed thrive and spread quickly in the warm snowball Earth aftermath. For these reasons, I only conclude that the biological carbon pump is a potential mechanism that can contribute to the reduction of the greenhouse conditions in the snowball Earth aftermath. How strong this contribution was and on which time scale it acts is, however, uncertain.

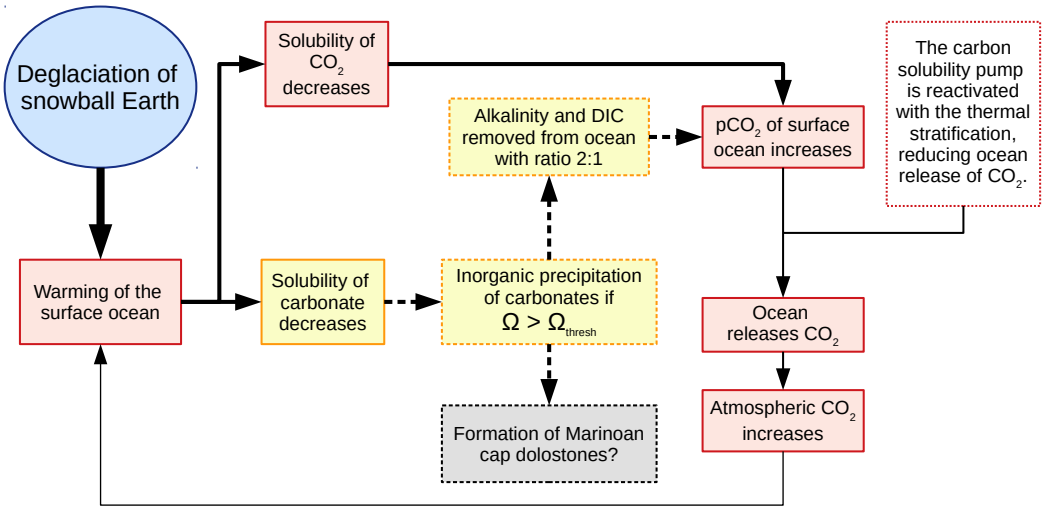

Figure 3.3: The positive feedback loop of ocean warming and outgassing of CO_2. Outgassing of CO_2 occurs via two pathways: 1. The solubility of CO_2 in seawater decreases at higher temperatures, which increases pCO_2 directly. However, the resulting CO_2 release is strongly reduced by the fact that the deep ocean warms much less, i.e., the carbon solubility pump is reactivated. 2. Also the solubility of carbonates decreases, which increases the pCO_2 of the ocean indirectly. The second pathway is only activated at high carbonate saturation states Ω. The additional warming that results from the increase in atmospheric CO_2 is small compared to the warming during the deglaciation.

3.1.4 *Ocean warming drives outgassing of CO_2*

So far, we have only discussed mechanisms that lead to a flux of CO_2 from the atmosphere into the ocean. Although a number of the ICON-ESM simulations do indeed show an overall reduction of the atmospheric CO_2 concentration in the snowball Earth aftermath, some simulations demonstrate that also a considerable outgassing of CO_2 from the ocean is possible (Fig. 3.1 and Appendix B). This outgassing is in large parts driven by the warming of the ocean and the impact of the warming on the solubility of the various carbonate species.

The warming-driven outgassing of CO_2 represents a positive feedback loop, because the resulting increase in atmospheric CO_2 intensifies the greenhouse conditions and warms the climate further. The CO_2 release is driven by two separate mechanisms (Fig. 3.3). On the one hand, the pCO_2 of the ocean is increased by the warming and the associated decrease in the solubility of CO_2 (Weiss, 1974). On the other hand, also the solubility of carbonate decreases in a warming ocean (Millero, 1979). This leads to the inorganic precipitation of carbonates from the water column if the solubility decrease lifts the carbonate saturation state above a threshold value (Zeebe and Westbroek, 2003). Thereby, alkalinity and DIC are removed from the ocean with a ratio of 2:1, which decreases the pH and increases pCO_2 through a shift in the differentiation between the carbonate species (e.g., Middelburg et al., 2020). In the following, I evaluate both processes separately.

Reduced solubility of CO_2 and effect of ocean circulation

In the aftermath of a snowball Earth, ocean surface temperatures increase rapidly. Hence, the post-snowball Earth warming will lead to a substantial increase of the surface pCO_2 of the ocean and possibly to an outgassing of CO_2. Surprisingly, the early stage of the deglaciation is also the phase where almost all the ICON-ESM simulations show a decrease of the atmospheric CO_2 concentration, despite the strong warming (Fig. 3.1). The mechanisms mentioned in the previous sections must therefore counteract the warming-induced increase in pCO_2 during this period. After $1-2$ kyr from the start of the deglaciation, the importance of other carbon cycle processes diminishes, and the long-term warming drives an oceanic release of CO_2 in most of the ICON-ESM simulations.

The reduction of the solubility of CO_2 during the warming of the ocean is the ultimate driver of the air-sea CO_2 exchange that I discuss in this section. However, the temperature increase at the surface is not representative for the warming of the whole ocean, since the deep ocean warms much less. This means that the carbon solubility pump (e.g., DeVries, 2022), which was not active in the well-mixed snowball ocean, comes into play again and reduces the warming-induced carbon release substantially. Because of this entanglement, I here only quantify the combined effect of the reduced solubility of CO_2 and the reintroduced thermal stratification.

The only simulation that indeed shows an outgassing of CO_2 during the main warming phase in the years $100-1000$ from the start of the deglaciation, is the one with suppressed primary production. I estimate that the warming of the ocean increases the atmospheric CO_2 concentration by about 25% in my ICON-ESM simulations. This is derived from a simulation in which the reservoir equilibration effect is zero, the dilution effect is weak, the inorganic precipitation of carbonates is inactive and the biological carbon pump is crudely estimated to reduce atmospheric CO_2 by 2000 ppm. In a warmer climate, at higher atmospheric CO_2 concentrations, the solubility reduction of CO_2 will lead to even more outgassing of CO_2, but the relative increase in atmospheric CO_2 is smaller.

Warming-driven inorganic precipitation of carbonates

Carbonate minerals like calcite, aragonite or dolomite become less soluble in a warming ocean. This can lead to outgassing of CO_2 via the inorganic precipitation of carbonates, as illustrated in Fig. 3.3. The inorganic precipitation of carbonates only occurs if the carbonate saturation state of the seawater is above a critical threshold. Therefore, the magnitude of the resulting increase in atmospheric CO_2 is highly dependent on the chemical state of the ocean. However, the critical threshold for the inorganic formation of dolomites, which was the main carbonate mineral formed after the Marinoan snowball Earth, is very uncertain (Bénézeth et al., 2018; Hood et al., 2022). As a consequence, the following description remains vague with respect to the conditions at which carbonate precipitation occurs or not. I refer the reader to Appendix B for a detailed explanation of the process and its implementation in my model, as well as for a more elaborate quantification of the results.

I find that the atmospheric CO_2 concentration is increased by $4-5\times10^3$ ppm for every 10^{18} mol of carbonate removed from the ocean. More inorganic precipitation of carbonates occurs at initially high ocean alkalinity and low atmospheric CO_2

concentrations. No inorganic precipitation will occur for ocean alkalinity of roughly < 15 mol m^{-3}. More than 10^{19} mol of carbonates could be formed inorganically for high ocean alkalinity around ~ 50 mol m^{-3}, implying a massive increase of the atmospheric CO_2 concentration. Depending on the ocean chemistry, the inorganic precipitation of carbonates will either not affect the post-snowball Earth carbon cycle at all, or it can lead to a massive intensification of the supergreenhouse climate.

3.2 DURATION OF THE SUPERGREENHOUSE CLIMATE

In the previous sections, I have described the main carbon cycle processes that are important in the first several thousand years after a snowball Earth. My findings suggest that the atmospheric CO_2 concentration could, in fact, be substantially altered through the exchange of CO_2 with the ocean. Here, I assess how the different carbon cycle processes might have acted together and shaped the evolution of the supergreenhouse climate after the Marinoan snowball Earth.

Three of the five major carbon cycle processes that I discussed in this thesis will certainly have contributed to the air-sea exchange of CO_2. These three processes are the dilution effect, the biological carbon pump and the warming-induced reduction of the solubility of CO_2. However, each of these three processes changed the atmospheric CO_2 concentration by < 25 % in my ICON-ESM simulations, and their magnitude would not be affected much by varying initial conditions. In two ICON-ESM simulations only these three processes were active. Both simulations show an initial reduction of the atmospheric CO_2 concentration and a long-term increase. In general, the atmospheric CO_2 concentration remained within ± 10 % of the initial CO_2 concentration at the start of the deglaciation in both simulations, showing that these three processes approximately balanced each other. Although the existence of such an approximate balance is far from certain, I argue that the combination of these three carbon cycle processes did not lead to a major alteration of the greenhouse conditions in the snowball Earth aftermath.

The two other carbon cycle processes, the reservoir equilibration effect and the warming-induced inorganic precipitation of carbonates, did not necessarily come into play in the snowball Earth aftermath. However, both processes have the potential to substantially modify the amount of CO_2 in the atmosphere. Their magnitude strongly depends on the uncertain ocean chemistry at the start of the deglaciation. The schematic in Fig. 3.4 summarizes this dependence. A set of different scenarios is possible, depending on the combination of the initial atmospheric CO_2 concentration and the ocean alkalinity. My ICON-ESM simulations only partly cover some of these scenarios, due to the limited range of ocean alkalinity ($2.4 - 15$ mol m^{-3}) and the fixed initial atmospheric CO_2 concentration (13,700 ppm) in the simulations. Nevertheless, the diverse pathways of the atmospheric CO_2 concentration in the different experiments (see Fig. 3.1 and Appendix B) provides an indication of what can be expected in the scenarios.

Scenario 1 At high initial atmospheric CO_2 concentrations and low ocean alkalinity, the transient carbon cycle dynamics in the snowball Earth aftermath are not strong enough to substantially reduce the atmospheric CO_2 concentration. The supergreenhouse climate will therefore persist for hundreds of thousands to millions of years, while continental weathering reduces the greenhouse

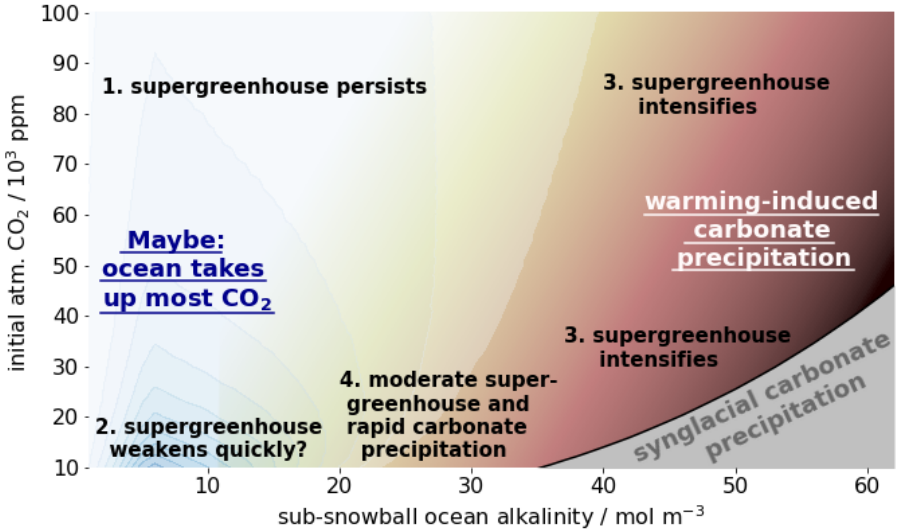

Figure 3.4: Illustration of the possible evolution of the supergreenhouse climate, depending on the uncertain ocean alkalinity and atmospheric CO_2 concentration at the start of the deglaciation. This schematic accounts for the reservoir equilibration effect (blue colors) and the warming-induced inorganic precipitation of carbonates (brown colors). The gray area represents incompatible combinations, where high carbonate saturation states would lead to the inorganic precipitation of carbonates already during the snowball state. The numbers refer to the different scenarios described in the text.

conditions slowly (Le Hir et al., 2008b). No ICON-ESM simulation covers high initial atmospheric CO_2 concentrations, but Exp. 3.1 and Exp. 4 are examples of how the greenhouse conditions are only weakly modified in the absence of the reservoir equilibration effect and the inorganic precipitation of carbonates.

Scenario 2 At low initial atmospheric CO_2 and an alkalinity of around 5-10 mol m^{-3}, the atmospheric CO_2 concentration will be reduced quickly, if the reservoir equilibration effect was strong. This could lead to a rapid end of the supergreenhouse climate within a few thousand years. A fast decline of the strong greenhouse conditions is conceivable also for a broader range of initial conditions, if other processes contribute to the oceanic CO_2 uptake more than they did in my simulations. The ICON-ESM simulations Exp. 1 and Exp. 2 are examples of this scenario. However, if the reservoir equilibration effect was zero, the supergreenhouse climate will likely persist in this scenario as well.

Scenario 3 The supergreenhouse climate will intensify over time, if an alkalinity-rich sub-snowball ocean warms and leads to the inorganic precipitation of carbonates from the water column. This effect is strongest at alkalinities that are higher than those used in my ICON-ESM simulations. Nevertheless, Exp. 3.2 indicates how the atmospheric CO_2 concentration is increased over time by the formation of carbonates.

Scenario 4 A mixed scenario occurs at initial atmospheric CO_2 concentrations of less than 5×10^4 ppm and moderate alkalinity of 15-30 mol m^{-3}. Here, potentially all the

discussed processes are active. The supergreenhouse climate might be moderate, but carbonates are formed readily. The combination of the different effects can lead to an initial reduction and a long-term increase of the atmospheric CO_2 concentration, as it occurs in Exp. 5 of the ICON-ESM simulations.

At this point, it should be asked whether we can exclude scenarios, or whether some scenarios are more likely than others. The existence of Marinoan cap dolostones gives us some insight in this regard. My findings presented in Chapter 2 have reduced the deposition time scale of Marinoan cap dolostones from about 50 kyr to just a few thousand years. This posed a problem, because continental weathering might not be able to provide the required alkalinity in such a short amount of time. In the previous sections, I have presented a solution for this problem, in terms of the warming-induced inorganic precipitation of carbonates from an alkalinity-rich ocean. This tells us that the ocean alkalinity probably had to be above ~ 15 mol m^{-3}, in order to induce the rapid formation of Marinoan cap dolostones. In addition to that, very high ocean alkalinities of > 40 mol m^{-3} might lead to such strong warming-induced outgassing of CO_2 that the resulting CO_2 concentrations are not reconcilable with the proxy record (Kasemann et al., 2005; Bao et al., 2008, 2009). Scenarios 1 and 2 are therefore problematic, as they cannot easily explain the rapid formation of Marinoan cap dolostones. Furthermore, the extreme cases of scenario 3 are also unlikely, due to the implied massive increase of atmospheric CO_2. Nevertheless, even with a reduced range of ocean alkalinity values, both a decline or an intensification of the greenhouse conditions are still possible. I conclude that a scenario for the snowball Earth aftermath that explains the rapid deposition of Marinoan cap dolostones and leads to a moderate supergreenhouse climate is entirely plausible.

4

CONCLUSIONS AND OUTLOOK

The overarching goal of my thesis was to improve our understanding of the Earth system dynamics in the aftermath of the Marinoan snowball Earth. In contrast to previous studies, I used a coupled Earth system model resolving the dynamical circulation of the ocean and the atmosphere. This allowed me to study the transient evolution of the climate, the ocean dynamics and the carbon cycle in the first several thousand years following the start of the deglaciation. At the end of Chapter 1, I laid out the specific research questions addressed in this thesis and discussed their relevance. Here, I provide the answers that I found to these questions, as well as a discussion of their implications and how they fit into the broader context of the snowball Earth hypothesis. Before that, however, I want to take a step back and reflect on a more general value of paleo modeling studies.

4.1 ON THE VALUE OF PALEO STUDIES FOR CLIMATE MODELING

The work presented in this thesis is an example of how climate models can provide helpful insights into the study of past states of our Earth. In this section, I want to turn this around and depict how using climate models for paleo studies also yields value in the opposite direction, in that studies of past climates are helpful for climate modeling as well. Tierney et al. (2020) and FAQ 1.3 of the contribution of working group I to the sixth assessment report of the IPCC (Chen et al., 2021) discuss in detail the scientific value of paleo studies, highlighting, for example, their role in rejecting unusually high climate sensitivities that emerged recently in some climate models (Meehl et al., 2020). My approach here is more personal. I emphasize the value of a paleo study for climate model development, as well as for the student or scientist conducting the study, based on the experience I had with ICON-ESM during the 3.5 years leading up to the writing of this essay.

Studies of paleo climates force modern climate models to "leave their comfort zone", i.e. to simulate conditions that vary substantially from a pre-industrial or a modern control climate. This can have several effects.

1. The unusual conditions and specific needs of the paleo setup might uncover previously hidden model errors (bugs). When I started with ICON-ESM, this was amplified by the fact that ICON was a new modeling framework. Consequently, the number of bugs was numerous, and, in fact, a paleo setup was not necessarily needed to uncover them. Nevertheless, the advantage of a coarse resolution paleo setup is that, through its low computational cost, it allows for extensive testing, making it easier to narrow down the location of the model error and fixing it. Additionally, paleo or idealized setups, such as aqua-planets, often have simpler and unusual boundary conditions that similarly make it easier to locate an existing model bug.

2. Paleo studies often need comprehensive model setups, partly because less information from observations can be provided as boundary condition. This forces the modeler to implement or improve existing model features. For example, to study the snowball Earth aftermath with ICON-ESM, I contributed to the development of a range of model components, such as the interactive carbon cycle, the "z^*" vertical ocean coordinate, a new implementation of sea-ice dynamics and the coupled ICON setup in general. Studies of past climates can combine this technical work with an interesting scientific question.

3. A climate model might become numerically unstable, as more extreme or uncommon conditions arise in the paleo setup. This forces the modeler to improve the stability of the model. While this is not necessarily an advantage for studies of the modern climate, this development, together with those mentioned in the previous points, leads to a reliable, comprehensive, computationally inexpensive and fast climate model. Such a model is valuable for finding model bugs and testing new implementations, but also for teaching and training purposes. The coarse resolution ICON-ESM version I used in this thesis now forms the basis for the model used in the Earth System Modeling School (EaSyMS) at the MPI for Meteorology in Hamburg.

4. The technical work is also valuable for the person developing the model and conducting the simulations. In order to build a comprehensive climate model for paleo studies, the modeler has to get to know the ins and outs of a variety of different model features from a physical as well as from a programming point of view. Additionally, simulating climates different from the modern one provides fascinating insights into the workings of the Earth system. The extensive tuning and testing of a new model setup in particular leads to an understanding of the climate model that is otherwise hard to achieve. More quantifiably, the large amount of technical work pays off for the modeler through his or her participation in technical or scientific publications, resulting from the collaborations that inevitably arise from such a project (Jungclaus et al., 2022; Mathis et al., 2022; Linardakis et al., 2022; Mehlmann and Ramme, in preparation). After all, studying past states of the Earth system with a climate model has a great range of benefits, the last one to mention here being that it is also a lot of fun.

4.2 FILLING THE GAP - ANSWERS TO THE RESEARCH QUESTIONS

In the first part of this thesis, I investigated the transient evolution of the ocean circulation in response to the deglaciation of a snowball Earth and the ensuing supergreenhouse climate. Special attention was given to the strong stratification that develops through the inflow of large amounts of freshwater. Specifically, I addressed the following question:

RQ1. How and over which time scale does the ocean destratify after a snowball Earth?

I have found that the time scale of destratification is just a few thousand years. Even under conditions that are most favorable for a strong stratification, it is unlikely

that a global freshwater layer could persist for more than 10 kyr. A main driver of the destratification is the strong circumpolar current that exists in the northern hemisphere, where continental barriers are missing and mid-latitude westerly winds accelerate the flow. This destratification time scale is substantially shorter than previous estimates of around 50 kyr (Yang et al., 2017). My findings highlight the importance of resolving three-dimensional ocean dynamics, even when studying "simple" global features like the stratification. The most direct consequence that follows from this shortened destratification time scale is that Marinoan cap dolostones must have formed within < 10 kyr from the start of the deglaciation, as they were deposited under the influence of a freshwater layer. The answer to this question therefore also represents a helpful constraint for the evolution of the carbon cycle in the snowball Earth aftermath.

If the temperatures in the snowball Earth aftermath were extremely high, they might have been threatening for the early forms of life that previously adapted to the freezing conditions of a snowball Earth lasting for millions of years (Brocks and Butterfield, 2009; Love et al., 2009; Erwin, 2015). The second research question I posed in this thesis was therefore:

RQ2. What were the temperatures in the supergreenhouse climate?

My simulations with ICON-ESM have shown that the supergreenhouse climate was maybe not as severe as previously thought (Le Hir et al., 2008b; Yang et al., 2017), with global mean surface temperatures possibly as low as 30°C. The novelty of my approach was that I included an ocean general circulation model and considered atmospheric CO_2 concentrations at the lower end of the possible range. Through the inclusion of a dynamical ocean, I could show that especially in the high latitudes moderate temperatures prevail even in the supergreenhouse climate.

Answering my third research question first required an investigation of the processes that impact the carbon cycle in the snowball Earth aftermath and an evaluation of their relative importance. I have shown here that there are indeed processes than can lead to a substantial oceanic uptake of CO_2 from the atmosphere in the first several thousand years after a snowball Earth. These processes are the dilution effect of the freshwater inflow, the biological carbon pump in combination with an enhanced stratification and possibly the equilibration of a depleted ocean that was previously disconnected from the atmosphere. On the other hand, the warming of the ocean induces outgassing through a reduced solubility of CO_2 (hampered by the introduction of a thermal stratification) and the warming-induced inorganic precipitation of carbonates from the water column.

RQ3. How did the supergreenhouse climate evolve?

The overarching answer to this question depends on the uncertain initial conditions at the start of the deglaciation. In fact, the opposing scenarios of either a rapid decline of the supergreenhouse climate or its long-term intensification are both entirely possible. The variety of the scenarios is a consequence of how the ocean regulates the carbon cycle in response to the dynamical evolution of the climate in the snowball Earth aftermath. Considering the implications of my findings for **RQ1.**, I highlight that a rapid deposition of Marinoan cap dolostones and a moderate, possibly even short-lived, supergreenhouse climate are readily achievable with a plausible set of initial conditions for the snowball Earth aftermath.

4.3 THE SNOWBALL EARTH CONTEXT AND OUTLOOK

Thus far, coupled atmosphere-ocean general circulation models (AOGCMs) have only been used in the snowball Earth context to study the initiation and the general plausibility of a snowball Earth (Poulsen et al., 2001; Poulsen and Jacob, 2004; Marotzke and Botzet, 2007; Voigt and Marotzke, 2010; Voigt et al., 2011; Ferreira et al., 2011; Rose, 2015). In that sense, my work complements the research on the snowball Earth hypothesis through the usage of an AOGCM in a study that specifically focuses on the snowball Earth aftermath. Additionally, I added an ocean biogeochemistry model and an interactive carbon cycle component to the AOGCM, a combination which I will refer to here as an Earth system model (ESM). Such an ESM has, in fact, never been applied in any study of the snowball Earth. I have highlighted the added value of such a model already throughout this thesis. Here, I put my results into context and review their relevance for the field of research on the snowball Earth hypothesis. In the end, I briefly discuss potential avenues for future research that may be inspired by this work.

My research has shown that the supergreenhouse climate following the snowball Earth was not as intense as previously expected (Le Hir et al., 2008b; Yang et al., 2017; Hoffman et al., 2017). The extremely warm estimates of global mean temperatures around 50°C are now especially unlikely, whereas the general existence of temperate regions is plausible. Additionally, the greenhouse conditions may have weakened quickly due to an oceanic uptake of CO_2. All these findings indicate that the temperatures in the aftermath of the Marinoan snowball Earth were probably not as threatening for the early forms of life that survived the snowball Earth period. The simulated conditions of the supergreenhouse climate that I have presented here provide helpful boundary conditions for future studies that try to understand the biological and geological evolution during that time.

By showing that the ocean stratification breaks up rapidly after the Marinoan snowball Earth, I have restricted the time scale of cap dolostone deposition to the period of the deglaciation or shortly after that. This corresponds to a reduction of the previous upper bound of 50 kyr (Yang et al., 2017) to very likely less than 10 kyr and possibly just $2-3$ kyr. While this new time scale agrees well with the signs of rapid deposition found in cap dolostones, it means that the mechanism of cap dolostone deposition has to be revisited. It is hard to imagine that continental weathering can deliver all the alkalinity that is required to produce the massive Marinoan cap dolostones within just a few thousand years, if the ocean had not gained any additional alkalinity already during the snowball period. Fortunately, Gernon et al. (2016) introduced shallow ridge volcanism during the snowball period as a process that can do exactly that. In this thesis, I have now shown that indeed the warming of an alkalinity-rich ocean can lead to a rapid and massive inorganic precipitation of carbonates. The results of this thesis therefore make a strong claim for a rapid deposition of Marinoan cap dolostones.

Although the model that I used for this thesis was already very complex, a lot of assumptions and simplifications had to be made. The main shortcomings of my model are the poor representation of the deglaciation process, the flat topography, the missing shelf regions and the omission of continental weathering, to name a few. It is easy to say that an even more complex model that includes all these features

could provide more and better insight into the topic, and this might indeed be the case for some specific questions. At the same time, however, there is a great range of uncertainties coming with the study of a climate from several hundred million years ago. These uncertainties will thwart any attempt to narrow the evolution of the Earth system down to a single pathway. This, however, does not at all mean that modeling studies of the snowball Earth aftermath are of little value. The work of this thesis has shown that there is still much to learn from modeling approaches, as long as the existing uncertainties are acknowledged.

At this point, I want to describe two potential pathways for future research that seem interesting, based on what we learned from the work presented in this thesis. Firstly, the ocean biogeochemistry model HAMOCC that was used here calculates the evolution of many more biogeochemical features than were discussed in this work. A study of the intertwined evolution of ocean anoxia, primary production and other chemical and biological processes in the snowball Earth aftermath could contribute helpful insights into the Neoproterozoic oxidation event and the evolution of life in the post-snowball Earth ocean. A tool like ICON-ESM is a good starting point for such a study, as it already includes many of the necessary processes.

Secondly, I previously mentioned that an ESM has never been used for modeling any part of the snowball Earth cycle so far. Regarding the initiation of a snowball Earth, previous studies mostly estimated the atmospheric CO_2 concentration that is required for triggering the inception of a snowball Earth (e.g. Voigt and Marotzke, 2010; Voigt et al., 2011; Yang et al., 2012; Liu et al., 2018b). They typically find very different values, because of the large number of uncertainties that exist also for the snowball Earth initiation, and because of the many different models and process parameterizations that further induce variability. My work has shown that we can improve our understanding of a range of different carbon cycle processes by using an ESM that includes an interactive carbon cycle. In that sense, a study with an ESM could lead to an improved understanding of the dynamical processes relevant during snowball Earth inception, while being less dependent on existing uncertainties.

Apart from the scientific contributions discussed here, I hope that this thesis has shown that ESMs are a useful tool for studying past, but also present and future states of the Earth system. The work presented in this thesis highlights that ocean biogeochemistry has an overarching control on the evolution of the Earth system under a changing climate on time scales of hundreds to thousands of years. The carbon cycle dynamics discussed in Chapter 3 are a telling example of how different carbon cycle processes interact and compensate each other, and how even the sign of the air-sea CO_2 flux can change over time, as the dominance hierarchy between the processes shifts. This serves as a reminder that the ocean is not necessarily a reliable sink for anthropogenic CO_2 under current climate change.

In this thesis, I investigated the dynamics of the ocean circulation and the carbon cycle in the aftermath of a snowball Earth. The work presented here has confined the time scales of ocean destratification and the possible conditions in the supergreenhouse climate. At the same time, this thesis also demonstrated that the evolution of the Earth system after the Marinoan snowball Earth could have followed very different scenarios, depending on the uncertain conditions at the start of the deglaciation.

Part II

APPENDICES

A

CLIMATE AND OCEAN CIRCULATION IN THE AFTERMATH OF A MARINOAN SNOWBALL EARTH

The work in this appendix has been published as:

Ramme, L. and Marotzke, J.: Climate and ocean circulation in the aftermath of a Marinoan snowball Earth, *Clim. Past*, 18, 759–774, https://doi.org/10.5194/cp-18-759-2022, 2022.

AUTHOR CONTRIBUTION

LR and JM designed the study. LR conducted the model simulations, performed the analysis and prepared the first draft of the manuscript. JM supervised the study. Both authors contributed to the scientific discussion and the writing of the manuscript.

CODE AND DATA AVAILABILITY

The model code of the specific setup used in this study, as well as model input, post-processed data and scripts used for the analysis and producing the figures, can be obtained from the Climate and Environmental Retrieval and Archive (CERA) of the World Data Center for Climate (WDCC) (Ramme, 2021).

Climate and ocean circulation in the aftermath of a Marinoan snowball Earth

Lennart Ramme[1,2] **and Jochem Marotzke**[1,3]

[1] Max-Planck-Institute for Meteorology, Hamburg, Germany
[2] International Max Planck Research School on Earth System Modelling, Hamburg, Germany
[3] Center for Earth System Research and Sustainability (CEN), Universität Hamburg, Germany

Received: 9 December 2021 - Discussion started: 20 December 2021 - Revised: 14 March 2022 - Accepted: 15 March 2022 - Published: 12 April 2022

ABSTRACT

When a snowball Earth deglaciates through a very high atmospheric CO_2 concentration, the resulting inflow of freshwater leads to a stably stratified ocean, and the strong greenhouse conditions drive the climate into a very warm state. Here, we use a coupled atmosphere-ocean general circulation model, applying different scenarios for the evolution of atmospheric CO_2, to conduct the first simulation of the climate and the three-dimensional ocean circulation in the aftermath of the Marinoan snowball Earth. The simulations show that the strong freshwater stratification breaks up on a timescale in the order of 10^3 years, mostly independent of the applied CO_2 scenario. This is driven by the upwelling of salty waters in high latitudes, mainly the northern hemisphere, where a strong circumpolar current dominates the circulation. In the warmest CO_2 scenario, the simulated Marinoan supergreenhouse climate reaches a global mean surface temperature of about 30°C under an atmospheric CO_2 concentration of 15×10^3 parts per million by volume, which is a moderate temperature compared to previous estimates. Consequently, the thermal expansion of seawater causes a sea-level rise of only 8 m, with most of it occurring during the first 3000 years. Our results imply that the surface temperatures of that time were potentially not as threatening for early metazoa as previously assumed. Furthermore, the short destratification timescale found in this study implies that Marinoan cap dolostones accumulated during the deglacial period, given that they were deposited under the influence of a freshwater environment.

A.1 INTRODUCTION

We apply a coupled atmosphere-ocean general circulation model (AOGCM) to study the transient period after the deglaciation of the Marinoan snowball Earth, including, for the first time, the three-dimensional ocean circulation. In contrast to the well studied snowball Earth climate and its initiation e.g. Poulsen and Jacob, 2004; Voigt et al., 2011; Fiorella and Poulsen, 2013; Abbot et al., 2012, 2013, the processes during the supergreenhouse aftermath are much less understood. Cap dolostone formations show signs of rapid accumulation (Allen and Hoffman, 2005; Hoffman, 2011), but also hold magnetic reversals indicating much longer accumulation times (Trindade et al., 2003; Font et al., 2010). At the same time, the hot climate, together with the physical and geochemical state of the ocean, could be severe for early metazoa, which possibly developed prior to the Marinoan snowball Earth (Dohrmann and Wörheide, 2017; Turner, 2021). For a better understanding of Earth's geological and biological record, an improved knowledge about the climate after the Marinoan snowball Earth is necessary.

The Marinoan snowball Earth was terminated around 635 million years ago (Ma) and had a duration of 5–15 million years (Kendall et al., 2006; Calver et al., 2013; Prave et al., 2016). During the globally frozen state kilometer-scale continental ice sheets and a several hundred meter, up to one kilometer, thick sea glacier formed (Hoffman, 2011; Abbot et al., 2013). Beneath this global ice cover the ocean was hypersaline, geochemically evolved through ridge volcanism and well mixed (Le Hir et al., 2008a; Gernon et al., 2016; Ashkenazy et al., 2013). The subsequent transition from the cold snowball to a warm greenhouse climate was rapid and globally synchronous, as can be inferred from the sharp contact between the glacial deposits of the panglacial state and the overlying carbonate formations (Kennedy, 1996; Hoffman et al., 1998; Calver et al., 2013; Hoffman, 2011). The deglaciation causes a strong stratification in which the freshwater of the molten ice caps overlies the cold and salty waters of the snowball Earth ocean (Shields, 2005). The stratification is then further increased by the rapid warming of the surface layer, as a strong greenhouse climate develops. The partial pressure of CO_2 is expected to have reached 0.01-0.1 bar at the end of the Marinoan snowball Earth (Kasemann et al., 2005; Le Hir et al., 2008c; Abbot et al., 2012), promoting very high temperatures in its aftermath.

In this study, we simulate the full transition from a globally frozen ocean into a supergreenhouse climate with an AOGCM including the Marinoan topography. The focus will be on the evolution of the global parameters of climate and ocean circulation. Yang et al. (2017) use a one-dimensional vertical mixing model to provide a first estimate of the destratification timescale of a strongly stratified ocean after a snowball Earth. However, including a temporally and spatially variable surface forcing and three-dimensional ocean dynamics can influence the outcome substantially. Furthermore, we conduct a set of sensitivity experiments, encompassing scenarios from very fast to no atmospheric CO_2 removal, to acknowledge the uncertain temporal evolution of the atmospheric CO_2 concentration (Le Hir et al., 2008b). Hence, we aim to give a first order estimate of possible scenarios for the ocean circulation and the prevailing climatic conditions in the aftermath of the Marinoan snowball Earth.

In the following section we describe the model used in our study and the adaptions that were made to create the Marinoan setup. Section A.3 then gives an overview

over the experimental strategy, and in Sec. A.4 we describe characteristics of the Marinoan control climate and the transition into and out of the snowball Earth. The transient response of the ocean in the aftermath of a snowball Earth is presented in Sec. A.5, and the ensuing supergreenhouse climate is described in Sec. A.6. We discuss the implications of our findings with respect to the climatic conditions and the ocean destratification process in Sec. A.7, before a conclusion is provided in Sec. A.8.

A.2 METHODS

A.2.1 *Model*

We use the icosahedral nonhydrostatic Earth system model (ICON-ESM), which couples the atmosphere general circulation model (AGCM) ICON-A to the ocean general circulation model (OGCM) ICON-O through the YAC coupler (Hanke et al., 2016). A specialty of the ICON model family is the unstructured grid consisting of triangles with quasi-uniform cell area. This allows us to flexibly adapt boundary conditions as the convergence of longitudes at the poles has no impact on the grid.

Giorgetta et al. (2018) and Crueger et al. (2018) give a detailed description of the atmospheric component ICON-A, and the implementation of the nonhydrostatic dynamical core on the icosahedral grid is described in Zängl et al. (2015). The atmosphere grid used in this study has a nominal mean horizontal resolution of 315.6 km and is divided into 47 levels reaching to a height of 83 km. The vertical spacing of levels increases with height, and lower levels follow the topography (Giorgetta et al., 2018). ICON-A has inherited its physics, that is, the parameterization of physical processes, from the well established AGCM ECHAM (Giorgetta et al., 2013) which, on its own or as part of a coupled AOGCM, has already been used in earlier studies on the snowball Earth (Marotzke and Botzet, 2007; Voigt and Marotzke, 2010; Voigt et al., 2011; Abbot et al., 2012).

The implementation of the primitive equations of the ocean on the ICON grid is described in Korn (2017). The nominal mean horizontal resolution of the ocean grid is 157.8 km with 35 vertical levels of increasing thickness with depth. The model uses a rescaled vertical "z^*" coordinate that follows the surface elevation and allows sea ice to become thicker than the first ocean layer (Campin et al., 2008). Eddy-induced transport is parameterized following Gent et al. (1995), and isopycnal mixing is described based on the formulation by Redi (1982). Both apply a constant diffusion coefficient of 1000 $m^2\ s^{-1}$. For vertical mixing we use the approach of Gaspar et al. (1990), which relates the vertical diffusivity parameter to the turbulent kinetic energy (TKE). The resulting vertical diffusivities are inversely proportional to the Brunt-Vaïsala frequency, so that the scheme is accounting for the inhibiting effect of stratification on vertical mixing. The parameters of this scheme are calibrated in order to achieve a good ocean circulation in a pre-industrial control simulation. Thereby, the minimum available TKE $\bar{e}_{min}$ and the calibration constant c_k are increased by factors of four and five respectively, compared to the values in Gaspar et al. (1990).

The freezing point of seawater is -1.8°C in our model, and sea ice is assumed to have a constant salinity of 5 psu. Sea-ice dynamics are included in the control simulation and during the snowball initiation as well as the greenhouse climate

after the snowball Earth. However, they are turned off during the period of global glaciation, because the current implementation of sea-ice dynamics is not suited for simulating the dynamics of a globally frozen ocean with large gradients in ice thickness. Sea-ice thermodynamics follow the 0-layer formulation by Semtner (1976) which has only three prognostic variables: ice thickness, snow thickness and surface temperature. The albedo of sea ice increases nonlinearly from 0.65 at 0°C to a maximum value of 0.7 at lower temperatures. Sea ice is considered snow-covered if the water equivalent of the snow depth exceeds 0.01 m, and the albedo of snow on sea ice increases from 0.7 at 0°C to a maximum of 0.85. The comparably high albedos of sea ice and snow follow from the formulation of sea-ice thermodynamics. They are set in a way to improve the sea ice distribution of the pre-industrial control simulation and to allow snowball initiation and melting at appropriate CO_2 concentrations.

The model is run with different time steps for the atmosphere, ocean and radiation components. The physical parameterizations of the atmosphere use a step size of 15 minutes, but the dynamical core performs ten substeps for every physics calculation. The ocean component uses a time step of 60 minutes, and the coupling between atmosphere and ocean is done after every ocean time step. The radiation is calculated every 120 minutes. When the melting of the snowball Earth is initiated, the atmosphere and radiation time steps are reduced, and stratospheric damping parameters are adapted to ensure numerical stability. During this phase, the atmosphere component uses a time step of 12 minutes with 12 substeps of the dynamical core, and the radiation is calculated every 48 minutes. The ocean and coupling time steps are set to 48 minutes accordingly. Once sea ice has retreated and the model has warmed sufficiently, time steps and damping parameters are set back to normal values.

The performance of ICON-ESM in a higher resolution setup has recently been evaluated by Jungclaus et al. (2022). The lower resolution used here produces similar but generally larger biases when simulating a pre-industrial climate. Characteristics of our pre-industrial control simulation are a strong overturning circulation and warm biases in upwelling regions and the Southern Ocean.

A.2.2 *Marinoan setup*

Based on the reconstructions of Li et al. (2013, Fig. 6) and Merdith et al. (2017, Fig. 11, 12), we adapted the distribution of continents for the time of the Marinoan snowball Earth (Fig. A.1). Continents are set to have a flat topography of 300 m above sea level. The ocean has a uniform depth of 3500 m, so that the total ocean volume is similar to the volume of the present-day oceans. This simplified topography is a first order approximation of the Marinoan conditions, but it is sufficient for the focus of this paper, which is on global transitions of the climate and the large scale ocean circulation

The land surface has uniform values with no vegetation, glaciers or lakes prescribed. Soil parameters are close to the values of sandy loam, and the surface albedo of land is chosen in a way that the background albedo of the Earth's surface is close to its present-day value. River runoff is distributed over all coastal grid cells weighted by latitude, with maximum runoff at the equator.

Figure A.1: Topography of the Marinoan setup. Land areas (dark grey) have an elevation of 300 m above sea level and the ocean (white) has a depth of 3500 m. The distribution of continents follows Li et al. (2013) and Merdith et al. (2017) and is simplified in a sense that closely located cratons are summarized in larger continental areas. The continents include the following cratons, 1: Australia, India and other, 2: Congo and other, 3: Kalahari and Rio Plata, 4: West Africa and other, 5: Laurentia and other, 6: Siberia, 7: North China.

We use a linear parameterization of ozone photochemistry (Cariolle and Teyssedre, 2007), which allows the distribution of ozone to follow the changing height of the troposphere. No aerosols are prescribed, and a constant orbit of the year 1850 C.E. is used, similar to the pre-industrial control simulation. Total solar irradiance is reduced to 95% of the present-day value to account for the weaker sun of the late Neoproterozoic (Gough, 1981). Water vapour and CO_2 are the only greenhouse gases, and the atmospheric CO_2 concentration is set to 1500 parts per million by volume (ppmv) in the control run, to create a control state with a global mean temperature comparable to the pre-industrial climate.

The Marinoan setup is initialized from a state of an earlier model version that included shelf regions and was spun-up for 3000 years starting from a homogeneous state at 5°C and a salinity of 34.3 psu. After the adaption of the ocean bottom topography, the model is run for another 1000 years until a stable climate is reached. The last 100 years of this simulation serve as the Marinoan control climate.

A.3 EXPERIMENTAL DESIGN

Our experiments are a continuous simulation from a control climate into a snowball Earth and subsequently into a strong greenhouse climate. Both transitions are induced through modulating the atmospheric CO_2 concentration. All simulations are summarized in table A.1.

Starting from the end of the control simulation, the CO_2 concentration is reduced to 10 ppmv in INIT to create a global glaciation. In order to achieve an ice thickness representative of the large sea glaciers of a "hard" snowball Earth, it would be necessary to integrate the model over several thousand years, and the following melting period would similarly require a very long simulation. Additionally, in our model setup no equilibrated snowball state could be achieved due to the missing

Table A.1: Prescribed CO_2 forcings for the set of simulations presented in this study. In scenario SC-CONST the CO_2 concentration is reduced stepwise to 18, 17, 16 and 15 $\times 10^3$ ppmv in years 4800, 6400, 7600 and 7940 to avoid model instability at too high temperatures. Similarly, there are stepwise reductions to 17 and 15 $\times 10^3$ ppmv in years 4600 and 7290 in SC-CONST-TKE.

name	years	CO_2 concentration
CONTROL	0–4000	1500 ppmv
INIT	4000–4300	10 ppmv
MELT[a]	4300–4600	20×10^3 ppmv
SC-CONST	4600–10,500	20–15$\times10^3$ ppmv
SC-SLOW	4600–10,500	0.05% annual decay
SC-FAST	4600–7000	1% annual decay
SC-CONST-TKE[a]	4500–10,500	20–15$\times10^3$ ppmv

[a]The salinity field is simplified to a two layer case in year 4500

implementation of geothermal heat flux. Therefore, we instead let the model create an only moderately thick layer of sea ice within 300 years, and already then initiate the deglaciation through an increased CO_2 concentration of 20×10^3 ppmv in MELT.

An atmospheric CO_2 concentration of 20×10^3 ppmv is within the 10^4–10^5 ppmv range of estimates for the aftermath of the Marinoan snowball Earth (Kasemann et al., 2005; Bao et al., 2008; Abbot et al., 2012). However, it is important to stress that this value is mainly a feature of the formulation of sea-ice thermodynamics and the albedos of ice and snow in our model. The impact of these parameters on snowball Earth dynamics was extensively discussed in the literature (Lewis et al., 2006; Abbot et al., 2010; Abbot and Pierrehumbert, 2010), and a much more sophisticated sea-ice and glacier model is needed for a reliable estimate of the snowball Earth deglaciation threshold (Abbot et al., 2010).

Two hundred years after the onset of deglaciation, when sea-ice extent has retreated to about 35% of the ocean area, the salinity distribution is modified manually to represent a much stronger stratification: In the first 23 levels, containing the upper 1020 m of the water column, salinity is set to a uniform value of 5 psu, whereas in the 12 lower levels, or 2480 m, the concentration is set to about 46.7 psu. Here, the salinity of the freshwater layer corresponds to the fixed salinity of sea ice used in our model, and the salinity of the brine layer is calculated so that the total amount of salt in the ocean stays the same. The distribution of temperature and all other parameters remains unchanged. This procedure avoids long integration times and potential numerical instabilities caused by large gradients in ice thickness.

Benn et al. (2015) estimate the volume of continental ice sheets to be around 170 million km^3 for CO_2 concentrations below 20×10^3 ppmv, which would translate into an oceanic freshwater layer of roughly 400 m thickness. This is 40% of the thickness of the freshwater layer applied in our study, and the freshwater amount would be even smaller for a higher CO_2 deglaciation threshold (Benn et al., 2015). Adding to that the uncertain freshwater amount of roughly 500–1500 m coming from melting sea glaciers (Tziperman et al., 2012; Abbot et al., 2013), we argue that the freshwater layer thickness used in our study is plausible, though potentially at the lower end

of possible thicknesses. As a consequence, the simulated destratification timescales could indeed be prolonged if the initial amount of freshwater was larger, and the continuous melting of land glaciers would keep surface salinities low for a longer time. However, this is counteracted by the two-layer assumption of the salinity field, which is a highly idealized scenario and more extreme than a possible stratification after the Marinoan snowball Earth. A less extreme scenario for the vertical salinity distribution could reduce the stratification timescale again.

After the adaption of the salinity distribution, the deglaciation run MELT is continued for another 100 years before the simulation is divided into three different scenarios. These scenarios are chosen to cover a broad range of possible evolutions of the atmospheric CO_2 concentration, going from no removal to an extremely rapid removal of CO_2. This procedure is motivated by the unknown contribution of the oceanic CO_2 uptake, which, in contrast to the long-term removal through continental weathering (Le Hir et al., 2008b), could cause a substantial reduction in the atmospheric CO_2 concentration on a timescale of several 10^3 years, depending on the CO_2 saturation state of the subglacial ocean (Le Hir et al., 2008c).

In the first scenario ("SC-CONST") the atmospheric concentration of CO_2 is kept constant at a high value. This scenario represents the case of maximum warming and no significant CO_2 uptake by either land or ocean. However, as the model is prone to numerical instabilities at too high temperatures, the CO_2 concentration is reduced in several steps from 20 to 15×10^3 ppmv. The scenario "SC-SLOW" deploys an exponential decay of 0.05 % per year and thereby emulates a modest removal of CO_2 from the atmosphere. This exponential decay is increased to 1 % per year in the scenario "SC-FAST" which serves as an extreme case of quick CO_2 removal. In SC-SLOW and SC-FAST the exponential decay of the atmospheric CO_2 concentration stops when the value used in CONTROL is reached, which happens in years 9780 and 4858, respectively.

In addition to the three scenarios with distinctive CO_2 concentration pathways, we conduct the experiment "SC-CONST-TKE", which follows a similar CO_2 pathway as SC-CONST, but uses different settings in the TKE scheme. Hence, this simulation serves us to test the robustness of our results with respect to vertical mixing. In this experiment the parameters of the vertical mixing scheme are set to the standard values suggested by Gaspar et al. (1990). The minimum available TKE is $\bar{e}_{min} = 10^{-6}$ m^{-2} s^{-2}, and the calibration constant is $c_k = 0.1$, implying much weaker vertical mixing. We note that when we use the smaller values of Gaspar et al. (1990) in a simulation with present-day continents, it leads to a complete breakdown of the Atlantic Meridional Overturning Circulation, and those parameters were specifically increased to reduce the bias between observations and the model simulation. SC-CONST-TKE starts at the time where the salinity distribution is adapted in MELT and is, similar to the other scenarios, stopped when the climate approaches an equilibrium.

A.4 CONTROL CLIMATE AND SNOWBALL PERIOD

Since the Neoproterozoic atmospheric CO_2 concentration is only loosely constrained (Hoffman et al., 1998), we here choose 1500 ppmv for the Marinoan control climate, because this leads to a global mean 2 m air temperature (from here on referred to

Table A.2: Comparison of the Marinoan control climate (CONTROL, CO_2 = 1500 ppmv, CH_4 = 0 ppmv, N_2O = 0 ppmv) and the pre-industrial control simulation with present-day continents (PI, CO_2 = 284 ppmv, CH_4 = 0.808 ppmv, N_2O = 0.273 ppmv). The total solar irradiance is reduced to 95% of its present-day strength in the Marinoan configuration. Both columns represent data averaged over 100 years.

	CONTROL	PI
GSAT (°C)	13.4	13.9
mean sea surface temperature (°C)	15.3	19.1
mean sea surface salinity (psu)	34.2	34.6
mean ocean potential temperature (°C)	1.9	3.8
sea-ice extent (10^6 km^2)	23.0	12.5
sea-ice volume (km^3)	19,519	32,050

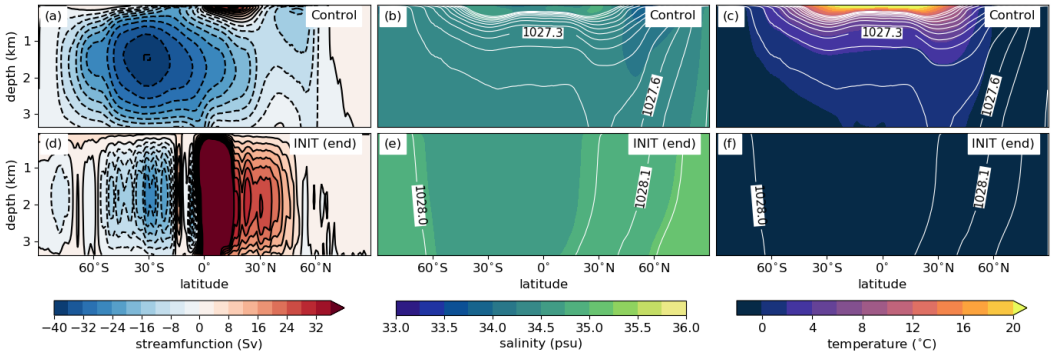

Figure A.2: Zonal averages of ocean properties from the Marinoan control climate (upper panels) and the end of the snowball initiation simulation INIT (averaged over the last 30 years, lower panels). The left colum shows the meridional overturning circulation, where negative values and blue colors refer to an anti-clockwise circulation. The middle and right column show salinity and potential temperature, respectively. The white contours represent isolines of potential density in intervals of 0.1 kg m^{-3} for densities above 1026.5 kg m^{-3}.

as GSAT) comparable to that of the pre-industrial control simulation, despite the weaker solar forcing. While the GSAT of the Marinoan control climate is similar to the pre-industrial one, sea surface temperatures are substantially lower (Tab. A.2). This is a consequence of the larger continental area in low latitudes. Furthermore, temperatures are below 0°C in large parts of the Marinoan deep ocean (Fig. A.2 (c)), making it colder than the pre-industrial deep ocean and causing a weaker resistance towards global glaciation due to the smaller thermal inertia. The deep waters of the ocean are formed at the south pole, where the waters sink to the ocean bottom during the austral winter. Additionally, convection occurs in both hemispheres along the sea-ice boundary. In the northern hemisphere there are no continents north of 51°N, leading to an extended sea-ice area with large seasonal fluctuations. The meridional overturning circulation (MOC) of the control climate, shown in Fig. A.2 (a), is characterized by a large cell with deep waters flowing northward along the ocean bottom from the deep water formation regions close to the south pole to

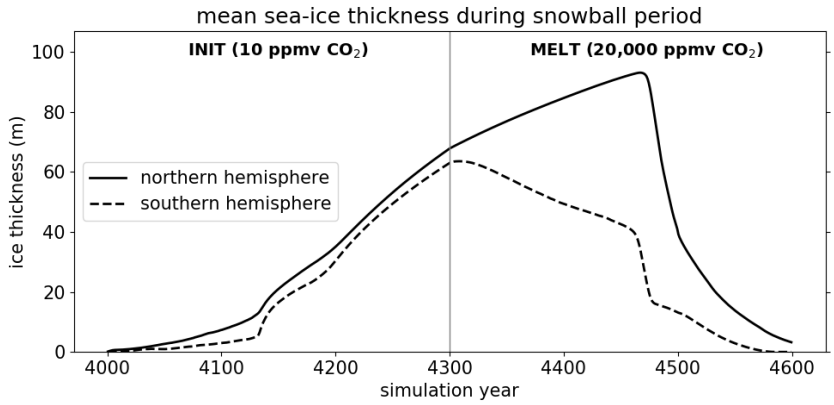

Figure A.3: Evolution of the mean sea-ice thickness in the hemispheres during the snowball period. The vertical line denotes the transition from a low CO_2 concentration in INIT to a high CO_2 concentrations in MELT.

a circumpolar current at 60°N. The single-celled shape of the Marinoan MOC is different from that of the present-day MOC, which consists of two counter-rotating cells. This is because in the present-day oceans the deep waters are formed in both hemispheres and with different density properties. In contrast to that, the location of continents in the Marinoan setup seems to favor deep water formation only at the south pole, and the flat ocean bottom allows those waters to penetrate far into the northern hemisphere, hindering the formation of deep waters there.

The northern circumpolar current of the Marinoan control climate has a transport of around 960 Sv and is therefore an important component of the ocean circulation. The relative strength of this flow, compared to the present-day Antarctic Circumpolar Current (ACC), is a consequence of the missing continental barriers north of 51°N and the weak bottom drag due to the flat ocean bathymetry. In a more realistic setup, including bathymetric features and a higher horizontal resolution, the circumpolar current would be slowed down substantially by topographic form stress and the downward momentum transport through eddies (Wolff et al., 1991). However, even though the circumpolar current is likely too strong in our simulation, the continental reconstructions of Li et al. (2013) and Merdith et al. (2017) are clear in that probably no continents were located north of 60°N. The existence of a circumpolar current, potentially stronger than the present-day ACC, is therefore conceivable. We will return to the influence of the circumpolar current on our model results during the discussion in Sec. A.7.3.

After the initial reduction of the atmospheric CO_2 concentration to 10 ppmv in run INIT, it takes 134 years until the sea ice covers more than 95% of the ocean surface area. The sea ice then quickly grows in vertical direction (Fig. A.3), and at the end of the 300-year long freezing period it reaches a global mean ice thickness of 65.6 m. The thickest sea ice can be found at the poles with 84 m in the southern hemisphere and up to 102 m in the northern hemisphere, while the thinnest ice is located in the subtropics and tropics with thicknesses between 50 m and 65 m in most parts.

The ocean under the ice cover (Fig. A.2 (d-f)) is well mixed and has a temperature of -1.8°C, the minimum value allowed in our model. Density largely follows the latitudinal variation of the salinity field, as differences in melting and freezing of sea ice create a gradient between the equator and the poles. This state of the ocean resembles the patterns found in earlier studies of the snowball Earth ocean (Ferreira et al., 2011; Ashkenazy et al., 2013). Differences can be attributed to model features like the coarse resolution, the missing geothermal heat flux and especially the transient character of the solution that is shown here.

When the atmospheric CO_2 concentration is increased in MELT, the global ice volume initially continues to grow in the northern hemisphere. A strong asymmetry between the hemispheres develops, with decreasing ice thickness in the subtropics of the southern hemisphere, mainly next to the western coast of the continents, and increasing or constant ice thickness in other regions. In year 4463, 163 years after the start of MELT, sea-ice cover falls below 95% of the ocean area and a rapid deglaciation sets in.

In year 4500 of MELT, when the salinity distribution of the water column is adapted to the two-layer case described in Sec. A.3, sea-ice cover has retreated to 34% of the ocean area and GSAT has reached 2.5°C. The adaption of the salinity field slows down the warming and the ice retreat in the first years, but then leads to a faster warming of the surface layer, as less cold waters reach the surface from the deep. One hundred years later, at the end of MELT, GSAT has already reached 22.6°C, and sea-ice cover has decreased to less than 5%.

A.5 TEMPORAL EVOLUTION OF CLIMATE AND OCEAN CIRCULATION IN THE SNOWBALL EARTH AFTERMATH

We now provide a description of the transient response of the climate and the ocean circulation to the different scenarios. Naturally, a CO_2 pathway that keeps the greenhouse conditions intact for a longer time will cause more warming than a fast CO_2 decrease, which is apparent in Fig. A.4 (a). As the climate is already very warm at the end of MELT in year 4600, the start of the 1% annual decay scenario SC-FAST causes the surface to start to cool within a few decades. From there on, a rapid cooling takes place and the surface temperature reaches the value of the control climate within 400 years from the start of SC-FAST, approximately 140 years after the CO_2 concentration reached the value of the control simulation. The surface then cools further, because the continuously low surface salinity promotes the formation of sea ice and the deep ocean is still cold. By contrast, the annual CO_2 reduction in SC-SLOW is much smaller. Here, the surface climate continues to warm for 160 years before the CO_2-induced cooling becomes visible. The warming of the global ocean persists for almost 2000 years. In SC-CONST the four individual CO_2 reductions, necessary to keep the model numerically stable, are visible as sudden drops in the surface temperature evolution. The first reduction in year 4800 stops the initial strong warming trend and a slow surface cooling sets in. However, the deep ocean keeps heating up, which causes a second phase of surface warming between years 5600 and 7600, where at the end the CO_2 concentration had to be reduced again. Afterwards, the warming of the surface, as well as the deep ocean, continues at a slower, decelerating pace.

The sea-level change due to the thermal expansion of the warming ocean largely follows the evolution of the mean ocean temperature (Fig. A.4 (b)). As our model does not include ice sheets on land, we cannot give an estimate about the much larger sea-level change from melting land glaciers. When in the following the terms sea-level rise or sea-level change are used, we therefore only refer to the change resulting from the thermal expansion of seawater. We derive the global mean sea-level rise on annual mean data by calculating the thermal expansion of each grid box from one year to the next using the formula from McDougall (1987). The individual values are then stacked up vertically and averaged horizontally to arrive at the global mean sea-level rise. During the 300 years of deglaciation in MELT, the thermal expansion of seawater already leads to a sea-level change of 1.2 m. In the fast CO_2 reduction pathway SC-FAST, however, the further sea-level change is small, as the deep ocean only warms slightly and the surface cools again. When applying the intermediate scenario SC-SLOW, the total sea-level rise since the deglaciation reaches a maximum of 3.3 m around year 6600, before the sea level drops again. Lastly, in SC-CONST the sea level continues to rise over the whole simulation, but the speed of the increase slows down, influenced also by the stepwise CO_2 reductions. At the end of the simulation, this increase has added up to 8 m, and a small trend of +0.2 mm per year is still visible.

The evolution of the ocean meridional overturning circulation (MOC), salinity and temperature are illustrated in Fig. A.5 for five different times during the scenario SC-CONST. The MOC of the control climate (see Fig. A.2 (a)) is dominated by a large anti-clockwise cell between 80°S and 30°N. However, directly after the melting of the snowball Earth, and after the adaption of the salinity field, this dominant cell is gone in all scenarios. Instead, there are distinct cells in the freshwater and the brine layer. All scenarios show a similar initial evolution of the MOC in the first 1000 years after the deglaciation and ultimately a recovery of the dominant anti-clockwise cell (Fig. A.6(a)). This recovery is rapid and occurs over a few hundred years in SC-FAST; it is slower in SC-SLOW, where there is an overshoot in the overturning strength before the circulation approaches the control state. In SC-CONST the MOC recovers gradually over a timescale of more than 2000 years and never reaches the strength of the control climate.

Potential temperature and salinity sections show that the break-up of the stratification starts in the high latitudes, especially in the northern hemisphere (Fig. A.5). Here, the isolines of density, which closely follow those of salinity in the first 1500 years, are sloping polewards under the influence of the strong circumpolar current. While the haline stratification is broken up, the whole ocean keeps warming, and even the deep ocean eventually arrives at temperatures of over 10°C in most areas. Only in the region of the circumpolar current do temperature and salinity decrease northwards and exhibit almost no vertical variation when the climate and the circulation have stabilized at the end of the simulation.

Circumpolar currents are an important feature when considering ocean destratification, as they are associated with exchange between surface waters and the deep ocean through deep Ekman cells. Figure A.5 shows that the largest initial deviation from the horizontally layered salinity field is through upwelling of salty waters northwards of 60°N, which occurs in all scenarios. To quantify the strength of the circumpolar current located there, we calculate the flux through a meridional section

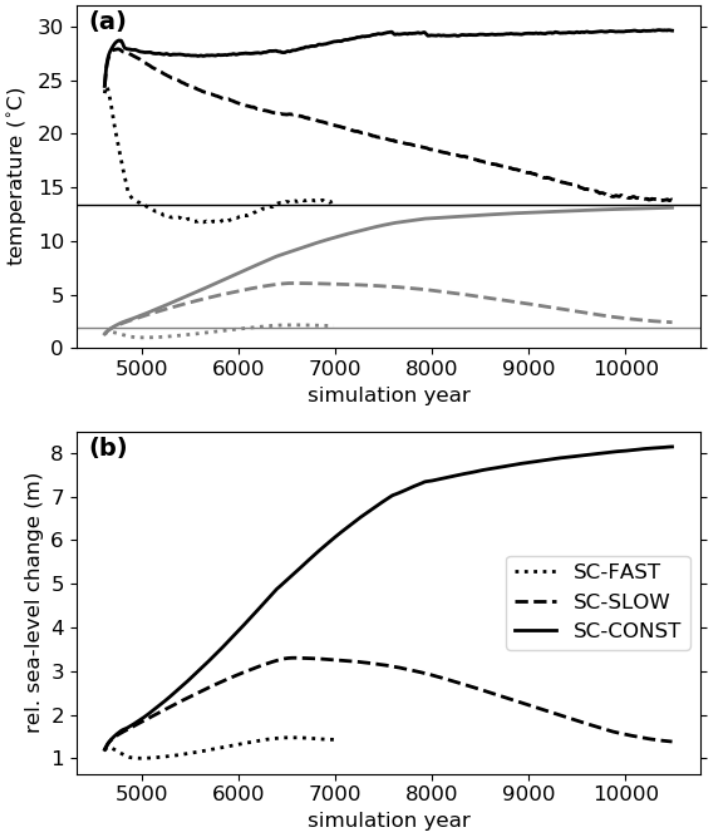

Figure A.4: Temporal evolution of **(a)** global mean 2 m air temperature (black) and ocean mean potential temperature (grey) and **(b)** relative sea-level change due to thermal expansion with respect to the starting point of each scenario. All plots show 30 year running means. The horizontal lines depict the value of the Marinoan control climate.

between the north pole and the northern tip of the conglomerate combining the Australian, Indian and other cratons (Fig. A.6 (b)). After an initial phase of about 500 years, where the model adapts to the idealized two-layer salinity field, the circumpolar current in SC-FAST approaches the strength it has in the control climate. It accelerates much quicker in SC-SLOW and SC-CONST, where the higher surface temperatures cause a strengthening and a shift of the westerly winds to higher latitudes, intensifying the surface drag (described in Sec. A.6). We elaborate on the implications that an overestimation of the current strength has on the inferred destratification timescales in Sec. A.7.3.

Next, we investigate the impact of the CO_2 pathway on the ocean stratification. As a first order approach, the strength of the ocean stratification can be determined from the density difference between the surface and the ocean bottom. Therefore, we calculate the horizontal means of salinity and temperature in the surface and bottom layer of our model. These values can then be used to divide the stratification into a thermal and a haline component, which are shown in Fig. A.6 (c) and (d). The thermal component should follow the CO_2 pathway more directly, while the haline component could give insight into whether certain CO_2 pathways accelerate or decelerate the break-up of the imposed freshwater stratification. At the start of the

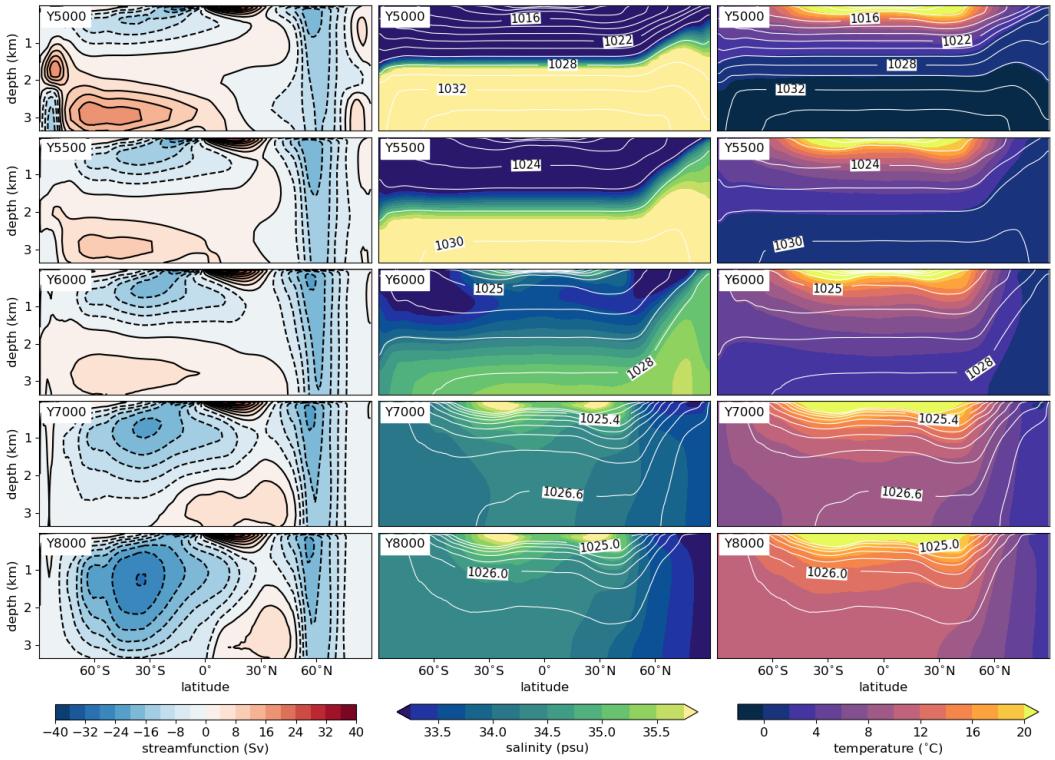

Figure A.5: Zonally averaged streamfunction (left), salinity (middle) and potential temperature (right) for five representative times during the strong warming scenario SC-CONST, depicted by 30 year averages around the given timestamp. Positive MOC values represent a clockwise circulation. Figure settings and color intervals are the same as in Fig. A.2. Contours of potential density are shown in intervals of 2 kg m^{-3} in the two upper rows, in intervals of 1 kg m^{-3} in the third row and in intervals of 0.2 kg m^{-3} for densities above 1025 kg m^{-3} in the two lower rows.

scenarios in year 4600, the haline stratification is more than ten times stronger than the thermal component, with values of 30 and 2.3 kg m^{-3}, respectively. The thermal component of the stratification then closely follows the evolution of the surface temperature (see Fig. A.4 (a)), with large differences between the scenarios and the strongest stratification in SC-CONST. In contrast to that, the haline stratification drops from 30 to 0.8 kg m^{-3} within 1500 years from the start of the scenarios and is mostly independent of the applied CO_2 pathway.

Lastly, we quantify the impact of the parameterized vertical mixing on the destratification timescale through the simulation SC-CONST-TKE. This simulation follows a similar CO_2 pathway as SC-CONST, but applies much weaker vertical mixing, as described in Sec. A.3. Figure A.7 shows the surface salinity 500 years after the insertion of the idealized salinity field for the simulations SC-CONST (a) and SC-CONST-TKE (b). Indeed, surface salinities in that year are approximately 10 psu smaller in SC-CONST-TKE than in SC-CONST, but also here the stratification break-up is driven from the high latitudes, and SC-CONST-TKE reaches surfaces salinities of 20 psu only about 500 years later than SC-CONST. Hence, a weaker parameterized vertical mixing can partly delay the stratification break-up, but it

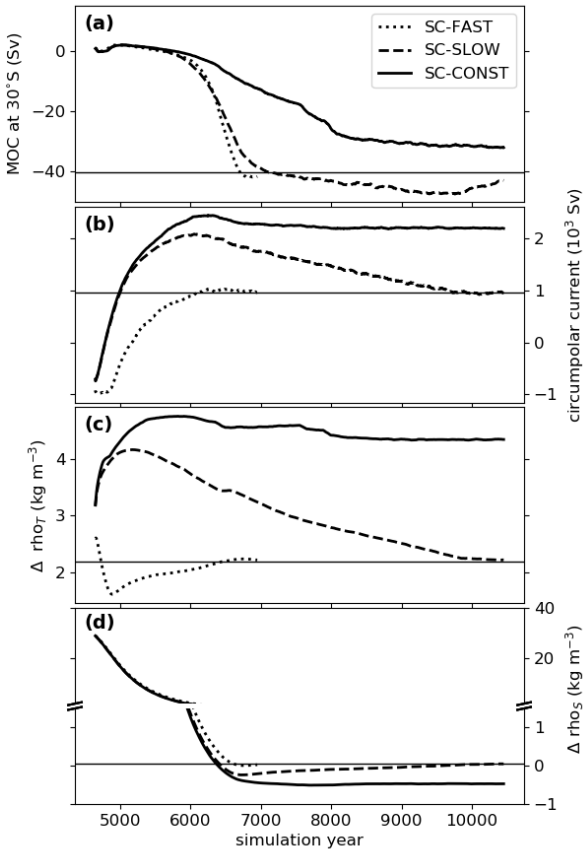

Figure A.6: Temporal evolution of the large scale ocean circulation. **(a)** Strength of the zonally averaged MOC at 30°S and 1365 m depth. **(b)** Mass flux of the depth-integrated circumpolar current through a meridional section between the north pole and the northernmost tip of the continents. Positive values refer to an eastward flow. **(c)** Global mean temperature contribution to the density difference from the ocean bottom to the surface. Higher values correspond to a stronger stratification. **(d)** Same as in (c), but for salinity; note the different scaling above and below the break in the y-axis. The plots show 100 year running means. The black horizontal lines depict the mean value of the Marinoan control climate.

does not lead to a qualitatively different behavior, in which the stratification would persist for 10^4 years or more.

A.6 SUPERGREENHOUSE CLIMATE

The deglaciation of a snowball Earth applies a strong evolutional pressure because it encompasses a very rapid transition between two climate states, but also because the ensuing warm climate could be threatening for some early metazoa. A scenario with long-lived extreme greenhouse conditions is therefore of particular interest, to understand how severe the climate could have possibly been in the aftermath of the Marinoan snowball Earth. In this section, we describe the supergreenhouse climate of the CO_2 scenario that gives the strongest warming in our simulations. For that we evaluate the mean climate of the last 100 years of SC-CONST, which represents a quasi-stable state under a CO_2 concentration of 15×10^3 ppmv.

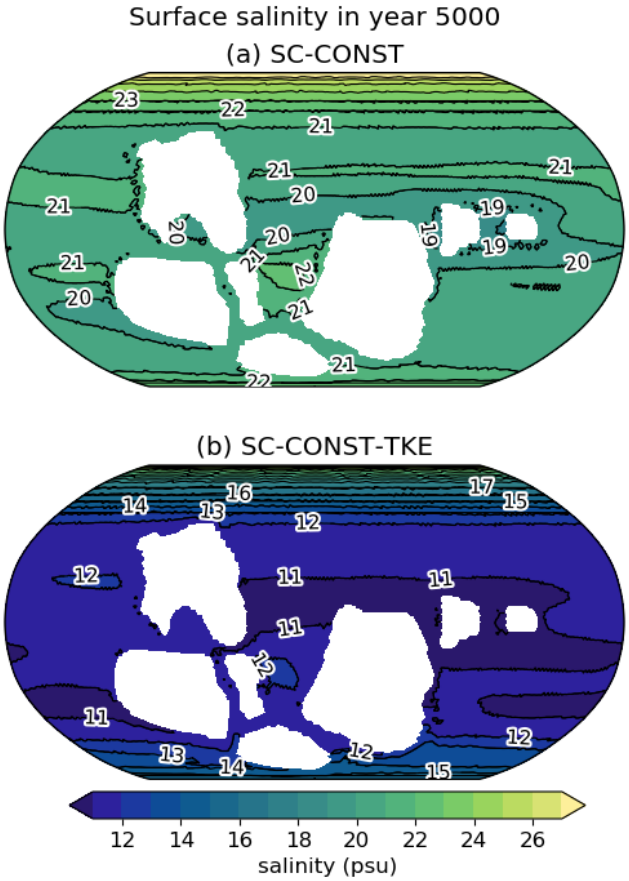

Figure A.7: Surface salinity in year 5000 of (a) SC-CONST and (b) SC-CONST-TKE. The latter uses the parameters of the TKE vertical mixing scheme as they were suggested in Gaspar et al. (1990). The data of both plots represent a 30 year mean around the specified year.

The annual global mean 2 m air temperature of the simulated supergreenhouse climate is 29.7°C, but there exist large regional and temporal variations. While the mean temperature reaches 50°C over some continental areas in the subtropics, mean sea surface temperatures are only 3°C at the north pole. Daily temperature averages can be as high as 68°C, while in other areas temperatures below -5°C are possible. In general, the meridional temperature distribution shows the same pattern as in the control climate, shifted towards higher values (Fig. A.8 (a), (d)).

Although GSAT is more than 16°C higher than in the control climate, precipitation and continental runoff are only increased by 37% and 38%, respectively, which is a slightly larger increase than found by Le Hir et al. (2008b). The main precipitation increase compared to the control climate occurs in the tropics and the mid to high latitudes, so that the general pattern of high precipitation in these regions and low precipitation in the subtropics is strengthened.

One of the reasons for the existence of still comparably cold regions in the Marinoan supergreenhouse climate is the circumpolar current in the northern hemisphere. Through the poleward shift of strengthened westerly winds (Fig. A.8 (f)), the circumpolar current has a water transport of 2190 Sv in the supergreenhouse climate, which is more than two times stronger than in the control climate. As discussed in Sec. A.4,

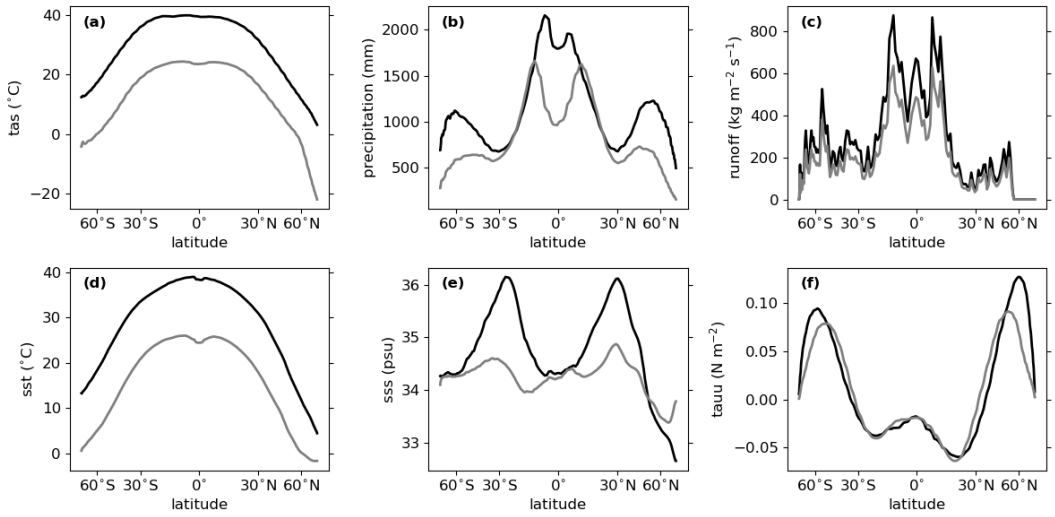

Figure A.8: Zonal averages of the supergreenhouse climate in SC-CONST (black) and the Marinoan control climate (grey) for **(a)** 2 m air temperature, **(b)** precipitation, **(c)** hydrological discharge from land grid cells, **(d)** sea surface temperature, **(e)** sea surface salinity and **(f)** zonal windstress.

the remarkable strength of the circumpolar current is mainly a consequence of the simplified ocean bathymetry in our setup, but the general existence of a circumpolar current is likely. Furthermore, that a circumpolar current strengthens in scenarios of increased greenhouse warming is known also from the warming of the present-day climate (Thompson and Solomon, 2002; Russell et al., 2006). The strong circumpolar current prevents warm water masses from penetrating into higher latitudes. As a consequence, sea surface temperature and salinity are both substantially lower in the high latitudes of the northern hemisphere than in those of the southern hemisphere (Fig. A.8 (d), (e)).

A.7 DISCUSSION

A.7.1 *Impact of CO_2-scenarios*

We included three different pathways for the atmospheric CO_2 concentration after the deglaciation, ranging from a very fast decline to no decline of the strong greenhouse conditions. The most straightforward difference between the scenarios is in the evolution of the global mean 2 m air temperature and consequently the mean ocean temperature and the associated sea-level rise. The scenario SC-CONST shows a permanent warming and a sea-level rise of up to 8 m, in SC-SLOW the surface warms for only a few hundred years, but the ocean temperature continues to increase for around 2000 years, and in SC-FAST the climate quickly approaches the control climate without any major sea-level rise (see Fig. A.4).

While the direct response of the surface temperature and the delayed response of the sea-level rise are readily derived differences coming from the implied different greenhouse forcing in the scenarios, the connection of the ocean circulation to the CO_2 pathways is less clear. The strength of the circumpolar current is shown to

depend on the scenario (Fig. A.6 (b)), with larger transports in warmer climates. This follows from the poleward shift of westerly winds under global warming, as described in Sec. A.6. Furthermore, the meridional overturning circulation (MOC) recovers on a similar timescale in SC-FAST and SC-SLOW, but much slower in SC-CONST (Fig. A.6 (a)). In the first thousand years after the deglaciation, the MOC is mostly gone in all scenarios, because the surface freshwater layer inhibits deep water formation. This haline stratification breaks up on the same timescale in all scenarios, but in SC-CONST a continuously strong thermal stratification limits the full recovery of the MOC (Fig. A.6 (c), (d)). The independence of the haline destratification timescale on the CO_2 pathway leads to the conclusion that it is not the MOC that is driving the break-up, as the slower MOC recovery in SC-CONST should otherwise also delay the destratification in the salinity field. The strength of the MOC is rather a consequence of the stratification strength. We return to the question of what is driving the destratification in Sec. A.7.3.

The procedure of applying different CO_2 pathways was motivated by the unknown carbon content of the ocean at the end of the deglaciation and the resultant possibility to either take up atmospheric CO_2 very quickly or not at all. It helps to test the robustness of the simulation results with respect to the greenhouse forcing and to give a range of possible climatic evolutions. However, prescribing the atmospheric CO_2 concentration neglects the interplay between the oceanic and atmospheric carbon reservoirs, and for future studies a model including an interactive carbon cycle component could help to better understand the climate after a snowball Earth.

In the following we will only discuss the warmest scenario SC-CONST, as we expect this to be the most likely case. This assumption is based on the fact that even small areas of open ocean are sufficient for an effective dissolution of CO_2 in the snowball ocean (Le Hir et al., 2008c), which means that afterwards the oceanic capacity to take up carbon is reduced strongly. Scenarios with a smaller or faster declining CO_2 concentration are also less extreme and therefore less consequential for the discussed properties. The possibility of even higher atmospheric CO_2 concentrations is included in the following discussion.

A.7.2 *Conditions after the Marinoan snowball Earth*

With the atmospheric CO_2 concentration at 15×10^3 ppmv, as chosen in our scenario SC-CONST, the global mean 2 m air temperature is simulated to be around 30°C, and large temperate areas exist in the higher latitudes. The supergreenhouse climate simulated in this study therefore probably does not represent a major restriction for early eukaryotic life (Rothschild and Mancinelli, 2001). With tropical sea surface temperatures of only up to 40°C, compared to previous estimates of 50–60°C (Yang et al., 2017), it is less clear whether cyanobacteria would indeed outcompete algea in the tropics and cause the observed "algal gap", as proposed by Brocks et al. (2017). However, temperatures could be considerably higher when pCO_2 was at the upper end of the range of 10^4–10^5 ppmv, which was estimated for the aftermath of the Marinoan snowball Earth (Kasemann et al., 2005; Bao et al., 2008; Abbot et al., 2012). To determine the possible GSAT at a CO_2 concentration of 10^5 ppmv, we calculate the Marinoan equilibrium climate sensitivity from the temperature difference between the supergreenhouse climate of SC-CONST and the Marinoan control simulation.

Thereby, we arrive at a temperature increase of 4.9 K per doubling of the CO_2 concentration. Using this value, we can estimate that the GSAT at 10^5 ppmv of CO_2 would be around 43°C. In such a climate, the tropical ocean would likely be dominated by cyanobacteria, but it is conceivable that polar regions still exhibit favorable conditions for early metazoa.

The sea-level rise due to thermal expansion is strongly related to the surface warming. It contributes to the overall sea-level change and can therefore influence the deposition of Marinoan cap dolostones. In our simulation SC-CONST, the thermal expansion of seawater accumulates to a sea-level rise of 8 m from the start of the deglaciation, and around 90% of it occurs within the first 3000 years. This means it mostly occurs on the same timescale as the much stronger sea-level rise due to the melting of continental ice sheets (Hyde et al., 2000), which is 1–2 orders of magnitude larger (Benn et al., 2015). Furthermore, a sea-level rise of 8 m is considerably smaller than the 40–50 m derived in Yang et al. (2017). This difference can be attributed to the much higher surface temperatures in Yang et al. (2017), causing the deep ocean to arrive at a potential temperature of 42°C, compared to 13°C in our setup. It can be argued that a deep ocean temperature of 42°C is too high, as it would probably require mean surface temperatures which are too high for the estimated possible range of CO_2 concentrations (discussed above). Our results therefore indicate that the thermal expansion of seawater is less important than it was previously assumed for the sea-level rise in the aftermath of a Marinoan snowball Earth.

Liu et al. (2014) show that isotope compositions of carbonate formations in South Australia and Mongolia indicate a deposition in two chemically distinct fluids: a plume of glacial meltwater overlying the salty waters of the snowball ocean. They discuss that this plume may have been either global or a regional phenomenom, and the most likely timescale for its existence is around 8000 years. Our simulations show that such a surface layer of low salinity is rapidly removed by the ocean circulation. Hence, the persistence of the described freshwater plume for more than just a few thousand years requires a long-term inflow of freshwater from the melting of continental ice sheets, as the stratification cannot be sustained for a long time under the influence of the ocean circulation. However, in the model of Hyde et al. (2000), the deglaciation of continental ice sheets takes less than 2000 years, only a quarter of the likely duration of the freshwater plume. As Liu et al. (2014) mention, the fact that part of the ice sheet sits below sea level could prolong the inflow of meltwater, but it is unlikely that the remaining inflow is sufficient to maintain a global freshwater layer. Therefore, we argue that any freshwater plume that is connected to the salty waters of the global ocean must have been either short-lived or regional in extent and fuelled by a prolonged inflow of meltwater. Accordingly, cap dolostones showing signs of deposition in two chemically distinct fluids must have been deposited within the deglacial period and cannot be attributed to a prolonged global ocean stratification. The finding that the ocean circulation can break up most of the haline stratification within a geologically very short time is discussed in the next section in more detail.

A.7.3 *Ocean destratification and vertical mixing*

Yang et al. (2017) use a one-dimensional vertical mixing model to estimate the destratification time of an idealized two-layer salinity field, similar to the one used in this study. They find timescales between 10^4 and 10^5 years, mostly depending on the vertical diffusivity of the ocean and the initial amount of freshwater. In contrast to that, our simulations indicate mixing times of just a few 10^3 years. In this section, we discuss why our destratification times are so much shorter and which timescales could be realistic.

The one-dimensional vertical mixing model used in Yang et al. (2017) and the AOGCM used in this study implement conceptually different mechanisms by which a vertical stratification can be removed. While the 1d-model describes all vertical motion through a vertical diffusion equation, the AOGCM attains the horizontal and vertical ocean circulation by solving the hydrostatic primitive equations on a three-dimensional grid (Korn, 2017), but it also adds vertical motion through a parameterization of small scale turbulent (vertical) mixing. Yang et al. (2017) argue that this mixing could be smaller in the warm snowball Earth aftermath than it is today, because of less energy input through weaker lunar tides and a weaker energy input from wind. Even though the second point is questionable in the light of increasing surface winds in our simulations of the supergreenhouse climate (see Fig. A.8 (f)), it could still be speculated that the short mixing times found with our model are a consequence of too much parameterized vertical mixing, because the mixing scheme was developed and adapted for a present-day climate. However, our simulation SC-CONST-TKE shows that also substantially weaker parameterized vertical mixing only delays the stratification break-up by some 500 years. Therefore, the parameterization of vertical mixing is unlikely to be the source for the order-of-magnitude difference in the destratification timescale.

Is it then the three-dimensional nature of the ocean circulation that is the main driver of the fast stratification break-up? The plots in Figs. A.5 and A.7 show that waters of higher salinity reach the surface through the high latitudes, especially in the northern hemisphere. Here, the strong westerly winds induce a massive circumpolar current that drives upwelling through surface divergence induced by Ekman transport. Furthermore, vertical shear within the current can also support the destratification. To investigate this, Fig. A.9 displays vertical profiles of the zonal ocean velocity in the circumpolar current for the pre-industrial and Marinoan control climates, as well as at different times during the snowball Earth aftermath. The circumpolar current is stronger in the Marinoan configuration than in the pre-industrial setup and is even stronger during the supergreenhouse climate. The vertical shear profiles also feature a very different shape in the direct aftermath of the snowball state. This shape includes a strong vertical shear of the zonal velocity, which is indicative of a baroclinic current. Through the thermal wind relation this vertical shear can be connected to the northward sloping isopycnals shown in Fig. A.5, which support the exchange of surface waters with the deeper ocean through mixing along those isopycnals. The clear correlation between the existence of a circumpolar current and the much stronger steepening of isohalines in the northern hemisphere is a convincing indicator that indeed the three-dimensional circulation, and not the small-scale vertical mixing, cause the fast break-up of the stratification.

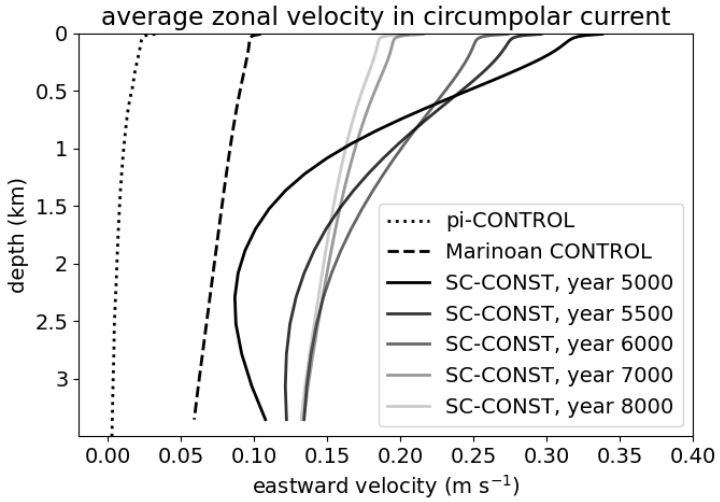

Figure A.9: Vertical profiles of the zonally averaged eastward velocity component over the region of the circumpolar current. Shown are profiles from the pre-industrial control simulation (dotted), from the Marinoan control simulation (dashed) and from the scenario SC-CONST (solid) for the same times as the sections shown in figure A.5. In the Marinoan setup, we define the region of the circumpolar current as the latitudes between 45°N and 75°N, and in the present-day configuration the current is averaged over the latitudes between 75°S and 45°S.

It is this crucial part of the ocean circulation that is missing in the vertical mixing model of Yang et al. (2017) and that explains a large part of the timescale differences.

Nevertheless, the question remains, how much of the timescale difference is due to an overestimation of the circumpolar current strength in our setup. As discussed in Sec. A.4, the simplified topography induces an unrealistically strong circumpolar current with a transport of 960 Sv during the control climate, which reaches up to 2190 Sv in the supergreenhouse climate after the snowball Earth. This is an order of magnitude stronger than the present-day ACC. Part of this difference can be attributed to the absence of continents north of 51°N during the Marinoan, which indeed favors a circumpolar current stronger than the ACC. A larger part of the difference, however, comes from the missing form drag at the flat ocean bottom, which is a typical issue in models with simplified topography (Bryan and Cox, 1972; Wolff et al., 1991). In a realistic circumpolar current, the eastward momentum imparted by the surface wind stress would be transferred downward through transient or standing eddies (Wolff et al., 1991). This slows down the circumpolar current substantially and leads to much less vertical transport in the deep Ekman cell, hindering the break-up of the stratification. However, the eddy activity itself is associated with turbulent vertical mixing. Therefore, even though the strength of the circumpolar current could be greatly reduced when using an eddy-resolving model with appropriate bottom topography, this is not necessarily the case for the vertical mixing linked to the current. So, while our model probably overestimates the vertical mixing induced by the Ekman cell, it possibly underestimates the vertical mixing through eddy activity, especially in the simulation SC-CONST-TKE.

In summary, the discrepancy in destratification timescales between the study of Yang et al. (2017) and our results can largely be explained by the addition of ocean

dynamics in our study. Although our simplified model topography favors a quick break-up of the stratification, it is still plausible that the ocean mixing timescale is much less than the 5×10^4 years that were suggested by Yang et al. (2017). The main reason for this is the following: The absence of continents north of 51°N at the time of the Marinoan glaciation favors a strong circumpolar current, which accelerates the break-up of the stratification through its initially baroclinic nature, a deep Ekman cell and strong eddy activity (It should be noted that the circumpolar current is not the only region where the three-dimensional circulation will lead to vertical transports, but it is presumably the strongest contributor to the destratification). These effects are not accounted for by the model of Yang et al. (2017), explaining their much longer mixing timescale. We propose that even when including the assumptions of Yang et al. (2017), a larger freshwater amount inserted over a few 10^3 years and a weaker circumpolar current the three-dimensional ocean circulation can break up the freshwater stratification after a snowball Earth in less than 10^4 years.

A.8 CONCLUSIONS

In this study, we simulate the transient period from the deglaciation of a Marinoan snowball Earth into a warm supergreenhouse climate using a coupled AOGCM. The main findings and implications of our simulation results are summarized by the following points:

1. By including the three-dimensional ocean circulation in a study of the snowball Earth aftermath, we show that the strong haline stratification can break up within just a few thousand years, mostly independent of the path the atmospheric CO_2 concentration takes. This finding is robust, even with significantly reduced vertical mixing, and shows the important contribution of the dynamical nature of the ocean circulation. Our results therefore indicate that cap dolostones where deposited during the period of deglaciation, given that they accumulated under the influence of a freshwater environment.

2. In a Marinoan supergreenhouse climate with an atmospheric CO_2 concentration of 15×10^3 ppmv, the Earth exhibits a global mean temperature of only around 30°C, and large temperate areas exist in the high latitudes. Even when accounting for the comparatively low CO_2 concentration here, this is a relative modest warming compared to previous estimates of GSAT of about 50°C. It is therefore conceivable that large parts of the estimated range of CO_2 concentrations after a snowball Earth would result in climates exhibiting large regions with still moderate temperatures. The impeding effect of temperature on eukaryotic life was potentially severe only with a CO_2 concentration at the upper end of the estimates.

3. Our simulations do not show a significant long-term sea-level rise due to thermal expansion, which is a consequence of the relatively lower surface and deep ocean temperatures, compared to previous studies (Yang et al., 2017). We therefore conclude that it was mainly the sea-level change through melting continental ice sheets and the ensuing glacio-isostatic adjustment affecting the deposition of Marinoan cap carbonates, while the thermal expansion of seawater probably only played a minor role.

A.9 APPENDIX: IMPACT OF MODEL ERRORS ON THE SIMULATIONS

The here used Earth system model ICON-ESM is a recently developed model (Jungclaus et al., 2022). Even though part of ICON's parameterizations are based on its predecessor MPI-ESM (Mauritsen et al., 2019), large parts of the code were built from scratch. Therefore, the frequency with which coding errors are detected is somewhat higher than in more established models. After the simulations presented in this study were finished, a set of bugs was detected, which are related to energy fluxes at the surface. On the one hand, both moisture and the dry static energy of moist air were diffused by the surface fluxes, effectively counting the moisture flux twice. On the other hand, the latent and sensible heat fluxes where accidentally set to zero when calculating the surface temperature of sea ice in the o-layer Semtner model. In the following, we explain why these errors do not influence the outcome of our work.

All conclusions of this paper are derived from first order components of the climate, like the broad-scale ocean circulation or the evolution of the global temperature distribution after the snowball Earth. Fixing the model errors does not change the qualitative nature of the simulation outcome. The first bug, causing the double counting of the moisture flux, potentially alters the conditions of the supergreenhouse climate, but a 100 year long simulation, including all bugfixes and a retuning of model parameters for a good pre-industrial simulation, produces a very similar supergreenhouse state, with an almost identical meridional temperature distribution. The second model error, found in the calculation of the surface temperature of sea ice, effectively warms the ice surface and therefore leads to generally thinner sea ice. This is balanced by the high ice and snow albedos of the sea-ice scheme used in our model. Lower sea-ice albedos would be used in a model version where this bug is fixed. Test runs show that fixing this bug and lowering the albedo leads to a similar behavior in a pre-industrial control simulation, but the deglaciation of a snowball Earth is much harder to achieve. However, shortly after the deglaciation, sea ice is gone completely, and it only recovers in SC-FAST and later in SC-SLOW, while it remains gone in SC-CONST and SC-CONST-TKE. Hence, large parts of our simulations are not affected by this second model error. It can thus confidently be said that the results and the conclusions of this work are robust with respect to both detected model errors.

Acknowledgements

We thank Chao Li for the internal review of the manuscript and Stephan Lorenz and Helmuth Haak for valuable technical support. Two anonymous reviewers provided very helpful comments. This work was supported by the Max Planck Society for the Advancement of Science and the International Max Planck Research School on Earth System Modelling. All model simulations and analyses were performed using resources of the German Climate Computing Center (DKRZ).

B

ASSESSMENT OF THE CARBON CYCLE EVOLUTION AFTER A SNOWBALL EARTH

The work in this appendix is in preparation for submission as:

Ramme, L., Ilyina, T. and Marotzke, J.: Assessment of the carbon cycle evolution after a snowball Earth, *in preparation*

Assessment of the carbon cycle evolution after a snowball Earth

Lennart Ramme,[1,2] **Tatiana Ilyina**[1] **and Jochem Marotzke**[1,3]

[1] Max-Planck-Institute for Meteorology, Hamburg, Germany
[2] International Max Planck Research School on Earth System Modelling, Hamburg, Germany
[3] Center for Earth System Research and Sustainability (CEN), Universität Hamburg, Germany

ABSTRACT

The aftermath of a snowball Earth is a period of rapid warming and a major transition in the biogeochemical conditions of the ocean. The extreme shifts represented threatening conditions for the early forms of life that previously adapted to the cold snowball Earth conditions. However, the severity and duration of the climatic and chemical excursions of this supergreenhouse climate are unknown. The carbon cycle dynamics that act on a time scale of less than ten thousand years after the start of the deglaciation have never been quantified. Here we show that the uncertain conditions at the start of the snowball Earth deglaciation allow for a wide range of scenarios, ranging from a rapid decline of the atmospheric CO_2 concentration to a supergreenhouse climate that intensifies over time. Our climate model simulations demonstrate that several processes could draw down substantial amounts of carbon from the atmosphere into the ocean quickly during the snowball Earth aftermath. These include the diluting effect of the freshwater inflow, the biological carbon pump and possibly the equilibration of a depleted ocean that was previously disconnected from the atmosphere. In contrast, the reduced solubility of CO_2 at higher temperatures leads to outgassing from the ocean. Furthermore, the warming-induced inorganic precipitation of carbonates can lead to massive outgassing of CO_2, and this mechanism can explain the formation of Marinoan cap dolostones within less than 10^4 years from the start of the deglaciation. We conclude that a rapid deposition of Marinoan cap dolostones and a moderate, possibly even short-lived, supergreenhouse climate are readily achievable if snowball Earth deglaciation is triggered at a low atmospheric CO_2 concentration and the ocean has gained a considerable amount of alkalinity during the snowball period.

B.1 INTRODUCTION

Carbon dioxide is a major greenhouse gas that prevents the Earth from freezing over, but it can also lead to severely warm climates when it accumulates in large amounts in the atmosphere. The Neoproterozoic Era (1000 - 541 million years ago, Ma) saw probably the most extreme climatic consequences of carbon cycle excursions in the Earth's history, with two long-lived periods of global glaciation that were caused by the removal of CO_2 from the atmosphere through weathering of silicate rocks (Kirschvink, 1992; Hoffman et al., 1998; Schrag et al., 2002; Donnadieu et al., 2004). As continental weathering sinks are shut down during these "snowball Earth" periods, CO_2 accumulates in the atmosphere until eventually a very high threshold concentration is reached, at which the greenhouse effect overcomes the strong reflection of sunlight by the glaciated surface (Walker et al., 1981; Pierrehumbert, 2005; Marotzke and Botzet, 2007; Hoffman et al., 2017). What follows is a fast deglaciation within a few thousand years (Hyde et al., 2000) and an ensuing supergreenhouse climate that can lead to global mean surface temperatures of $\sim 30 - 50°C$ (Le Hir et al., 2008b; Yang et al., 2017; Ramme and Marotzke, 2022). In this study, we focus on the evolution of the carbon cycle in the aftermath of the second snowball event, the Marinoan snowball Earth, which ended at around 635 Ma (Hoffmann et al., 2004; Calver et al., 2013).

The dynamics of the carbon cycle determine the climatic and chemical boundary conditions that set the scene for the biological evolution. Especially the rapid transition into a hot greenhouse climate, potentially accompanied by substantial changes in the chemical properties of the ocean, is a major burden for biota that previously adapted to the freezing conditions of a snowball Earth lasting for millions of years (Brocks and Butterfield, 2009; Love et al., 2009; Erwin, 2015). However, the central questions of the severity and the duration of the supergreenhouse climate are so far unresolved. Reconstructions of the weathering carbon sink indicate that atmospheric CO_2 concentrations may have remained elevated for hundreds of thousands to millions of years (Higgins and Schrag, 2003; Le Hir et al., 2008b), but some isotope data suggest moderate CO_2 levels already shortly after the deglaciation (Kasemann et al., 2005; Sansjofre et al., 2011). An assessment of the possible scenarios for the evolution of the carbon cycle is therefore essential to determine the climatic and biogeochemical conditions that represented a potential bottleneck in the evolution of life, but this assessment is lacking so far.

Some insights into the climatic and chemical evolution during the aftermath of the Marinoan snowball Earth can be gained from both modelling and the geological rock record, but the available data are associated with large uncertainties and sometimes contradicting outcomes (Hoffman et al., 2017). While climate models initially suggested that very high atmospheric CO_2 concentrations are needed for triggering the deglaciation of a snowball Earth (Pierrehumbert, 2005), new estimates are more in line with data from the geological record pointing to more moderate CO_2 concentrations (Abbot et al., 2012). Still, the possible range for the atmospheric CO_2 concentration is only loosely constrained to $10^4 - 10^5$ ppmv (Kasemann et al., 2005; Bao et al., 2008, 2009). Similarly, the ocean chemistry at the start of the deglaciation is another source of uncertainty, where the major unknowns are related to the amount of alkalinity dissolved in the ocean (Le Hir et al., 2008a; Gernon et al., 2016) and the

question whether the oceanic carbon reservoir experienced an efficient exchange with the rising atmospheric CO_2 concentration (Hoffman et al., 1998; Le Hir et al., 2008c). Furthermore, Marinoan glacial deposits are commonly overlain by a distinctive layer of dolomite rock (Hoffman, 2011), indicating that coastal waters were supersaturated with respect to carbonate minerals. The existence of those "cap dolostones" and their specific features of rapid deposition can provide helpful constraints when reconstructing the evolution of the carbon cycle and the supergreenhouse climate. But again, the origin of the required alkalinity and the mechanism of the formation of those cap dolostones are not well understood (Higgins and Schrag, 2003; Le Hir et al., 2008a; Fabre and Berger, 2012; Gernon et al., 2016).

Here, we acknowledge the existing major uncertainties, namely the atmospheric CO_2 concentration at the start of the deglaciation, the amount of alkalinity stored in the ocean and the question whether the oceanic pCO_2 was in equilibrium with the atmospheric CO_2 concentration. Our simulations with the comprehensive climate model ICON-ESM (Jungclaus et al., 2022), which we extend by further calculations with a carbonate chemistry model, are aimed at exploring different scenarios for the evolution of the carbon cycle in the aftermath of the Marinoan snowball Earth. Thereby, we assess the different pathways in which the climate and the biogeochemical conditions could have evolved during the supergreenhouse climate, and we discuss how a rapid deposition of Marinoan cap carbonates can be reconciled with those scenarios.

B.2 SIMULATING THE CARBON CYCLE DYNAMICS AFTER A SNOWBALL EARTH

The exchange of carbon between the atmosphere and the ocean after a snowball Earth is determined by a variety of different processes (Fig. B.1a), and their magnitude and time scale largely depend on the ocean chemistry and other uncertain parameters. Most of the processes are represented in ICON-ESM, but a number of model limitations and a large range of possible initial conditions exist. The main spread in uncertainty that we consider here can be represented as a two-dimensional space determined by the possible ranges of the atmospheric CO_2 concentration (atm. CO_2) and the total alkalinity (TA) concentration in the ocean at the start of the deglaciation. The atmospheric CO_2 concentration required to trigger the deglaciation is assumed to be between 10^4 and 10^5 parts per million by volume (ppmv). However, all ICON-ESM simulations are started with the same initial atm. CO_2 of 13,700 ppmv, because the model becomes unstable at too high CO_2 concentrations. Therefore, a carbonate chemistry model is used to cover the full range of atm. CO_2. We further discuss a large range of TA of up to 60 mol m^{-3}, as this determines the oceanic capacity to store large amounts of carbon. Very high TA are inconsistent with low atmospheric CO_2 concentrations, because either the carbonate saturation states are unrealistically high and would cause synglacial carbonate formation, or the oceanic pCO_2 would need to be higher than atm. CO_2. Therefore, and because high TA can lead to substantial outgassing of CO_2 into the atmosphere, as discussed later, the ICON-ESM simulations only cover scenarios with TA $\leq$ 15 mol m^{-3}. Again, the carbonate chemistry model is used to incorporate also higher TA.

Figure B.1b shows the ocean pCO_2 and TA at the start of the deglaciation in the ICON-ESM simulations. While the initial atm. CO_2 is the same in all simulations, the

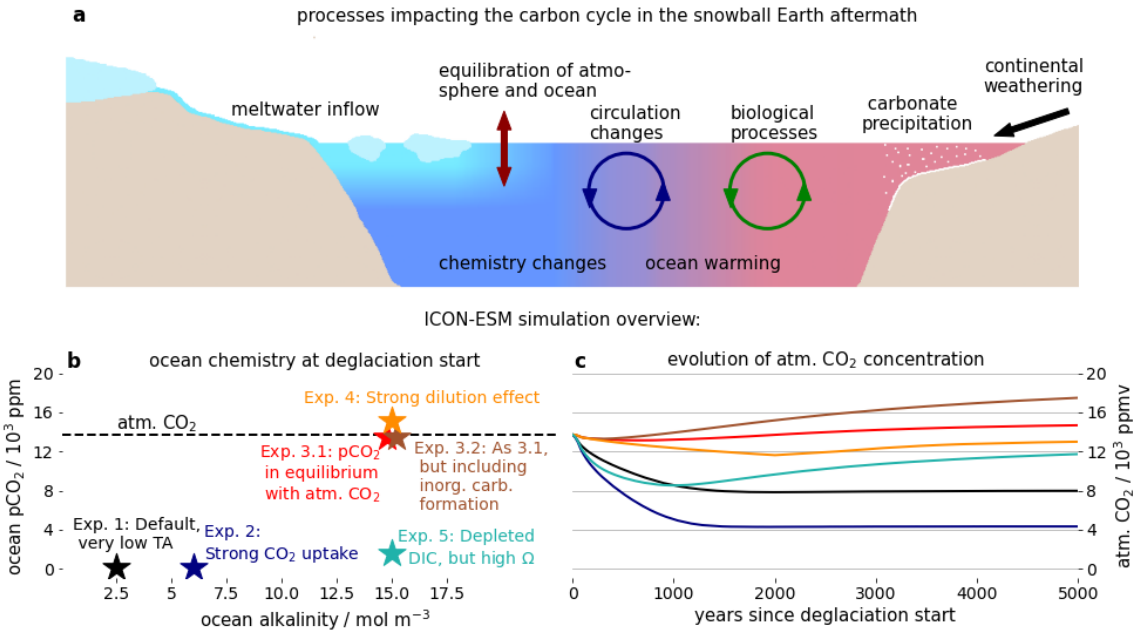

Figure B.1: **Air-sea CO_2 exchange after a snowball Earth and simulation overview. a**, Schematic representation of the different processes that impact the air-sea CO_2-flux after a snowball Earth. **b**, The ocean alkalinity concentration, TA, and pCO_2 at the start of the deglaciation for the different ICON-ESM simulations. The initial atmospheric CO_2 concentration (atm. CO_2) was around 13,700 ppmv in all simulations, indicated by the dashed line. **c**, Evolution of atm. CO_2 in the ICON-ESM simulations. More details on the experiment settings are found in the supporting information.

ocean pCO_2 is varied in terms of a modified initial reservoir of dissolved inorganic carbon (DIC). The simulations can largely be divided into two groups. In the first group (Exp. 1, Exp. 2, Exp. 5) the oceanic carbon reservoir is depleted, reflecting an inefficient exchange with the atmosphere, while in the second group (Exp. 3.1, Exp. 3.2, Exp. 4), the ocean's pCO_2 is similar to the initial atm. CO_2. The evolution of atm. CO_2 in the snowball Earth aftermath (Fig. B.1c) is very sensitive to the ocean chemistry, and we discuss the impact of the most important carbon cycle processes in the following sections. More details on the settings of the individual simulations can be found in the supporting information.

B.3 OCEAN CARBON UPTAKE DURING DEGLACIATION

The dilution of the sub-snowball brine by the inflow of meltwater reduces, among all other tracer concentrations, the concentration of DIC and hence the pCO_2 of the ocean, which will lead to a flux of CO_2 from the atmosphere into the ocean. Similarly, if the ocean was disconnected from the atmosphere during the snowball state and has a depleted carbon reservoir, this can also lead to a major uptake of CO_2, as the reservoirs equilibrate during the deglaciation. While the dilution effect is a predictable mechanism with uncertainties related only to its magnitude, the reservoir equilibration effect will only have occurred if there was no efficient gas exchange during the snowball Earth period. In the following, we quantify the isolated effect of both mechanisms in idealized calculations using a carbonate chemistry model and discuss how these effects appear in the ICON-ESM simulations.

In order to quantify the magnitude of the dilution effect, we consider a case where pure freshwater with a volume of 1000 m of sea-level equivalent is instantaneously mixed into a cold ocean previously in equilibrium with atm. CO_2. This reduces all tracer concentrations in the ocean by about 30%, leading to a lower pCO_2 in all cases. In the calculations, CO_2 is then removed from the atmosphere and added to the ocean in the form of DIC until a new equilibrium is found between the ocean surface pCO_2 and atm. CO_2. The relative reduction in atm. CO_2 is depicted in Fig. B.2a for the full uncertainty range of initial atm. CO_2 and ocean TA. Over almost the entire range, the atmospheric CO_2 concentration is reduced by 10-15%, with larger reductions only for very low initial atm. CO_2. Test calculations show that about 30% of this reduction are driven by an increase in the solubility of CO_2, which comes from the reduced salinity after the dilution. The further uptake results from a combination of the dilution of the DIC concentration directly and a shift in the carbonate chemistry that causes a rearrangement between the different carbonate species. We can quantify the dilution effect in a more complex setup by comparing two of our ICON-ESM simulations (Exp. 3.1 and Exp. 4), which only differ by a strong dilution effect that is comparable to the idealized calculations described above (see experiment description in the SI). At the end of the simulations, the atmospheric CO_2 concentration is about 11.5% smaller in the experiment including the strong dilution effect. This reduction is comparable to the reduction derived with the idealized carbon chemistry calculation shown in Fig. B.2a (orange star), which predicts a 13.5% reduction of atm. CO_2. This indicates that these idealized calculations can give a good first order approximation of the potential reduction

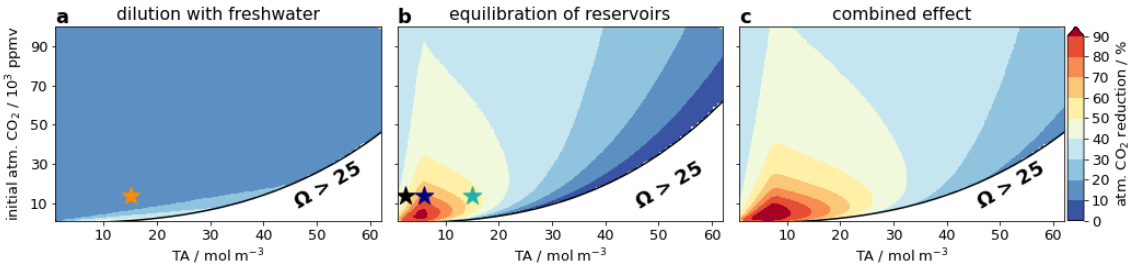

Figure B.2: **The potential reduction in the atmospheric CO_2 due to the effects of dilution and reservoir equilibration.** Both effects are considered in isolation of any other potential mechanism affecting the carbon exchange.**a**, Potential atmospheric CO_2 reduction due to the dilution of the ocean through the mixing of a 1000 m thick layer of freshwater that is void of any biogeochemical tracers. The orange star indicates the conditions of Exp. 4. **b**, Potential atmospheric CO_2 reduction due to the effect of reservoir equilibration. The initial oceanic concentration of DIC is here set to be at the lowest possible value that still fulfills two conditions: pCO_2 > 100 ppm and Ω_{CaCO_3} < 25 under snowball conditions. The three stars indicate the conditions of Exp. 1 (black), Exp. 2 (blue) and Exp. 5 (cyan). **c**, Combined effect of **a** and **b**, where 1000 m of freshwater are mixed into an ocean that is initially depleted in DIC. In **a** and **c**, the ocean initially only has a depth of 2500m and 1000m of freshwater are then added. In **b** already the initial state has the full ocean depth of 3500m.

of atm. CO_2 for a given volume and chemical composition of the meltwater inflow during the deglaciation of a snowball Earth.

After all, the CO_2 uptake potential of the dilution effect is very dependent on the volume, as well as the chemistry of the freshwater. Here, we assumed that the deglacial waters are void of any biogeochemical tracers. However, some DIC and TA are normally also present in sea ice, often with a ratio of TA:DIC that is larger than one (Fransson et al., 2011; Grimm et al., 2016), and further alkalinity could come with the meltwater flushes from the continents (Fabre and Berger, 2012). Therefore, DIC in the ocean could easily be diluted stronger than TA, which would lower pCO_2 even further, causing an even stronger dilution effect than predicted here.

The second mechanism potentially causing an oceanic CO_2 uptake during the deglaciation, the reservoir equilibration effect, can be best quantified in isolation when assuming a scenario in which the sea-ice cover is suddenly permeable for the exchange of CO_2. We again consider the case of a cold sub-snowball ocean that is now depleted in DIC. This, however, does not at all mean that there is no DIC in the ocean, but that the DIC concentration is reduced to the lowest possible value that still fulfills two conditions: the ocean surface pCO_2 (below the ice) is still larger than 100 ppm, which is roughly the atm. CO_2 needed for snowball initiation in our model, and the calcium carbonate saturation state Ω_{CaCO_3} must be lower than 25, as otherwise the syn-glacial precipitation of carbonates would reduce TA again. The threshold value at which inorganic precipitation of carbonates occurs is not well constrained (Ridgwell and Zeebe, 2005). We here choose a high value of 25 to reflect the difficulty to initiate inorganic carbonate precipitation in a cold ocean under sea ice, which lacks organic particles that could act as condensation nuclei. Different threshold values would only shift the observed pattern to higher or smaller TA. With

the settings defined here, the first criterion of a lower bound on pCO_2 comes into play for TA < 8 mol m^{-3}, while the second criterion is effective at higher TA. The DIC concentration is in all cases still very similar to TA. Without these two criteria, at substantially reduced DIC concentrations, the ocean could theoretically suck almost all CO_2 out of the atmosphere and drive the climate back into a snowball state already during the period of deglaciation.

The relative reduction of atm. CO_2 due to the reservoir equilibration effect is displayed in Fig. B.2b. At very low TA (< 3 mol m^{-3}), the atmospheric carbon reservoir is of a comparable size or even larger than the ocean carbon reservoir. Hence, already small relative reductions in atm. CO_2 increase the ocean pCO_2 substantially and lead to a new equilibrium. At high TA ($> 10 - 15$ mol m^{-3}), the large carbonate saturation states do not allow for a significant disequilibrium between the two reservoirs, and the relative reduction in atm. CO_2 through the reservoir equilibration effect is small as well. However, there is a maximum of the relative reduction of atm. CO_2 centered at very low initial atm. CO_2 and intermediate to low TA concentrations ($3 - 10$ mol m^{-3}), where the reservoir equilibration effect can reduce the atmospheric CO_2 concentration by more than 90%. Here, TA is large enough to accommodate a substantial flux of carbon into the ocean, and the carbonate saturation states are still low, so that a large difference between the ocean's pCO_2 and atm. CO_2 can be sustained. These calculations show that the reservoir equilibration effect can end the supergreenhouse climate already during the deglaciation, for specific combinations of TA and initial atm. CO_2.

Three ICON-ESM simulations (Exp. 1, Exp. 2, Exp. 5) were designed with a depleted ocean DIC, in order to test the possibility of a significant reduction of atm. CO_2. Many more processes are affecting the carbon cycle in these simulations, but the large predicted reductions in atm. CO_2 mean that the carbon cycle evolution is possibly dominated by the reservoir equilibration effect. The starting conditions of the ICON-ESM simulations are marked by the coloured stars in Fig. B.2b, and more details about the simulations are given in the supporting information. The predicted and simulated relative reductions in atm. CO_2 are, respectively, 48% and 42% for Exp. 1, 72% and 68% for Exp. 2 and 54% and 14% for Exp. 5. The respective values are very similar in Exp. 1 and Exp. 2, showing that the idealized calculations are approximately correct and that the reservoir equilibration effect indeed dominates the air-sea CO_2 exchange. The fact that the simulated reduction is slightly smaller than the predicted reduction indicates that the sum of all other carbon cycle processes leads to an overall outgassing in these simulations. In contrast, the simulated reduction in Exp. 5 is significantly smaller than the predicted oceanic uptake of CO_2. In that experiment, an additional process plays a major role and counteracts the CO_2 uptake by the reservoir equilibration effect. This process is the inorganic precipitation of carbonates from the ocean, which we discuss later.

The ICON-ESM simulations Exp. 1, Exp. 2, Exp. 5 and the idealized calculations of the reservoir equilibration effect were designed in order to achieve a maximum oceanic uptake of CO_2. The possible reductions in atmospheric CO_2 that we present here should therefore be seen as the maximum CO_2 uptake, and the reservoir equilibration effect could also only play a minor role. Nevertheless, we suggest that the combination of the dilution and the reservoir equilibration effect (Fig. B.2c) can

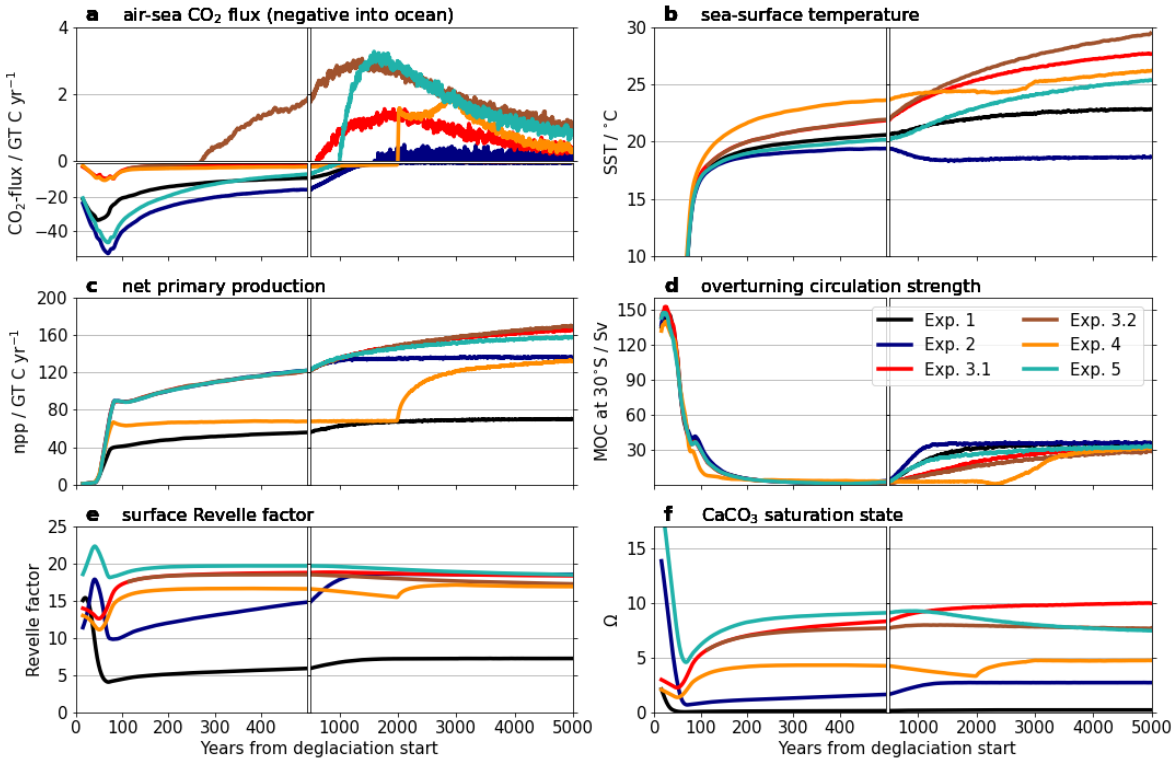

Figure B.3: **Timeseries of global variables from the ICON-ESM simulations. a**, Annual air-sea CO_2-flux, note the change in scale of the y-axis, **b**, mean sea-surface temperature, **c**, sum of global annual primary production by phytoplankton and cyanobacteria, **d**, strength of meridional overturning circulation at the location of its maximum in the control simulation, **e**, mean surface Revelle sensitivity factor, **f**, mean surface calcium carbonate saturation state. Timeseries of more variables can be found in the supporting information. For more information on the experiment settings see Fig. B.1b and the list of experiments in the supporting information. All timeseries show 30-year running mean data. Note the change in scale of the time axis at year 500. In year 2000 of Exp. 4 the surface freshwater input is stopped, causing the kink of the timeseries at that point.

lead to a significant reduction of the atmospheric CO_2 concentration already during the period of deglaciation. This would mean that temperatures may never get as high as it could be expected from the high CO_2 concentration required to trigger snowball Earth termination. This is important especially because the counteracting effects that lead to outgassing of CO_2 are often driven by the temperature increase.

B.4 OCEAN WARMING, CIRCULATION CHANGES AND THE BIOLOGICAL CARBON PUMP

The solubility of CO_2 in seawater decreases with rising temperatures. During the snowball state, ocean temperatures are close to the freezing point, which corresponds to -1.8°C in ICON-ESM. Global mean sea-surface temperatures then increase to values around 20°C within just a few hundred years from the start of the deglaciation in our simulations, and they may reach 25-30°C in the long term (Fig. B.3b). Using the temperature dependence of pCO_2 (Weiss, 1974), one can estimate that the mean

surface ocean pCO_2 would increase by about $140 - 180\%$ through the warming, depending on the initial pCO_2 and the ocean alkalinity. However, it is not practical to calculate the coupled atm. CO_2 change for this mechanism in an idealized calculation, as it was done for the dilution and the reservoir equilibration effects. This is because of the large spatial variations of temperature and the fact that the deep ocean pCO_2 is rather set by the circulation and biological processes. For this reason, we investigate here the carbon cycle evolution of our simulation Exp. 3.1, where the warming effect should be best visible. In this simulation, the CO_2 concentration of the atmosphere increases by only about 7 % over the course of 5000 years. However, atm. CO_2 actually drops initially by 4% during the phase of the strongest surface warming within the first few hundred years from the start of the deglaciation. Other mechanisms must therefore counteract the warming-driven outgassing in this period. One of them is the already discussed dilution effect from the melting of a 147 m thick layer of sea ice in this simulation. Another factor that could counteract the outgassing is the reviving biosphere.

Carbon is removed from the surface ocean through primary production of phytoplankton and cyanobacteria and released in the deeper ocean, where the organic material is remineralized. This biological carbon pump therefore leads to a reduction in pCO_2 in the surface layers and an increase in pCO_2 in the deep ocean. Primary production ramps up to very high values in our simulations of the snowball Earth aftermath (Fig. B.3c), as a result of the high availability of nutrients and the increasing temperatures. In a test simulation with suppressed primary production, we notice a strong outgassing of CO_2 from the ocean during the main phase of deglaciation, while the original simulation Exp. 3.1 shows a strong uptake of CO_2. After 1000 years from the start of the deglaciation, the atmospheric CO_2 concentration is 2000 ppm higher in the simulation with suppressed primary production than it is in the simulation where the biological carbon pump is active. This highlights that primary production and the associated organic matter transport into the deep ocean counteract and even reverse the outgassing of CO_2 that is expected from the warming of the ocean.

Primary production reappears rapidly after the snowball Earth in our model, because it is implemented in HAMOCC to represent the modern primary producers of the ocean (Ilyina et al., 2013). However, it is questionable whether those biota that adapted to a snowball Earth state could indeed thrive and spread quickly in the hot snowball Earth aftermath. It is conceivable that there would at least be a delay in the reappearance of the biological carbon pump, while the biology adapts to the changed climatic boundary conditions.

The temporal uncertainty of the effect of the biological carbon pump is increased further by the changing ocean circulation. The meridional overturning circulation (MOC) recovers quickly in most of our ICON-ESM simulations (Fig. B.3d), because the amount of meltwater is comparably small and because the dynamics of the ocean circulation break up the stratification quickly (Ramme and Marotzke, 2022). The MOC is suppressed for a longer time only in the simulation with a sustained freshwater influx (Exp. 4). The recovery of the MOC, which is best visible around year 3000 in Exp. 4, then triggers a period of increased outgassing, because the upwelling of carbon-rich deep waters strengthens. The large jump in year 2000 of this simulation is artificial and caused by the end of the freshwater input period,

when the dilution of the surface waters is stopped. Overall, the effect of the recovery of the MOC is only adding to an already existing trend of CO_2 outgassing. It seems that the long-term warming is dominating the carbon cycle once the periods of deglaciation and rapidly increasing primary production are over.

Apart from the large climatic shifts during the snowball Earth deglaciation, also the chemical composition of the sub-snowball ocean is important for the evolution of the carbon cycle in the snowball Earth aftermath. The ocean's TA and DIC concentrations set the pH of the ocean, which then determines how efficient the buffering capacity of the ocean is in the snowball aftermath. This was implicitly already included in the discussion of the reservoir equilibration effect, where the efficiency of this mechanism was strongly dependent on TA. More generally, the importance of the chemical composition of the ocean can also be quantified by the Revelle factor (Fig. B.3e), which is defined as the relative change in pCO_2 for a given relative change in DIC (Egleston et al., 2010; Middelburg et al., 2020). In most of our simulations, the global mean surface Revelle factor is above 15. This indicates that, despite the large CO_2 fluxes during the deglaciation, the ocean buffering capacity is actually smaller than in the modern ocean, where the mean Revelle factor is $\sim$10 (Middelburg et al., 2020). Similarly, the carbonate saturation state of the ocean (Fig. B.3f) is dependent on TA and DIC. This can massively affect the carbon cycle, when very high saturation states lead to the inorganic precipitation of carbonates in a warming ocean. Therefore, we dedicate the following sections to the quantification of this process.

B.5 WARMING-INDUCED INORGANIC PRECIPITATION OF CARBONATES

Carbonate forms inorganically in seawater if the saturation state Ω is above a very high supercritical value. During the snowball state, the ocean is very cold, the salinity is high and the thick sea-ice cover increases the pressure even in the shallowest ocean waters. All these factors lower the carbonate saturation state. In addition, the absence of biologically produced particles that could act as condensation nuclei suggests that the threshold for the inorganic precipitation of carbonates is even higher in the snowball ocean than in the modern ocean. Together, this means that very large amounts of alkalinity could be stored in the snowball ocean at the start of the deglaciation, possibly provided by shallow-ridge volcanism during the snowball Earth period (Gernon et al., 2016). In Fig. B.4a, we show the calcium carbonate saturation state as black contours for the already discussed two-dimensional uncertainty space formed by TA and atm. CO_2 at the start of the deglaciation. We here use the conditions of the snowball state in the ICON-ESM simulations, where there is just a thin sea-ice cover and the salinity is only weakly increased to 35.5 psu. The pCO_2 of the ocean is assumed to be in equilibrium with the atmosphere. When the ocean warms rapidly in the snowball Earth aftermath, the carbonate saturation state increases to values which can trigger the inorganic precipitation of carbonate (red contours in Fig. B.4b).

We reconstruct the total mass of warming-induced precipitated carbonate (Fig. B.4b) with a carbonate chemistry model that uses ICON-ESM simulation results as boundary conditions. Furthermore, we also conduct ICON-ESM simulations, where the process of inorganic precipitation of carbonates is implemented. Details about the implementation of inorganic carbonate precipitation can be found in

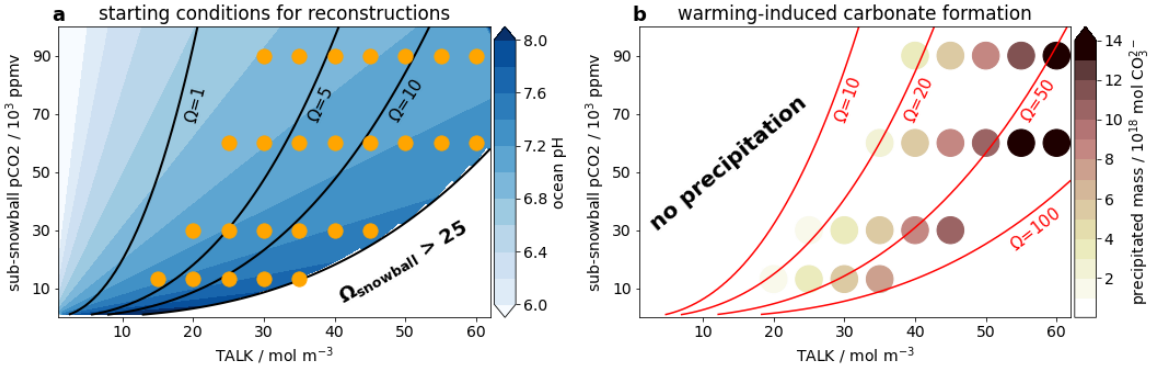

Figure B.4: **Relationship between sub-snowball ocean chemistry and carbonate precipitation. a,** Sub-snowball ocean chemistry of the reconstructions with our carbonate chemistry model. Seawater conditions are identical to the snowball state of the ICON-ESM simulation with 147 m of sea ice and T = −1.8°C, S = 35.5 psu. The orange dots represent the calculations with a carbonate chemistry model that use reference data from the ICON-ESM simulation Exp. 3.1. **b,** The reconstructed mass of carbonates that is precipitated within 5000 years through the effect of ocean warming for each calculation with the carbonate chemistry model. Note that the colored dots are plotted at the chemical conditions of the snowball state, while the red lines indicate the values of Ω under warmer conditions (T = 25°C, S = 34.3 psu, P = 1 atm) to show how ocean warming impacts $CaCO_3$ saturation. Details on the carbonate chemistry model and how inorganic carbonate precipitation is implemented are given in the method section.

the method section. We calculate that the total mass of carbonates that is formed through the warming within 5000 years from the deglaciation start can be more than 10^{19} mol CO_3^2, for the range of TA and atm. CO_2 considered here. These large amounts suggest that, for high initial ocean TA concentrations, the warming-induced carbonate precipitation was a major contributor to the formation of Marinoan cap dolostones.

The regions where carbonate precipitation occurs in ICON-ESM are mostly determined by the distribution of surface temperature. Hence, carbonate precipitation occurs only in the tropics and subtropics in our model (Fig. B.5a, b). The highest chance for carbonate precipitation is simulated to be off the western coast of Laurentia. Although there is a rough agreement between the carbonate formation regions of our model and the Marinoan rock record, a much improved representation of the continental topography and the deglaciation process is necessary for an actual reconstruction of Marinoan cap dolostone accumulation. The evolution of the deposition rate shows that most carbonate is formed in the very early stages of the deglaciation, where the warming of the ocean is most rapid. Again, a better representation of the deglaciation process could alter this temporal evolution significantly, as the meltwater inflow dilutes the carbonate concentration. Nevertheless, the total amount of carbonate formation is mostly determined by the ocean chemistry and the amount of warming. For these quantities, our calculations provide a good first-order approximation, so that also the calculated total carbonate formation is a good first-order approximation.

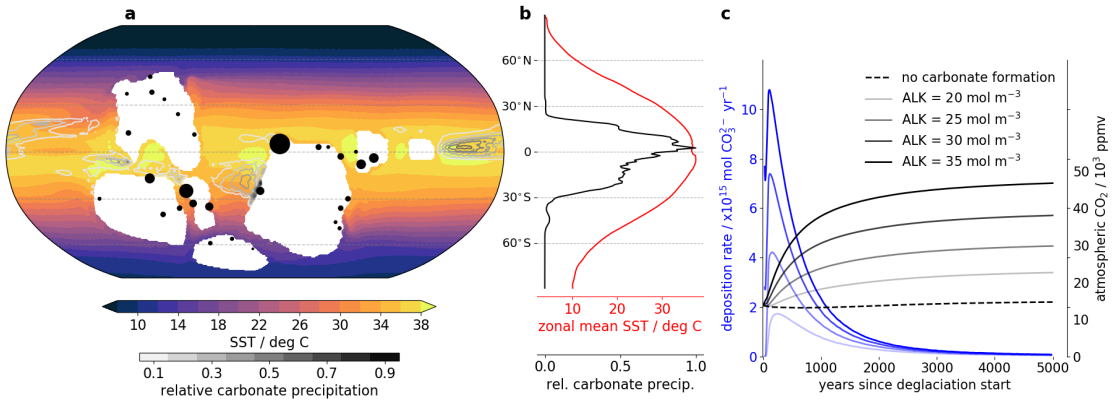

Figure B.5: **Patterns of inorganic carbonate precipitation induced by ocean warming after a snowball Earth. a**, the mean sea-surface temperature averaged over the full 5000 years from the start of the deglaciation, overlain by contour lines of relative carbonate formation as simulated with the ICON-ESM simulation Exp. 3.2. The black dots indicate the location of Marinoan cap dolostones in the geological record (data from Hoffman, 2011). The area of the dots is proportional to the thickness of the cap dolostone formation. **b**, zonal averages of the data in **a**. **c**, annual precipitation rates of carbonate (blue lines) for the reconstructions of the carbonate chemistry model with $pCO_2 = 13,200$ in the ocean at the start of the deglaciation. The black lines show the rise in atmospheric CO_2 corresponding to the carbonate formation in the reconstructions.

In contrast to carbonate formation sustained by continental weathering, carbonate formation caused by the warming of an alkaline ocean effectively removes alkalinity from the ocean, which reduces the carbon storage capacity of the ocean. Hence, this process is associated with a flux of CO_2 from the ocean into the atmosphere. We calculate here that warming-induced carbonate formation has the potential to massively strengthen the already strong greenhouse conditions (Fig. B.5c), with an approximate increase of $4 - 5 \times 10^3$ ppmv in the atmospheric CO_2 concentration for every 10^{18} mol of carbonate that are removed from the ocean. This process is partly driven by a positive feedback between the atmospheric rise in CO_2 and further increases in the saturation state as a consequence of the higher temperatures. For certain conditions, the severity of the supergreenhouse climate is therefore not set by the CO_2 level required to melt the snowball Earth, but by the chemical state of the sub-snowball ocean and the positive feedbacks acting during the supergreenhouse climate.

So far, we have assumed that the ocean pCO_2 and atm. CO_2 are in equilibrium at the start of the deglaciation. Indeed, the largest amounts of carbonate will be formed for combinations of TA and atm. CO_2 that lead to high synglacial saturation states under equilibrated conditions. If this is not the case, and the previously mentioned reservoir equilibration effect comes into play, the initial uptake of CO_2 by the ocean will reduce the carbonate saturation state and prevent the precipitation of carbonates to some degree. However, a smaller initial pCO_2 also signifies larger initial saturation states for a given initial TA and atm. CO_2 combination. Therefore, when a disequilibrium between the atmosphere and the ocean is sustainable, the total carbonate formation is actually larger for a lower initial oceanic pCO_2. Nevertheless, at higher TA, where the deposition rates are largest, no significant disequilibrium

can be sustained, due to the high carbonate saturation states. At intermediate TA concentration, both mechanisms, the reservoir equilibration and the inorganic carbonate precipitation, can occur. Our ICON-ESM simulation Exp. 5 is located at such a starting condition. Here, initially the reservoir equilibration effect causes a substantial drop in atm. CO_2, but in the long term the inorganic precipitation of carbonates leads to a flux of CO_2 from the ocean into the atmosphere. The atmospheric CO_2 concentration then stabilizes at a much higher value than what it would have without the warming-induced formation of carbonates.

B.6 A POSSIBLE MECHANISM FOR THE RAPID FORMATION OF MARINOAN CAP DOLOSTONES

The massive Marinoan cap dolostones feature various indicators that they were deposited rapidly: The dolostones are transgressive (Hoffman et al., 2017), include sedimentary features of rapid accumulation (Allen and Hoffman, 2005; Hoffman and Macdonald, 2010), and they accumulated in a freshwater-influenced environment (Liu et al., 2014; Wei et al., 2019). While a transgressive setting driven by isostatic adjustments could maybe occur for up to 6×10^4 years after a snowball Earth (Creveling and Mitrovica, 2014), a global freshwater influence can only persist for a few thousand years after the deglaciation ended (Ramme and Marotzke, 2022). The Marinoan cap dolostones therefore require a mechanism that can explain their deposition on a timescale of $\sim 10^4$ years. Gernon et al. (2016) introduced shallow-ridge volcanism as a process that could lead to a build-up of alkalinity in the ocean already during the snowball Earth period. In this study, we demonstrate that for an increased ocean alkalinity reservoir, the warming of the ocean during the deglacial period is sufficient to explain the formation of the cap dolostones in a geologically short time.

Alkalinities of > 40 mol m^{-3} will almost unavoidably lead to the inorganic formation of massive carbonate rocks within 10^4 years from the start of the deglaciation, even under extremely high atmospheric CO_2 concentrations. Within the range of $20 - 40$ mol m^{-3}, a rapid deposition of the Marinoan cap dolostones is also readily achieved if the threshold CO_2 concentration required to trigger snowball Earth deglaciation is not too large. Other contributing factors are required to explain the rapid formation of Marinoan cap dolostones at even lower alkalinities. In this study, we did not consider the alkalinity provided by continental weathering during the deglacial period. Le Hir et al. (2008b) and Le Hir et al. (2008a) have shown that the peak weathering rates in the snowball Earth aftermath can also provide large amounts of alkalinity. We therefore deduce that the formation of Marinoan cap dolostones in less than 10^4 years is also possible at sub-snowball ocean alkalinities of < 20 mol m^{-3}. In these cases, carbonates would mostly be formed in warm regions, where additional alkalinity input by rivers raises the local carbonate saturation state above the critical threshold. In summary, we conclude that the warming-induced inorganic precipitation of carbonates is a mechanism that can explain the rapid accumulation of Marinoan cap dolostones.

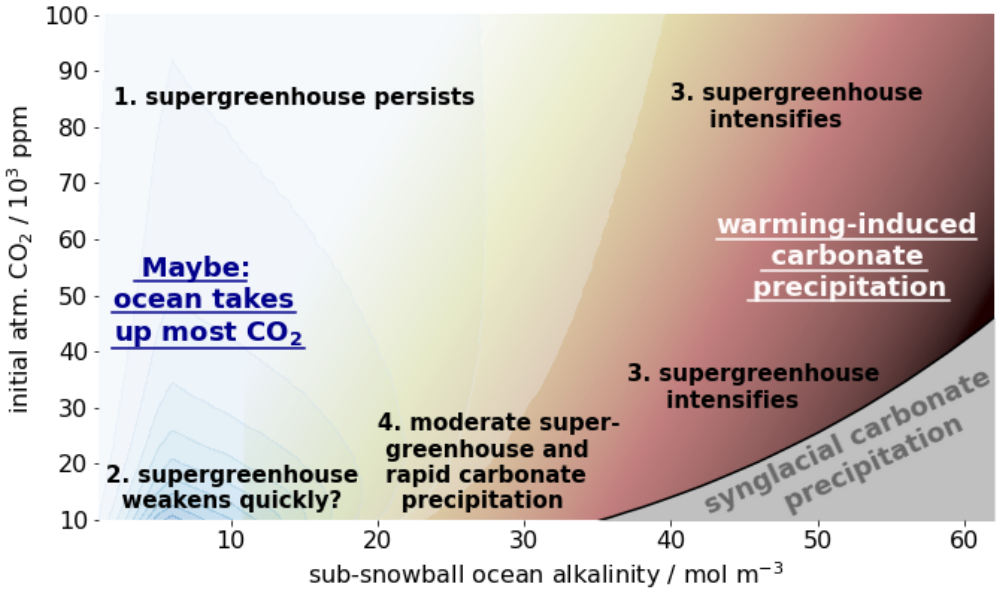

Figure B.6: **The evolution of the supergreenhouse climate after a snowball Earth.** Illustration of the different possibilities for the evolution of the supergreenhouse climate, depending on the atmospheric CO_2 concentration and the ocean chemistry at the start of the deglaciation. The numbers refer to the different scenarios described in the text.

B.7 WHAT IS THE FATE OF ATMOSPHERIC CO_2 IN THE SNOWBALL EARTH AFTERMATH?

Here, we have described how different processes impact the evolution of the carbon cycle during the first 5000 years from the start of the deglaciation of a snowball Earth. However, the major uncertainties considered here, i.e., the atmospheric CO_2 concentration required to trigger snowball termination, the sub-snowball ocean alkalinity and the efficiency of the gas exchange through the sea ice during the snowball period, allow for a wide range of possible scenarios (Fig. B.6). Now, we discuss the conditions under which the different scenarios are to be expected.

1. In the scenario that is most commonly assumed in the literature (Hoffman et al., 1998; Le Hir et al., 2008a), incorporating a very high initial atmospheric CO_2 concentration around 10^5 ppmv and a comparably low ocean alkalinity, the supergreenhouse climate will indeed persist for hundreds of thousands to millions of years (Le Hir et al., 2008b). Due to the logarithmic nature of the greenhouse effect of CO_2, reductions of atmospheric CO_2 during the deglaciation will only slightly reduce the temperatures during the supergreenhouse climate. This scenario is hard to reconcile with the deposition of Marinoan cap dolostones within 10^4 years from the start of the deglaciation because of very low carbonate saturation states in an acidic ocean.

2. The atmospheric CO_2 concentration will be reduced quickly if the ocean carbon reservoir was not in equilibrium with the high atmospheric CO_2 concentration and depleted at the start of the deglaciation. For initial alkalinity of around

5-10 mol m^{-3}, this could lead to a rapid end of the supergreenhouse climate within a few thousand years if the initial atmospheric CO_2 concentration was low. A fast decline of the strong greenhouse conditions is conceivable also for a broader range of initial alkalinity and atmospheric CO_2 concentrations if other processes contribute to the oceanic CO_2 uptake more than they did in our model simulations.

3. The supergreenhouse climate will intensify over time if an alkalinity-rich ocean warms and leads to the inorganic precipitation of carbonates from the water column. While this scenario is consistent with the rapid deposition of Marinoan cap dolostones, it is questionable whether the associated massive increase in atmospheric CO_2 concentrations can be reconciled with geological proxy data (Kasemann et al., 2005; Bao et al., 2008, 2009; Sansjofre et al., 2011).

4. A compelling scenario occurs for an initial atmospheric CO_2 concentration of less than about 5×10^4 ppmv and moderate alkalinities of 15-30 mol m^{-3}. Here, the warming of the ocean can already cause the inorganic precipitation of carbonates. At the same time, a relatively fast weakening of the supergreenhouse conditions is possible if the mechanisms that reduce atmospheric CO_2 are strong and continental weathering keeps the ocean alkalinity high. Consequently, this scenario can explain a rapid deposition of Marinoan cap dolostones and may lead to a moderate supergreenhouse climate.

We conclude that the opposing scenarios of either a rapid decline or a long-term increase of the atmospheric CO_2 concentration are both possible because of the large uncertainties that come with the deglaciation of a snowball Earth. Our results suggest that the severity of the supergreenhouse climate is not only set by the atmospheric CO_2 concentration required to trigger snowball termination, but also by the chemical state of the ocean at the start of the deglaciation. We demonstrate that a rapid formation of Marinoan cap dolostones and a moderate and short-lived supergreenhouse climate are explainable features of the snowball Earth aftermath.

B.8 METHODS

B.8.1 *ICON-ESM model description*

The icosahedral nonhydrostatic model ICON-ESM is a recently developed Earth system model with an unstructured grid and quasi-uniform grid cell areas (Jungclaus et al., 2022). It couples the atmosphere general circulation model ICON-A (Giorgetta et al., 2018) with the ocean general circulation model ICON-O (Korn, 2017; Korn et al., 2022) and the ocean biogeochemistry model HAMOCC (Ilyina et al., 2013). It furthermore includes an interactive carbon cycle, meaning that carbon is handled as a mass-conserving, prognostic tracer in all components. We here use ICON-ESM in a coarse resolution setup that is adapted to the boundary conditions of the Marinoan snowball Earth. The setup of the two physical components (atmosphere and ocean) is largely identical to the model version that was used and described in more detail in Ramme and Marotzke (2022), but includes an improved representation of sea-ice dynamics (Mehlmann and Korn, 2021). Therefore, we here only present a description

of the specifics of the ocean biogeochemistry component that are important for this study and refer the reader to the cited literature for more information.

The HAMOCC model describes the biogeochemical dynamics of at least 17 prognostic state variables that are advected by the circulation calculated in the ocean model. These tracers include total alkalinity (TA) and dissolved inorganic carbon (DIC), which are sufficient to calculate the carbonate chemistry, as well as tracers for primary producers, the main nutrients, dissolved gases and further biogeochemical components (see Ilyina et al., 2013, for the full list). As the model is run with an interactive carbon cycle, HAMOCC receives information on the concentration of CO_2 in the overlying atmospheric grid cell at every ocean time step (60 minutes) and calculates the surface flux of CO_2 based on the difference to the pCO_2 in the ocean surface layer. We tuned HAMOCC for a good representation of the modern biogeochemistry in a setup with present-day continents and then use the calibrated parameter settings in the Marinoan setup.

Some modifications of the biogeochemical implementations are made in order to adapt the model for an application to the Neoproterozoic conditions: 1. Shell production by phytoplankton was turned off, as both silicate shell producers and marine calcifiers had not yet developed in the late Neoproterozoic (Knoll, 2003). 2. The standard implementation of phytoplankton growth uses an exponential dependence on temperature in the default HAMOCC setup. This would lead to unrealistically high growth rates during the supergreenhouse climate. Therefore, we modified the dependence to let the growth rate of phytoplankton decrease at temperatures above 35°C. Cyanobacteria growth is only limited by temperatures below 25°C 3. In the standard HAMOCC model, iron is added to the ocean in the form of a time-invariant dust deposition at the ocean surface coming from present-day observations. We modified this input to a globally uniform, high value, only reducing northwards in the ocean-dominated latitudes >50°N. This accounts for the high rates of dust production on the bare Neoproterozoic continents (Liu et al., 2020). 4. The atmospheric concentration of oxygen is assumed to be 50% of the present atmospheric level and is constant in time. 5. Calcium is added to the list of state variables in those simulations, where the inorganic precipitation of carbonate is activated.

B.8.2 *Simulation design*

All our simulations incorporate the ocean biogeochemistry component and a prognostic carbon cycle at all times, and transitions in the climate are initiated by prescribing positive or negative emissions of CO_2 into the atmosphere. As the focus of this study is on the aftermath of a snowball Earth, the initiation and the snowball state itself are simplified. The simulation procedure starts with a stable control climate at an atmospheric CO_2 concentration of 1500 ppmv. The model is then forced into a cold pre-snowball state at 112 ppmv CO_2. The snowball state itself is then triggered by removing another 400 GT C over a short time of 200 years. After 300 years without carbon emissions to allow for some growth of the sea ice, carbon is added to the atmosphere at an extremely high rate of 100 GT C yr^{-1} for another 300 years. This causes a rise of the atmospheric CO_2 concentration to 13,710 ppmv, which is not enough to initiate deglaciation in our model. As higher CO_2 concentrations

would cause instabilities in the atmosphere component, we trigger the deglaciation through a 100-year long reduction of the albedo of snow on ice to a value of 0.6. The onset of this reduction is what we refer to as the start of the deglaciation in this paper, and from that point on the model simulations are let run freely without prescribing any further emissions of CO_2.

At the start of the deglaciation, the ocean under the ice is well mixed with largely uniform values. We make use of this property by adapting the inventories of some of the biogeochemical tracers to create a set of additional simulations. In the control climate and during the snowball cycle, the biogeochemical inventories of the ocean are still similar to modern values - a remnant of the initialisation of the model. These inventories remain unchanged in the reference simulation Exp. 1. In all other simulations, we adapt some of the state variables to represent a chemically evolved state more representative for a sub-snowball ocean (Le Hir et al., 2008a; Gernon et al., 2016; Reinhard et al., 2017). All modified values (see Tab. B.1 in the SI) are identical in the different additional experiments, except for TA and DIC, which we use to cover a range of possible scenarios for the post-snowball evolution. A detailed overview of the different ICON-ESM simulations is presented in the supporting information.

B.8.3 *Carbonate chemistry model*

The idealized carbonate chemistry calculations that extend the ICON-ESM simulations are based on a model that is mostly a translation of the carbonate chemistry implementation of HAMOCC into an easy-to-use python code. The model then derives the chemical conditions based on two state variables of the carbonate system, TA and DIC, using information about temperature, salinity and pressure for calculating the dissociation constants. Solutions to this carbonate chemistry system are described comprehensively in the literature (e.g. Sarmiento, 2013). The source code of the carbonate chemistry model is available from the authors upon request.

The ICON-ESM simulations that include the inorganic precipitation of carbonate from supersaturated waters calculate the carbonate formation rate as

$$R = \begin{cases} k(\Omega_{CaCO_3} - \Omega_{thresh})^3 & \text{if } \Omega_{CaCO_3} > \Omega_{thresh} \\ 0 & \text{otherwise,} \end{cases} \tag{B.1}$$

following Zeebe and Westbroek (2003) and Hood et al. (2022), where k is a rate constant and $\Omega_{thresh} = 15$ is the threshold saturation above which the inorganic carbonate precipitation starts. We use the saturation state of calcium carbonate, Ω_{CaCO_3}, as a proxy for the inorganic precipitation of $CaMg(CO_3)_2$, because of the large uncertainties regarding the formation of dolomite (Bénézeth et al., 2018; Hood et al., 2022). We further assume that any TA concentration that is substantially higher than the modern concentration was added in the form of Ca^{2+} or Mg^{2+} and that the seawater ratio of Mg^{2+} to Ca^{2+} is 3:1. As we assume the formation of dolomite, only one mole of Ca^{2+} is removed for every two moles of carbonate, and we only track Ca^{2+} explicitly in the model. These assumptions reflect the large uncertainties in carbonate precipitation dynamics and the seawater composition during the aftermath of the Marinoan snowball Earth. However, the results presented in this study are

mostly of a qualitative nature, and different assumptions would only shift a certain scenario to a different location within the spread of uncertainties related to the ocean's chemical conditions of that time.

In this paper, we also present a set of carbonate chemistry model calculations that extend the ICON-ESM simulations to a larger range of ocean chemistries and initial atmospheric CO_2 concentrations. These calculations are designed in order to reconstruct the amount of carbonate that could have possibly precipitated from supersaturated ocean waters, and we refer to these calculations as reconstructions here. The reconstructions use the annual mean simulation output of Exp. 3.1, which has an ocean pCO_2 initially equilibrated with the atmospheric CO_2 concentration and a sub-snowball ocean alkalinity of 15 mol m^{-3}. The simulation itself did not include the process of inorganic precipitation of carbonates. The fields of TA and DIC are adapted by adding globally uniform concentrations. The reconstruction model works with a time step of one year. In each time step, Ω_{CaCO_3} is calculated for every grid cell of the surface ocean, and if $\Omega_{CaCO_3} > \Omega_{thresh}$, TA, DIC and Ca^{2+} are removed with a ratio of 2:1:0.5 until the saturation state in this grid cell is below the threshold. As this process increases pCO_2, DIC is removed from the global surface ocean in order to reflect outgassing of CO_2. The CO_2 concentration of the atmosphere is increased accordingly until a new equilibrium is established. The increased atmospheric CO_2 concentration then feeds back to the temperature in the surface ocean, assuming a constant climate sensitivity of 4.9 K per doubling of CO_2 (Ramme and Marotzke, 2022). The depleted local reservoirs of TA and DIC in each surface grid cell are then resupplied on two timescales from a global surface ocean and a deep ocean reservoir. The parameterization of this resupply is the largest contributer to uncertainties in the timescale of carbonate formation. All parameterizations of the carbonate chemistry model were tuned for a good reconstruction of the inorganic precipitation dynamics simulated in Exp. 3.2.

B.9 SUPPORTING INFORMATION

B.9.1 *List of experiments*

We here provide a list of the different ICON-ESM simulations presented in this paper. An overview of the chemical conditions at the start of the deglaciation and the conditions after 5000 simulation years can be found in Table B.1. Apart from the default simulation Exp. 1, all other simulations adopt the idea of a "chemically evolved ocean", which results from the chemical alteration of the seawater during the snowball state, driven by hydrothermal and weathering activities (Le Hir et al., 2008a; Gernon et al., 2016; Reinhard et al., 2017). In these simulations, the phosphate inventory is increased to approximately 5 times the modern concentration (Planavsky et al., 2010). Similarly, iron is increased by the same factor, while oxygen is reduced to anoxic conditions, in order to replicate largely reducing conditions during the snowball state (Hoffman and Schrag, 2002). The nitrate inventory is unchanged, because of sparse information and the fact that the nitrate inventory is not closed due to the processes of denitrification and N2-fixation by cyanobacteria (Peng et al., 2020). In the following, we present a short description of the individual

experiments and their motivation.

Exp. 1: This is the default simulation that represents a continuous simulation from a pre-snowball control climate through the snowball state into the supergreenhouse climate without any adaptions of the inventories. In contrast to all other simulations, in Exp. 1 the ocean is not chemically evolved and the tracer inventories are similar to modern values. As the snowball cycle itself is short, the model has no time for an equilibration of the atmosphere and ocean carbon reservoirs, so that DIC in the ocean is largely depleted. Due to the low alkalinity of TA=2.47 mol m^{-3}, the calcium carbonate saturation state is far below the critical threshold value in the snowball state, and the pH of the ocean drops very quickly during the deglaciation, as the ocean equilibrates with the high atm. CO_2. All other simluations, except for Exp. 4, are started from the end of the snowball cycle in this simulation, so that the experiments only differ from the start of the deglaciation onwards.

Exp. 2: Here, we try to achieve a maximum reduction of the atmospheric CO_2 concentration through the reservoir equilibration effect. Therefore, TA is 6 mol m^{-3}, close to the maximum depicted in Fig. B.2b of the main text, and DIC is reduced to a very low value, resulting in an ocean pCO_2 of 180 ppm at the start of the deglaciation. As the sub-snowball calcium carbonate saturation state is already quite high, the inorganic precipitation of carbonates is activated in this simulation. However, it does not play a significant role, because the saturation state drops quickly during the phase of reservoir equilibration.

Exp. 3.1 and 3.2 Exp. 3.1 is a reference simulation for many other experiments, and it provides the simulation output that is fed into the reconstructions with the carbonate chemistry model. It has a comparably high TA of 15 mol m^{-3} and the DIC concentration is chosen so that the ocean pCO_2 is in equilibrium with atm. CO_2 at the start of the deglaciation. Exp. 3.2 is identical to Exp. 3.1, only that Exp. 3.2 includes the inorganic precipitation of carbonates from the water column, while this process is deactivated in Exp. 3.1. This allows for an isolated quantification of the effect of inorganic carbonate precipitation on the evolution of the climate, which we use in order to tune our reconstructions with the carbonate chemistry model to produce a similar behavior.

Exp. 4: This simulation is based on a different snowball cycle experiment, and its main purpose is to quantify the effect of dilution on the oceanic carbon uptake. Here, a total freshwater volume of 1000 m of sea-level equivalent was removed over a time scale of several thousand years during the transition from our control climate into a cold pre-snowball state. The snowball period itself is then similar to the representation in the default simulation Exp. 1, with a terminal mean sea-ice thickness of 149 m. Together with the start of the deglaciation, a globally distributed freshwater flux is implemented, adding every year freshwater with a volume of 0.5 m of sea level back to the ocean over a timescale of 2000 years. As this freshwater input suddenly stops in year 2000 from the deglaciation start, most timeseries of this simulation show a kink at this time (Fig. B.3 in the main text and Fig. B.7 in the SI). The biogeochemical concentrations of the ocean at the start of the deglaciation are

identical to those in Exp. 3.1, so that all differences to Exp. 3.1 are direct or indirect consequences of the dilution effect.

Exp. 5: Exp. 5 has the same TA as Exp. 3.1, but DIC is reduced to a very low value, which leads to a calcium carbonate saturation state of 24.3 at the start of the deglaciation. This simulation was designed in order to study the interplay of the competing effects of the oceanic uptake of CO_2 through the reservoir equilibration mechanism and the possible outgassing of CO_2 during the inorganic precipitation of carbonates. Inorganic precipitation of carbonates is implemented as described in Eq. B.1, so that here the initial calcium carbonate saturation state is already larger than the threshold. This is motivated by the idea that during the snowball state there are no organic particles that could function as condensation nuclei, and higher saturation states than in an ice-free ocean are sustainable. Due to the melting of the sea ice and the equilibration with the high atm. CO_2, the oversaturation initially drops below the threshold value, but then increases again, as the ocean warms and waters with higher alkalinity are mixed to the surface.

B.9.2 *Supplementary figures and tables*

Table B.1: **Overview table of the ICON-ESM simulations.** Presented are the physical and chemical conditions at the start of the deglaciation, which either result from the preceding modelling procedure or were set manually (italic font). The values in the second part of the table show the globally averaged conditions after 5000 simulation years. A description of the experiments is given in the supporting information text.

	Exp. 1	Exp. 2	Exp. 3.1	Exp. 3.2	Exp. 4	Exp. 5
Conditions at start of deglaciation						
- atm. CO_2 [ppmv]	13710	13710	13710	13710	13720	13710
- ice thickness [m]	147	147	147	147	149	147
- ocean salinity [psu]	35.5	35.5	35.5	35.5	*50.5*	35.5
- ocean temperature [°C]	-1.8	-1.8	-1.8	-1.8	-1.8	-1.8
- TA [mol m^{-3}]	2.47	*6*	*15*	*15*	*15*	*15*
- DIC [mol m^{-3}]	2.12	*5.05*	*15.75*	*15.75*	*15.75*	*14.1*
- PO_4 [mol m^{-3}]	0.0026	*0.01*	*0.01*	*0.01*	*0.01*	*0.01*
- NO_3 [mol m^{-3}]	0.025	0.025	0.025	0.025	0.036	0.025
- O_2 [mol m^{-3}]	0.16	*0.001*	*0.001*	*0.001*	*0.001*	*0.001*
- Fe [mol m^{-3}]	10^{-6}	$5{\cdot}10^{-6}$	$5{\cdot}10^{-6}$	$5{\cdot}10^{-6}$	$5{\cdot}10^{-6}$	$5{\cdot}10^{-6}$
- ocean pCO_2 [ppm]	117	180	13420	13420	15200	1532
- mean surface pH	8.5	8.7	7.3	7.3	7.3	8.2
- Ω_{CaCO_3} (below ice)	5.4	19.0	3.5	3.5	2.7	24.3
Conditions after 5000 simulation years						
- atm. CO_2 [pppmv]	7969	4319	14681	17492	12993	11728
- GSAT [°C]	23.3	17.6	29.3	31.4	27.5	26.5
- GSAT Drift [K (100 yr)$^{-1}$]	±0.0	±0.0	+0.05	+0.1	+0.05	+0.07
- mean surface pH	6.68	7.36	7.30	7.20	7.19	7.31
- carb. formation [10^{15} mol]	0.0	0.01	-	691	-	1532
- NPP (phyto.) [GT C yr^{-1}]	38	55	63	62	58	61
- NPP (cyano.) [GT C yr^{-1}]	32	81	102	107	75	96

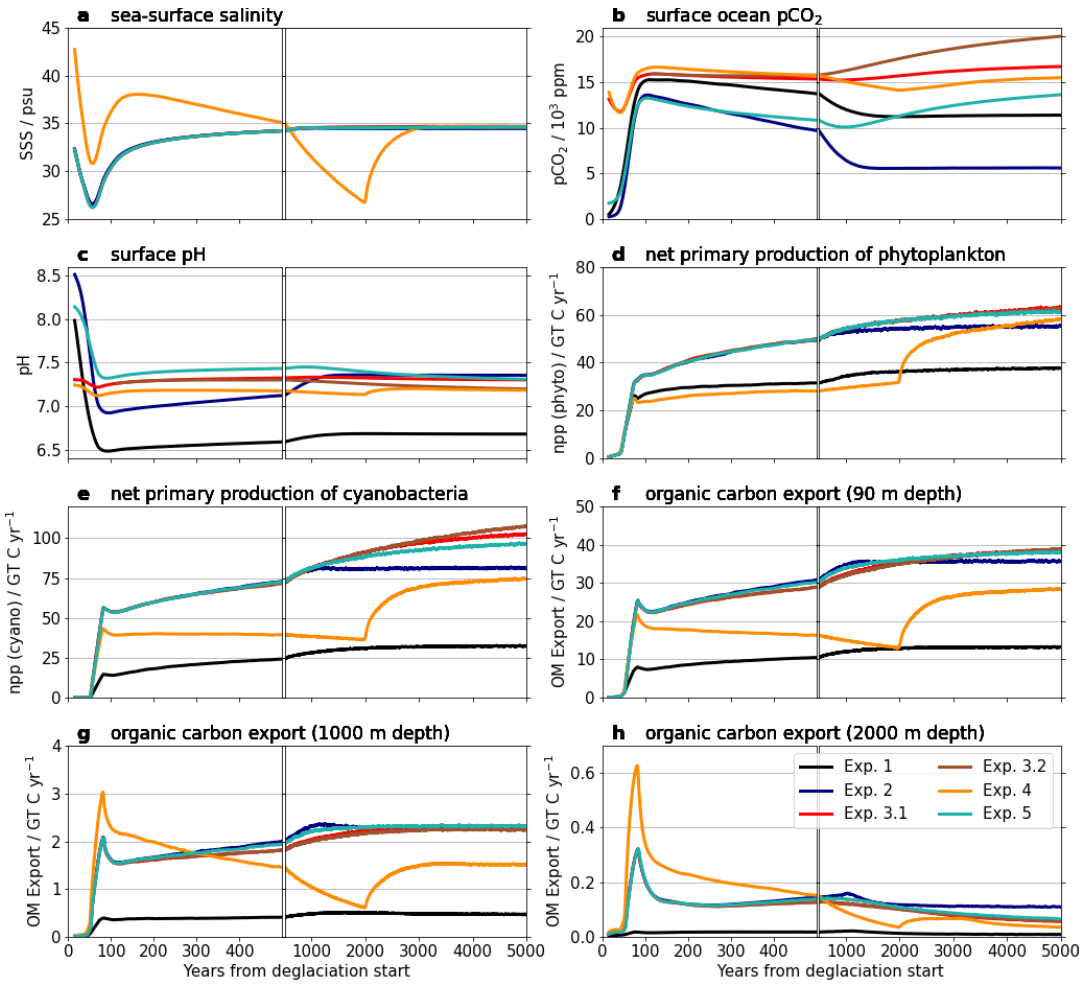

Figure B.7: **Timeseries of global carbon cycle variables from the ICON-ESM simulations.** For more information on the experiment settings see the list of experiments in the supporting information. All timeseries show 30-year running mean data. Note the change in scale of the time axis at year 500. Timeseries of more variables can be found in the main text.

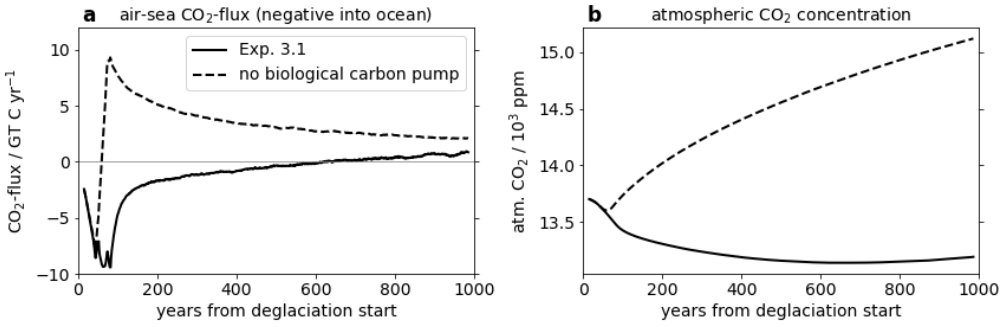

Figure B.8: **Effect of suppressed primary production on the carbon cycle.** Shown are the air-sea CO_2-flux and the atmospheric CO_2 concentration of Exp. 3.1 and a test simulation with suppressed primary production. The chosen time period represents the main phase of the deglaciation, where, both, temperature and primary production increase strongly. The data is represented by 30-year running means.

BIBLIOGRAPHY

Abbot, D. S., Eisenman, I., and Pierrehumbert, R. T. (2010). "The importance of ice vertical resolution for Snowball climate and deglaciation." In: *J. Climate* 23.22, pp. 6100–6109. DOI: 10.1175/2010JCLI3693.1.

Abbot, D. S. and Pierrehumbert, R. T. (2010). "Mudball: Surface dust and snowball Earth deglaciation." In: *J. Geophys. Res.-Atmos.* 115.D3. DOI: 10.1029/2009JD012007.

Abbot, D. S., Voigt, A., Branson, M., Pierrehumbert, R. T., Pollard, D., Le Hir, G., and Koll, D. D. (2012). "Clouds and snowball Earth deglaciation." In: *Geophys. Res. Lett.* 39.20. DOI: 10.1029/2012GL052861.

Abbot, D. S., Voigt, A., Li, D., Hir, G. L., Pierrehumbert, R. T., Branson, M., Pollard, D., and B. Koll, D. D. (2013). "Robust elements of Snowball Earth atmospheric circulation and oases for life." In: *J. Geophys. Res.-Atmos.* 118.12, pp. 6017–6027. DOI: 10.1002/jgrd.50540.

Ahm, A.-S. C., Maloof, A. C., Macdonald, F. A., Hoffman, P. F., Bjerrum, C. J., Bold, U., Rose, C. V., Strauss, J. V., and Higgins, J. A. (2019). "An early diagenetic deglacial origin for basal Ediacaran "cap dolostones"." In: *Earth Planet. Sc. Lett.* 506, pp. 292–307. DOI: 10.1016/j.epsl.2018.10.046.

Allen, P. A. and Hoffman, P. F. (2005). "Extreme winds and waves in the aftermath of a Neoproterozoic glaciation." In: *Nature* 433.7022, pp. 123–127. DOI: 10.1038/nature03176.

Appen, W.-J. von, Waite, A. M., Bergmann, M., Bienhold, C., Boebel, O., Bracher, A., Cisewski, B., Hagemann, J., Hoppema, M., Iversen, M. H., et al. (2021). "Sea-ice derived meltwater stratification slows the biological carbon pump: results from continuous observations." In: *Nat. comm.* 12.1, pp. 1–16. DOI: 10.1038/s41467-021-26943-z.

Ashkenazy, Y., Gildor, H., Losch, M., Macdonald, F. A., Schrag, D. P., and Tziperman, E. (2013). "Dynamics of a Snowball Earth ocean." In: *Nature* 495.7439, pp. 90–93. DOI: 10.1038/nature11894.

Bao, H., Fairchild, I. J., Wynn, P. M., and Spötl, C. (2009). "Stretching the envelope of past surface environments: Neoproterozoic glacial lakes from Svalbard." In: *Science* 323.5910, pp. 119–122. DOI: 10.1126/science.1165373.

Bao, H., Lyons, J., and Zhou, C. (2008). "Triple oxygen isotope evidence for elevated CO 2 levels after a Neoproterozoic glaciation." In: *Nature* 453.7194, pp. 504–506. DOI: 10.1038/nature06959.

Benn, D. I., Le Hir, G., Bao, H., Donnadieu, Y., Dumas, C., Fleming, E. J., Hambrey, M. J., McMillan, E. A., Petronis, M. S., Ramstein, G., et al. (2015). "Orbitally forced ice sheet fluctuations during the Marinoan Snowball Earth glaciation." In: *Nat. Geosci.* 8.9, pp. 704–707. DOI: 10.1038/ngeo2502.

Brocks, J. J. and Butterfield, N. J. (2009). "Early animals out in the cold." In: *Nature* 457.7230, pp. 672–673. DOI: 10.1038/457672a.

Brocks, J. J., Jarrett, A. J., Sirantoine, E., Hallmann, C., Hoshino, Y., and Liyanage, T. (2017). "The rise of algae in Cryogenian oceans and the emergence of animals." In: *Nature* 548.7669, pp. 578–581. DOI: 10.1038/nature23457.

Bryan, K. and Cox, M. D. (1972). "The circulation of the world ocean: a numerical study. Part I, a homogeneous model." In: *J. Phys. Oceanogr.* 2.4, pp. 319–335. DOI: 10.1175/1520-0485(1972)002<0319:TCOTWO>2.0.CO;2.

Budyko, M. I. (1969). "The effect of solar radiation variations on the climate of the Earth." In: *Tellus* 21.5, pp. 611–619. DOI: 10.3402/tellusa.v21i5.10109.

Bénézeth, P., Berninger, U.-N., Bovet, N., Schott, J., and Oelkers, E. H. (2018). "Experimental determination of the solubility product of dolomite at 50–253°C." In: *Geochim. Cosmochim. Ac.* 224, pp. 262–275. ISSN: 0016-7037. DOI: 10.1016/j.gca.2018.01.016.

Caldeira, K. and Kasting, J. F. (1992). "Susceptibility of the early Earth to irreversible glaciation caused by carbon dioxide clouds." In: *Nature* 359.6392, pp. 226–228. DOI: 10.1038/359226a0.

Calver, C., Crowley, J., Wingate, M., Evans, D., Raub, T., and Schmitz, M. (2013). "Globally synchronous Marinoan deglaciation indicated by U-Pb geochronology of the Cottons Breccia, Tasmania, Australia." In: *Geology* 41.10, pp. 1127–1130. DOI: 10.1130/G34568.1.

Campin, J.-M., Marshall, J., and Ferreira, D. (2008). "Sea ice–ocean coupling using a rescaled vertical coordinate z." In: *Ocean Model.* 24.1-2, pp. 1–14. DOI: 10.1016/j.ocemod.2008.05.005.

Cariolle, D. and Teyssedre, H. (2007). "A revised linear ozone photochemistry parameterization for use in transport and general circulation models: multi-annual simulations." In: *Atmos. Chem. Phys.* 7.9, pp. 2183–2196. DOI: 10.5194/acp-7-2183-2007.

Chen, D., Rojas, M., Samset, B., Cobb, K., Diongue Niang, A., Edwards, P., Emori, S., Faria, S., Hawkins, E., Hope, P., Huybrechts, P., Meinshausen, M., Mustafa, S., Plattner, G.-K., and Tréguier, A.-M. (2021). "Framing, Context, and Methods." In: *Climate Change 2021: The Physical Science Basis. Contribution of Working Group I to the Sixth Assessment Report of the Intergovernmental Panel on Climate Change*. Ed. by V. Masson-Delmotte, P. Zhai, A. Pirani, S. Connors, C. Péan, S. Berger, N. Caud, Y. Chen, L. Goldfarb, M. Gomis, M. Huang, K. Leitzell, E. Lonnoy, J. Matthews, T. Maycock, T. Waterfield, O. Yelekçi, R. Yu, and B. Zhou. Cambridge, United Kingdom and New York, NY, USA: Cambridge University Press, 147–286. DOI: 10.1017/9781009157896.003.

Creveling, J. R. and Mitrovica, J. X. (2014). "The sea-level fingerprint of a Snowball Earth deglaciation." In: *Earth Planet. Sc. Lett.* 399, pp. 74–85. DOI: 10.1016/j.epsl.2014.04.029.

Crueger, T., Giorgetta, M. A., Brokopf, R., Esch, M., Fiedler, S., Hohenegger, C., Kornblueh, L., Mauritsen, T., Nam, C., Naumann, A. K., et al. (2018). "ICON-A, The atmosphere component of the ICON Earth system model: II. Model evaluation." In: *J. Adv. Model. Earth. Sy.* 10.7, pp. 1638–1662. DOI: 10.1029/2017MS001233.

Curry, J. A., Schramm, J. L., and Ebert, E. E. (1995). "Sea Ice-Albedo Climate Feedback Mechanism." In: *J. Climate* 8.2, pp. 240 –247. DOI: 10.1175/1520-0442(1995)008<0240:SIACFM>2.0.CO;2.

DeVries, T. (2022). "The Ocean Carbon Cycle." In: *Annual Review of Environment and Resources* 47.1, pp. 317–341. DOI: 10.1146/annurev-environ-120920-111307.

Dessert, C., Dupré, B., François, L. M., Schott, J., Gaillardet, J., Chakrapani, G., and Bajpai, S. (2001). "Erosion of Deccan Traps determined by river geochemistry:

impact on the global climate and the 87Sr/86Sr ratio of seawater." In: *Earth Planet. Sc. Lett.* 188.3, pp. 459–474. DOI: 10.1016/S0012-821X(01)00317-X.

Dohrmann, M. and Wörheide, G. (2017). "Dating early animal evolution using phylogenomic data." In: *Sci. Rep.* 7.1, pp. 1–6. DOI: 10.1038/s41598-017-03791-w.

Donnadieu, Y., Goddéris, Y., Ramstein, G., Nédélec, A., and Meert, J. (2004). "A 'snowball Earth' climate triggered by continental break-up through changes in runoff." In: *Nature* 428.6980, pp. 303–306. DOI: 10.1038/nature02408.

Droser, M. L. and Gehling, J. G. (2015). "The advent of animals: The view from the Ediacaran." In: *P. Natl. Acad. Sci.* 112.16, pp. 4865–4870. DOI: 10.1073/pnas.1403669112.

Edkins, N. J. and Davies, R. (2021). "Atmospheric Pressure and Snowball Earth Deglaciation." In: *J. Geophys. Res.-Atmospheres* 126.24, e2021JD035423. DOI: 10.1029/2021JD035423.

Egleston, E. S., Sabine, C. L., and Morel, F. M. M. (2010). "Revelle revisited: Buffer factors that quantify the response of ocean chemistry to changes in DIC and alkalinity." In: *Global Biogeochem. Cy.* 24.1. DOI: 10.1029/2008GB003407.

Erwin, D. H. (2015). "Early metazoan life: divergence, environment and ecology." In: *Philos. T. Roy. Soc. B.* 370.1684, p. 20150036. DOI: 10.1098/rstb.2015.0036.

Erwin, D. H., Laflamme, M., Tweedt, S. M., Sperling, E. A., Pisani, D., and Peterson, K. J. (2011). "The Cambrian Conundrum: Early Divergence and Later Ecological Success in the Early History of Animals." In: *Science* 334.6059, pp. 1091–1097. DOI: 10.1126/science.1206375.

Fabre, S. and Berger, G. (Nov. 2012). "How tillite weathering during the snowball Earth aftermath induced cap carbonate deposition." In: *Geology* 40.11, pp. 1027–1030. DOI: 10.1130/G33340.1.

Fabre, S., Berger, G., and Nédélec, A. (2011). "Modeling of continental weathering under high-CO2 atmospheres during Precambrian times." In: *Geochem. Geophy. Geosy.* 12.10. DOI: 10.1029/2010GC003444.

Ferreira, D., Marshall, J., and Rose, B. (2011). "Climate determinism revisited: Multiple equilibria in a complex climate model." In: *J. Climate* 24.4, pp. 992–1012. DOI: 10.1175/2010JCLI3580.1.

Fiorella, R. P. and Poulsen, C. J. (2013). "Dehumidification over tropical continents reduces climate sensitivity and inhibits snowball Earth initiation." In: *J. Climate* 26.23, pp. 9677–9695. DOI: 10.1175/JCLI-D-12-00820.1.

Font, E, Nédélec, A, Trindade, R., and Moreau, C (2010). "Fast or slow melting of the Marinoan snowball Earth? The cap dolostone record." In: *Palaeogeogr. Palaeoclimatol. Palaeoecol.* 295.1-2, pp. 215–225. DOI: 10.1016/j.palaeo.2010.05.039.

Fransson, A., Chierici, M., Yager, P. L., and Smith Jr., W. O. (2011). "Antarctic sea ice carbon dioxide system and controls." In: *J. Geophys. Res.-Oceans* 116.C12. DOI: 10.1029/2010JC006844.

Gaspar, P., Grégoris, Y., and Lefevre, J.-M. (1990). "A simple eddy kinetic energy model for simulations of the oceanic vertical mixing: Tests at station Papa and Long-Term Upper Ocean Study site." In: *J. Geophys. Res.-Oceans* 95.C9, pp. 16179–16193. DOI: 10.1029/JC095iC09p16179.

Gent, P. R., Willebrand, J., McDougall, T. J., and McWilliams, J. C. (1995). "Parameterizing eddy-induced tracer transports in ocean circulation models." In:

J. Phys. Oceanogr. 25.4, pp. 463–474. DOI: 10.1175/1520-0485(1995)025<0463:PEITTI>2.0.CO;2.

Gernon, T., Hincks, T., Tyrrell, T, Rohling, E., and Palmer, M. (2016). "Snowball Earth ocean chemistry driven by extensive ridge volcanism during Rodinia breakup." In: *Nat. Geosci.* 9.3, pp. 242–248. DOI: 10.1038/ngeo2632.

Giorgetta, M. A., Brokopf, R., Crueger, T., Esch, M., Fiedler, S., Helmert, J, Hohenegger, C., Kornblueh, L., Köhler, M, Manzini, E., et al. (2018). "ICON-A, the atmosphere component of the ICON Earth System Model: I. Model description." In: *J. Adv. Model. Earth. Sy.* 10.7, pp. 1613–1637. DOI: 10.1029/2017MS001242.

Giorgetta, M. A., Roeckner, E., Mauritsen, T., Bader, J., Crueger, T., Esch, M., Rast, S., Kornblueh, L., Schmidt, H., Kinne, S., et al. (2013). "The atmospheric general circulation model ECHAM6-model description." In.

Gough, D. (1981). "Solar interior structure and luminosity variations." In: *Physics of solar variations*. Springer, pp. 21–34. DOI: 10.1007/978-94-010-9633-1_4.

Griffiths, H. J., Whittle, R. J., and Mitchell, E. G. (2022). "Animal survival strategies in Neoproterozoic ice worlds." In: *Global Change Biol.* DOI: 10.1111/gcb.16393.

Grimm, R., Notz, D., Glud, R., Rysgaard, S., and Six, K. (Nov. 2016). "Assessment of the sea-ice carbon pump: Insights from a three-dimensional ocean-sea-ice-biogeochemical model (MPIOM/HAMOCC)." In: *Elementa, Science of the Anthropocene* 4. DOI: 10.12952/journal.elementa.000136.

Gulev, S., Thorne, P., Ahn, J., Dentener, F., Domingues, C., Gerland, S., Gong, D., Kaufman, D., Nnamchi, H., Quaas, J., Rivera, J., Sathyendranath, S., Smith, S., Trewin, B., Schuckmann, K. von, and Vose, R. (2021). "Changing State of the Climate System." In: *Climate Change 2021: The Physical Science Basis. Contribution of Working Group I to the Sixth Assessment Report of the Intergovernmental Panel on Climate Change*. Ed. by V. Masson-Delmotte, P. Zhai, A. Pirani, S. Connors, C. Péan, S. Berger, N. Caud, Y. Chen, L. Goldfarb, M. Gomis, M. Huang, K. Leitzell, E. Lonnoy, J. Matthews, T. Maycock, T. Waterfield, O. Yelekçi, R. Yu, and B. Zhou. Cambridge, United Kingdom and New York, NY, USA: Cambridge University Press, 287–422. DOI: 10.1017/9781009157896.004.

Hambrey, M. J. and Harland, W. B. (1981). *Earth's pre-Pleistocene glacial record*. Cambridge, United Kingdom: Cambridge University Press.

Hanke, M., Redler, R., Holfeld, T., and Yastremsky, M. (2016). "YAC 1.2. 0: new aspects for coupling software in Earth system modelling." In: *Geosci. Model Dev.* 9, pp. 2755–2769. DOI: 10.5194/gmd-9-2755-2016.

Harland, W. B. (1964). "Evidence of Late Precambrian glaciation and its significance." In: *Problems in palaeoclimatology* 705, pp. 119–149.

Hartmann, J., Moosdorf, N., Lauerwald, R., Hinderer, M., and West, A. J. (2014). "Global chemical weathering and associated P-release — The role of lithology, temperature and soil properties." In: *Chem. Geol.* 363, pp. 145–163. DOI: 10.1016/j.chemgeo.2013.10.025.

Heinze, M. and Ilyina, T. (2015). "Ocean biogeochemistry in the warm climate of the late Paleocene." In: *Clim. Past* 11.1, pp. 63–79. DOI: 10.5194/cp-11-63-2015.

Held, I. M. and Suarez, M. J. (1974). "Simple albedo feedback models of the icecaps." In: *Tellus* 26.6, pp. 613–629. DOI: 10.1111/j.2153-3490.1974.tb01641.x.

Higgins, J. A. and Schrag, D. P. (2003). "Aftermath of a snowball Earth." In: *Geochem. Geophy. Geosy.* 4.3. DOI: 10.1029/2002GC000403.

Hoffman, P. F., Abbot, D. S., Ashkenazy, Y., Benn, D. I., Brocks, J. J., Cohen, P. A., Cox, G. M., Creveling, J. R., Donnadieu, Y., Erwin, D. H., Fairchild, I. J., Ferreira, D, Goodman, J, Halverson, G. P., Jansen, M. F., Le Hir, G, Love, G. D., MacDonald, F. A., Maloof, A. C., Partin, C. A., Ramstein, G, Rose, B. E. J., Rose, C. V., Sadler, P. M., Tziperman, E, Voigt, A, and Warren, S (2017). "Snowball Earth climate dynamics and Cryogenian geology-geobiology." In: *Sci. Adv.* 3.11, e1600983. DOI: 10.1126/sciadv.1600983.

Hoffman, P. F. (2011). "Strange bedfellows: glacial diamictite and cap carbonate from the Marinoan (635 Ma) glaciation in Namibia." In: *Sedimentology* 58.1, pp. 57–119. DOI: 10.1111/j.1365-3091.2010.01206.x.

Hoffman, P. F., Kaufman, A. J., Halverson, G. P., and Schrag, D. P. (1998). "A Neoproterozoic snowball earth." In: *Science* 281.5381, pp. 1342–1346. DOI: 10.1126/science.281.5381.1342.

Hoffman, P. F. and Macdonald, F. A. (2010). "Sheet-crack cements and early regression in Marinoan (635Ma) cap dolostones: Regional benchmarks of vanishing ice-sheets?" In: *Earth Planet. Sci. Let.* 300.3, pp. 374–384. DOI: 10.1016/j.epsl.2010.10.027.

Hoffman, P. F. and Schrag, D. P. (2002). "The snowball Earth hypothesis: testing the limits of global change." In: *Terra Nova* 14.3, pp. 129–155. DOI: 10.1046/j.1365-3121.2002.00408.x.

Hoffmann, K.-H., Condon, D., Bowring, S., and Crowley, J. (Sept. 2004). "U-Pb zircon date from the Neoproterozoic Ghaub Formation, Namibia: Constraints on Marinoan glaciation." In: *Geology* 32.9, pp. 817–820. ISSN: 0091-7613. DOI: 10.1130/G20519.1.

Hood, A. v. S., Penman, D. E., Lechte, M. A., Wallace, M. W., Giddings, J. A., and Planavsky, N. J. (2022). "Neoproterozoic syn-glacial carbonate precipitation and implications for a snowball Earth." In: *Geobiology* 20.2, pp. 175–193.

Hyde, W. T., Crowley, T. J., Baum, S. K., and Peltier, W. R. (2000). "Neoproterozoic 'snowball Earth' simulations with a coupled climate/ice-sheet model." In: *Nature* 405.6785, p. 425. DOI: 10.1038/35013005.

IPCC (2022). *Climate Change 2022: Impacts, Adaptation, and Vulnerability. Contribution of Working Group II to the Sixth Assessment Report of the Intergovernmental Panel on Climate Change*. Vol. In Press. Cambridge, United Kingdom and New York, NY, USA: Cambridge University Press.

Ilyina, T. and Heinze, M. (2019). "Carbonate Dissolution Enhanced by Ocean Stagnation and Respiration at the Onset of the Paleocene-Eocene Thermal Maximum." In: *Geophys. Res. Lett.* 46.2, pp. 842–852. DOI: 10.1029/2018GL080761.

Ilyina, T., Six, K. D., Segschneider, J., Maier-Reimer, E., Li, H., and Núñez-Riboni, I. (2013). "Global ocean biogeochemistry model HAMOCC: Model architecture and performance as component of the MPI-Earth system model in different CMIP5 experimental realizations." In: *J. Adv. Model. Earth. Sy.* 5.2, pp. 287–315. DOI: 10.1029/2012MS000178.

Johnson, B. W., Poulton, S. W., and Goldblatt, C. (2017). "Marine oxygen production and open water supported an active nitrogen cycle during the Marinoan Snowball Earth." In: *Nat. Comm.* 8.1, pp. 1–10. DOI: 10.1038/s41467-017-01453-z.

Jungclaus, J. H., Lorenz, S. J., Schmidt, H, Brovkin, V, Brüggemann, N, Chegini, F, De-Vrese, P, Gayler, V, Giorgetta, M. A., Gutjahr, O., Haak, H, Hagemann, S,

Hanke, M, Ilyina, T, Korn, P, Kröger, J, Linardakis, L, Mehlmann, C, Mikolajewicz, U, Müller, W. A., Nabel, J. E. M. S., Notz, D, Pohlmann, H, Putrasahan, D, Raddatz, T, Ramme, L, Redler, R, Reick, C. H., Riddick, T, Sam, T, Schneck, R, Schnur, R, Schupfner, M, Storch, J.-S. von, Wachsmann, F, Wieners, K.-H., Ziemen, F, Stevens, B, Marotzke, J, and Claussen, M (2022). "The ICON Earth System Model Version 1.0." In: *J. Adv. Model. Earth. Sy.* DOI: 10.1029/2021MS002813.

Kasemann, S. A., Hawkesworth, C. J., Prave, A. R., Fallick, A. E., and Pearson, P. N. (2005). "Boron and calcium isotope composition in Neoproterozoic carbonate rocks from Namibia: evidence for extreme environmental change." In: *Earth Planet. Sc. Lett.* 231.1-2, pp. 73–86. DOI: 10.1016/j.epsl.2004.12.006.

Kendall, B., Creaser, R. A., and Selby, D. (2006). "Re-Os geochronology of postglacial black shales in Australia: Constraints on the timing of "Sturtian" glaciation." In: *Geology* 34.9, pp. 729–732. DOI: 10.1130/G22775.1.

Kennedy, M. J. (1996). "Stratigraphy, sedimentology, and isotopic geochemistry of Australian Neoproterozoic postglacial cap dolostones; deglaciation, delta 13 C excursions, and carbonate precipitation." In: *J. Sediment Res.* 66.6, pp. 1050–1064. DOI: 10.2110/jsr.66.1050.

Kirschvink, J. L. (1992). "Late Proterozoic low-latitude global glaciation: The Snowball Earth." In: *The Proterozoic Biosphere: A Multidisciplinary study*, pp. 51–52.

Knoll, A. H. (2003). "Biomineralization and evolutionary history." In: *Rev. Mineral. Geochem.* 54.1, pp. 329–356. DOI: 10.2113/0540329.

Knoll, A. H., Summons, R. E., Waldbauer, J. R., and Zumberge, J. E. (2007). "CHAPTER 8 - The Geological Succession of Primary Producers in the Oceans." In: *Evolution of Primary Producers in the Sea*. Ed. by P. G. Falkowski and A. H. Knoll. Burlington: Academic Press, pp. 133–163. ISBN: 978-0-12-370518-1. DOI: 10.1016/B978-012370518-1/50009-6.

Korn, P., Brüggemann, N., Jungclaus, J. H., Lorenz, S. J., Gutjahr, O., Haak, H., Linardakis, L., Mehlmann, C., Mikolajewicz, U., Notz, D., Putrasahan, D. A., Singh, V., Storch, J.-S. von, Zhu, X., and Marotzke, J. (2022). "ICON-O: The Ocean Component of the ICON Earth System Model—Global Simulation Characteristics and Local Telescoping Capability." In: *J. Adv. Model. Earth. Sy.* 14.10, e2021MS002952. DOI: 10.1029/2021MS002952.

Korn, P. (2017). "Formulation of an unstructured grid model for global ocean dynamics." In: *J. Comput. Phys.* 339, pp. 525–552. DOI: 10.1016/j.jcp.2017.03.009.

Lan, Z., Huyskens, M. H., Le Hir, G., Mitchell, R. N., Yin, Q.-Z., Zhang, G., and Li, X.-H. (2022). "Massive Volcanism May Have Foreshortened the Marinoan Snowball Earth." In: *Geophys. Res. Lett.* 49.6, e2021GL097156. DOI: 10.1029/2021GL097156.

Le Hir, G, Goddéris, Y, Donnadieu, Y, and Ramstein, G (2008a). "A geochemical modelling study of the evolution of the chemical composition of seawater linked to a" snowball" glaciation." In: *Biogeosciences* 5.1, pp. 253–267. DOI: 10.5194/bg-5-253-2008.

Le Hir, G., Donnadieu, Y., Goddéris, Y., Pierrehumbert, R. T., Halverson, G. P., Macouin, M., Nédélec, A., and Ramstein, G. (2008b). "The snowball Earth aftermath: Exploring the limits of continental weathering processes." In: *Earth Planet. Sc. Lett.* 277.3-4, pp. 453–463. DOI: 10.1016/j.epsl.2008.11.010.

Le Hir, G., Donnadieu, Y., Krinner, G., and Ramstein, G. (2010). "Toward the snowball Earth deglaciation. . . " In: *Clim. Dyn.* 35.2, pp. 285–297. DOI: 10.1007/s00382-010-0748-8.

Le Hir, G., Ramstein, G., Donnadieu, Y., and Goddéris, Y. (2008c). "Scenario for the evolution of atmospheric pCO2 during a snowball Earth." In: *Geology* 36.1, pp. 47–50. DOI: 10.1130/G24124A.1.

Lewis, J. P., Weaver, A. J., and Eby, M. (2006). "Deglaciating the snowball Earth: Sensitivity to surface albedo." In: *Geophys. Res. Lett.* 33.23. DOI: 10.1029/2006GL027774.

Li, G., Hartmann, J., Derry, L. A., West, A. J., You, C.-F., Long, X., Zhan, T., Li, L., Li, G., Qiu, W., Li, T., Liu, L., Chen, Y., Ji, J., Zhao, L., and Chen, J. (2016). "Temperature dependence of basalt weathering." In: *Earth Planet. Sc. Lett.* 443, pp. 59–69. ISSN: 0012-821X. DOI: 10.1016/j.epsl.2016.03.015.

Li, Z.-X., Evans, D. A., and Halverson, G. P. (2013). "Neoproterozoic glaciations in a revised global palaeogeography from the breakup of Rodinia to the assembly of Gondwanaland." In: *Sediment. Geol.* 294, pp. 219–232. DOI: 10.1016/j.sedgeo.2013.05.016.

Linardakis, L., Stemmler, I., Hanke, M., Ramme, L., Chegini, F., Ilyina, T., and Korn, P. (2022). "Improving scalability of Earth System Models through coarse-grained component concurrency – a case study with the ICON v2.6.5 modeling system." In: *Geoscientific Model Development Discussions* 2022, pp. 1–32. DOI: 10.5194/gmd-2022-214.

Liu, C., Wang, Z., and Macdonald, F. A. (2018a). "Sr and Mg isotope geochemistry of the basal Ediacaran cap limestone sequence of Mongolia: Implications for carbonate diagenesis, mixing of glacial meltwaters, and seawater chemistry in the aftermath of Snowball Earth." In: *Chem. Geol.* 491, pp. 1–13. ISSN: 0009-2541. DOI: 10.1016/j.chemgeo.2018.05.008.

Liu, C., Wang, Z., Raub, T. D., Macdonald, F. A., and Evans, D. A. (2014). "Neoproterozoic cap-dolostone deposition in stratified glacial meltwater plume." In: *Earth Planet. Sc. Lett.* 404, pp. 22–32. DOI: 10.1016/j.epsl.2014.06.039.

Liu, P., Liu, Y., Peng, Y., Lamarque, J.-F., Wang, M., and Hu, Y. (2020). "Large influence of dust on the Precambrian climate." In: *Nat. Comm.* 11.1, pp. 1–8. DOI: 10.1038/s41467-020-18258-2.

Liu, Y., Peltier, W. R., Yang, J., and Hu, Y. (2018b). "Influence of Surface Topography on the Critical Carbon Dioxide Level Required for the Formation of a Modern Snowball Earth." In: *J. Climate* 31.20, pp. 8463 –8479. DOI: 10.1175/JCLI-D-17-0821.1.

Love, G. D., Grosjean, E., Stalvies, C., Fike, D. A., Grotzinger, J. P., Bradley, A. S., Kelly, A. E., Bhatia, M., Meredith, W., Snape, C. E., et al. (2009). "Fossil steroids record the appearance of Demospongiae during the Cryogenian period." In: *Nature* 457.7230, pp. 718–721. DOI: 10.1038/nature07673.

Lyons, T. W., Reinhard, C. T., and Planavsky, N. J. (2014). "The rise of oxygen in Earth's early ocean and atmosphere." In: *Nature* 506.7488, pp. 307–315. DOI: 10.1038/nature13068.

Marotzke, J. and Botzet, M. (2007). "Present-day and ice-covered equilibrium states in a comprehensive climate model." In: *Geophys. Res. Lett.* 34.16. DOI: 10.1029/2006GL028880.

Marshall, J. and Speer, K. (2012). "Closure of the meridional overturning circulation through Southern Ocean upwelling." In: *Nature Geoscience* 5.3, pp. 171–180. DOI: 10.1038/ngeo1391.

Mathis, M., Logemann, K., Maerz, J., Lacroix, F., Hagemann, S., Chegini, F., Ramme, L., Ilyina, T., Korn, P., and Schrum, C. (2022). "Seamless Integration of the Coastal Ocean in Global Marine Carbon Cycle Modeling." In: *J. Adv. Model. Earth. Sy.* 14.8. e2021MS002789 2021MS002789, e2021MS002789. DOI: 10.1029/2021MS002789.

Mauritsen, T., Bader, J., Becker, T., Behrens, J., Bittner, M., Brokopf, R., Brovkin, V., Claussen, M., Crueger, T., Esch, M., et al. (2019). "Developments in the MPI-M Earth System Model version 1.2 (MPI-ESM1. 2) and its response to increasing CO2." In: *J. Adv. Model. Earth. Sy.* 11.4, pp. 998–1038. DOI: 10.1029/2018MS001400.

McDougall, T. J. (1987). "Neutral surfaces." In: *J. Phys. Oceanogr.* 17.11, pp. 1950–1964. DOI: 10.1175/1520-0485(1987)017<1950:NS>2.0.CO;2.

McGuffie, K. and Henderson-Sellers, A. (2005). *The climate modelling primer*. Chichester: John Wiley & Sons.

McInerney, F. A. and Wing, S. L. (2011). "The Paleocene-Eocene Thermal Maximum: A Perturbation of Carbon Cycle, Climate, and Biosphere with Implications for the Future." In: *Annu. Rev. Earth Pl. Sc.* 39.1, pp. 489–516. DOI: 10.1146/annurev-earth-040610-133431.

Meehl, G. A., Senior, C. A., Eyring, V., Flato, G., Lamarque, J.-F., Stouffer, R. J., Taylor, K. E., and Schlund, M. (2020). "Context for interpreting equilibrium climate sensitivity and transient climate response from the CMIP6 Earth system models." In: *Science Advances* 6.26, eaba1981. DOI: 10.1126/sciadv.aba1981.

Mehlmann, C. and Korn, P. (2021). "Sea-ice dynamics on triangular grids." In: *J. Comput. Phys.* 428, p. 110086. ISSN: 0021-9991. DOI: 10.1016/j.jcp.2020.110086.

Mehlmann, C. and Ramme, L. (in preparation). "The numerical representation of sea ice strongly effects climate dynamics." In: *Nat. Comm.*

Merdith, A. S., Collins, A. S., Williams, S. E., Pisarevsky, S., Foden, J. D., Archibald, D. B., Blades, M. L., Alessio, B. L., Armistead, S., Plavsa, D., et al. (2017). "A full-plate global reconstruction of the Neoproterozoic." In: *Gondwana Res.* 50, pp. 84–134. DOI: 10.1016/j.gr.2017.04.001.

Middelburg, J. J., Soetaert, K., and Hagens, M. (2020). "Ocean Alkalinity, Buffering and Biogeochemical Processes." In: *Rev. Geophys.* 58.3, e2019RG000681. DOI: 10.1029/2019RG000681.

Millero, F. J. (1979). "The thermodynamics of the carbonate system in seawater." In: *Geochim. Cosmochim. Ac.* 43.10, pp. 1651–1661. ISSN: 0016-7037. DOI: 10.1016/0016-7037(79)90184-4.

Mitchell, J. F. B. (1989). "The "Greenhouse" effect and climate change." In: *Rev. Geophys.* 27.1, pp. 115–139. DOI: 10.1029/RG027i001p00115.

Moczydłowska, M. (2008). "The Ediacaran microbiota and the survival of Snowball Earth conditions." In: *Precambrian Res.* 167.1-2, pp. 1–15. DOI: 10.1016/j.precamres.2008.06.008.

Morris, J. L., Puttick, M. N., Clark, J. W., Edwards, D., Kenrick, P., Pressel, S., Wellman, C. H., Yang, Z., Schneider, H., and Donoghue, P. C. J. (2018). "The timescale of early land plant evolution." In: *P. Natl. Acad. Sci.* 115.10, E2274–E2283. DOI: 10.1073/pnas.1719588115.

Myrow, P. M., Lamb, M., and Ewing, R. (2018). "Rapid sea level rise in the aftermath of a Neoproterozoic snowball Earth." In: *Science* 360.6389, pp. 649–651. DOI: 10.1126/science.aap8612.

Och, L. M. and Shields-Zhou, G. A. (2012). "The Neoproterozoic oxygenation event: Environmental perturbations and biogeochemical cycling." In: *Earth-Sci. Rev.* 110.1, pp. 26–57. DOI: 10.1016/j.earscirev.2011.09.004.

Olbers, D., Willebrand, J., and Eden, C. (2012). *Ocean dynamics*. ISBN: 9783642234491.

Opdyke, B. N. and Wilkinson, B. H. (1990). "Paleolatitude distribution of Phanerozoic marine ooids and cements." In: *Palaeogeogr. Palaeoclimatol. Palaeoecol.* 78.1, pp. 135–148. DOI: 10.1016/0031-0182(90)90208-O.

Pan, Y., Li, Y., Ma, Q., He, H., Wang, S., Sun, Z., Cai, W.-J., Dong, B., Di, Y., Fu, W., and Chen, C.-T. A. (2021). "The role of Mg2+ in inhibiting CaCO3 precipitation from seawater." In: *Mar. Chem.* 237, p. 104036. ISSN: 0304-4203. DOI: 10.1016/j.marchem.2021.104036.

Peng, Y., Dong, L., Ma, H., Wang, R., Lang, X., Peng, Y., Qin, S., Liu, W., and Shen, B. (2020). "Surface ocean nitrate-limitation in the aftermath of Marinoan snowball Earth: Evidence from the Ediacaran Doushantuo Formation in the western margin of the Yangtze Block, South China." In: *Precambrian Res.* 347, p. 105846. ISSN: 0301-9268. DOI: 10.1016/j.precamres.2020.105846.

Pierrehumbert, R. T. (2005). "Climate dynamics of a hard snowball Earth." In: *J. Geophys. Res.-Atmospheres* 110.D1. DOI: 10.1029/2004JD005162.

Pierrehumbert, R., Abbot, D., Voigt, A., and Koll, D. (2011). "Climate of the Neoproterozoic." In: *Annual Review of Earth and Planetary Sciences* 39.1, pp. 417–460. DOI: 10.1146/annurev-earth-040809-152447.

Planavsky, N. J., Rouxel, O. J., Bekker, A., Lalonde, S. V., Konhauser, K. O., Reinhard, C. T., and Lyons, T. W. (2010). "The evolution of the marine phosphate reservoir." In: *Nature* 467.7319, pp. 1088–1090. DOI: 10.1038/nature09485.

Poulsen, C. J. and Jacob, R. L. (2004). "Factors that inhibit snowball Earth simulation." In: *Paleoceanography* 19.4. DOI: 10.1029/2004PA001056.

Poulsen, C. J., Pierrehumbert, R. T., and Jacob, R. L. (2001). "Impact of ocean dynamics on the simulation of the neoproterozoic "snowball Earth"." In: *Geophys. Res. Lett.* 28.8, pp. 1575–1578. DOI: 10.1029/2000GL012058.

Prave, A. R., Condon, D. J., Hoffmann, K. H., Tapster, S., and Fallick, A. E. (2016). "Duration and nature of the end-Cryogenian (Marinoan) glaciation." In: *Geology* 44.8, pp. 631–634. DOI: 10.1130/G38089.1.

Puttick, M. N., Morris, J. L., Williams, T. A., Cox, C. J., Edwards, D., Kenrick, P., Pressel, S., Wellman, C. H., Schneider, H., Pisani, D., and Donoghue, P. C. (2018). "The Interrelationships of Land Plants and the Nature of the Ancestral Embryophyte." In: *Curr. Biol.* 28.5, 733–745.e2. DOI: 10.1016/j.cub.2018.01.063.

Qin, B., Jia, Q., Xiong, Z., Li, T., Algeo, T. J., and Dang, H. (2022). "Sustained Deep Pacific Carbon Storage After the Mid-Pleistocene Transition Linked to Enhanced Southern Ocean Stratification." In: *Geophys. Res. Lett.* 49.4, e2021GL097121. DOI: 10.1029/2021GL097121.

Ramme, L. and Marotzke, J. (2022). "Climate and ocean circulation in the aftermath of a Marinoan snowball Earth." In: *Clim. Past* 18.4, pp. 759–774. DOI: 10.5194/cp-18-759-2022. URL: https://cp.copernicus.org/articles/18/759/2022/.

Ramme, L. (2021). *Publication data for "Ramme and Marotzke: Climate and Ocean Circulation in the Aftermath of a Marinoan Snowball Earth"*. URL: http://cera-www.dkrz.de/WDCC/ui/Compact.jsp?acronym=DKRZ_LTA_033_ds00011.

Redi, M. H. (1982). "Oceanic isopycnal mixing by coordinate rotation." In: *J. Phys. Oceanogr.* 12.10, pp. 1154–1158. DOI: 10.1175/1520-0485(1982)012<1154:OIMBCR>2.0.CO;2.

Reinhard, C. T., Planavsky, N. J., Gill, B. C., Ozaki, K., Robbins, L. J., Lyons, T. W., Fischer, W. W., Wang, C., Cole, D. B., and Konhauser, K. O. (2017). "Evolution of the global phosphorus cycle." In: *Nature* 541.7637, pp. 386–389. DOI: 10.1038/nature20772.

Ridgwell, A. and Zeebe, R. E. (2005). "The role of the global carbonate cycle in the regulation and evolution of the Earth system." In: *Earth Planet. Sc. Lett.* 234.3, pp. 299–315. ISSN: 0012-821X. DOI: 10.1016/j.epsl.2005.03.006.

Roberts, J. D. (1976). "Late Precambrian Dolomites, Vendian Glaciation, and Synchroneity of Vendian Glaciations." In: *The Journal of Geology* 84.1, pp. 47–63. DOI: 10.1086/628173.

Rose, B. E. J. (2015). "Stable "Waterbelt" climates controlled by tropical ocean heat transport: A nonlinear coupled climate mechanism of relevance to Snowball Earth." In: *J. Geophys. Res.-Atmospheres* 120.4, pp. 1404–1423. DOI: 10.1002/2014JD022659.

Rothschild, L. J. and Mancinelli, R. L. (2001). "Life in extreme environments." In: *Nature* 409.6823, pp. 1092–1101. DOI: 10.1038/35059215.

Russell, J. L., Dixon, K. W., Gnanadesikan, A., Stouffer, R. J., and Toggweiler, J. (2006). "The Southern Hemisphere westerlies in a warming world: Propping open the door to the deep ocean." In: *J. Climate* 19.24, pp. 6382–6390. DOI: 10.1175/JCLI3984.1.

Sabine, C. L. and Tanhua, T. (2010). "Estimation of Anthropogenic CO2 Inventories in the Ocean." In: *Annu. Rev. Mar. Sci.* 2.1, pp. 175–198. DOI: 10.1146/annurev-marine-120308-080947.

Sansjofre, P, Ader, M, Trindade, R., Elie, M, Lyons, J, Cartigny, P, and Nogueira, A. (2011). "A carbon isotope challenge to the snowball Earth." In: *Nature* 478.7367, pp. 93–96. DOI: 10.1038/nature10499.

Sarmiento, J. L. (2013). *Ocean Biogeochemical Dynamics*. Princeton: Princeton University Press. ISBN: 9781400849079. DOI: 10.1515/9781400849079.

Schmittner, A. (2005). "Decline of the marine ecosystem caused by a reduction in the Atlantic overturning circulation." In: *Nature* 434.7033, pp. 628–633. DOI: 10.1038/nature03476.

Schrag, D. P., Berner, R. A., Hoffman, P. F., and Halverson, G. P. (2002). "On the initiation of a snowball Earth." In: *Geochem. Geophy. Geosy.* 3.6, pp. 1–21. DOI: 10.1029/2001GC000219.

Sellers, W. D. (1969). "A Global Climatic Model Based on the Energy Balance of the Earth-Atmosphere System." In: *J. Appl. Meteorol.* 8.3, pp. 392–400. DOI: 10.2307/26174552.

Semtner, A. J. (1976). "A model for the thermodynamic growth of sea ice in numerical investigations of climate." In: *J. Phys. Oceanogr.* 6.3, pp. 379–389. DOI: 10.1175/1520-0485(1976)006<0379:AMFTTG>2.0.CO;2.

Shaojun, Z. and Mucci, A. (1993). "Calcite precipitation in seawater using a constant addition technique: A new overall reaction kinetic expression." In: *Geochim. Cosmochim. Ac.* 57.7, pp. 1409–1417. DOI: 10.1016/0016-7037(93)90002-E.

Shen, W., Zhu, X., Yan, B., Li, J., Liu, P., and Poulton, S. W. (Aug. 2022). "Secular variation in seawater redox state during the Marinoan Snowball Earth event and implications for eukaryotic evolution." In: *Geology* 50.11, pp. 1239–1244. DOI: 10.1130/G50147.1.

Shields, G. A. (2005). "Neoproterozoic cap carbonates: a critical appraisal of existing models and the plumeworld hypothesis." In: *Terra Nova* 17.4, pp. 299–310. DOI: 10.1111/j.1365-3121.2005.00638.x.

Siegenthaler, U. and Sarmiento, J. L. (1993). "Atmospheric carbon dioxide and the ocean." In: *Nature* 365.6442, pp. 119–125. DOI: 10.1038/365119a0.

Stephens, G. L., O'Brien, D., Webster, P. J., Pilewski, P., Kato, S., and Li, J.-l. (2015). "The albedo of Earth." In: *Rev. Geophys.* 53.1, pp. 141–163. DOI: 10.1002/2014RG000449.

Stephenson, D. A., Fleming, A. H., and Mickelson, D. M. (Jan. 1988). "Glacial deposits." In: *Hydrogeology*. Geological Society of America. ISBN: 9780813754673. DOI: 10.1130/DNAG-GNA-O2.301.

Thompson, D. W. J. and Solomon, S. (2002). "Interpretation of recent Southern Hemisphere climate change." In: *Science* 296.5569, pp. 895–899. DOI: 10.1126/science.1069270.

Tierney, J. E., Poulsen, C. J., Montañez, I. P., Bhattacharya, T., Feng, R., Ford, H. L., Hönisch, B., Inglis, G. N., Petersen, S. V., Sagoo, N., Tabor, C. R., Thirumalai, K., Zhu, J., Burls, N. J., Foster, G. L., Goddéris, Y., Huber, B. T., Ivany, L. C., Turner, S. K., Lunt, D. J., McElwain, J. C., Mills, B. J. W., Otto-Bliesner, B. L., Ridgwell, A., and Zhang, Y. G. (2020). "Past climates inform our future." In: *Science* 370.6517, eaay3701. DOI: 10.1126/science.aay3701.

Trindade, R. I. F., Font, E, D'Agrella-Filho, M. S., Nogueira, A. C. R., and Riccomini, C (2003). "Low-latitude and multiple geomagnetic reversals in the Neoproterozoic Puga cap carbonate, Amazon craton." In: *Terra Nova* 15.6, pp. 441–446. DOI: 10.1046/j.1365-3121.2003.00510.x.

Turner, E. C. (2021). "Possible poriferan body fossils in early Neoproterozoic microbial reefs." In: *Nature*, pp. 1–5. DOI: 10.1038/s41586-021-03773-z.

Tziperman, E., Abbot, D. S., Ashkenazy, Y., Gildor, H., Pollard, D., Schoof, C. G., and Schrag, D. P. (2012). "Continental constriction and oceanic ice-cover thickness in a Snowball-Earth scenario." In: *J. Geophys. Res.-Oceans* 117.C5. DOI: 10.1029/2011JC007730.

Voigt, A, Abbot, D. S., Pierrehumbert, R. T., and Marotzke, J (2011). "Initiation of a Marinoan Snowball Earth in a state-of-the-art atmosphere-ocean general circulation model." In: *Clim. Past* 7, pp. 249–263. DOI: 10.5194/cp-7-249-2011.

Voigt, A. and Marotzke, J. (2010). "The transition from the present-day climate to a modern Snowball Earth." In: *Clim. Dyn.* 35.5, pp. 887–905. DOI: 10.1007/s00382-009-0633-5.

Vrese, P. de, Stacke, T., Caves Rugenstein, J., Goodman, J., and Brovkin, V. (2021). "Snowfall-albedo feedbacks could have led to deglaciation of snowball Earth starting from mid-latitudes." In: *Communications Earth & Environment* 2.1, pp. 1–9. DOI: 10.1038/s43247-021-00160-4.

Walker, J. C. G., Hays, P. B., and Kasting, J. F. (1981). "A negative feedback mechanism for the long-term stabilization of Earth's surface temperature." In: *J. Geophys. Res.-Oceans* 86.C10, pp. 9776–9782. DOI: 10.1029/JC086iC10p09776.

Warren, J. (2000). "Dolomite: occurrence, evolution and economically important associations." In: *Earth-Sci. Rev.* 52.1, pp. 1–81. ISSN: 0012-8252. DOI: 10.1016/S0012-8252(00)00022-2.

Wei, G.-Y., Hood, A. v.S., Chen, X., Li, D., Wei, W., Wen, B., Gong, Z., Yang, T., Zhang, Z.-F., and Ling, H.-F. (2019). "Ca and Sr isotope constraints on the formation of the Marinoan cap dolostones." In: *Earth Planet. Sc. Lett.* 511, pp. 202–212. ISSN: 0012-821X. DOI: 10.1016/j.epsl.2019.01.024.

Weiss, R. F. (1974). "Carbon dioxide in water and seawater: the solubility of a non-ideal gas." In: *Mar. Chem.* 2.3, pp. 203–215. ISSN: 0304-4203. DOI: 10.1016/0304-4203(74)90015-2.

Winton, M. (2003). "On the Climatic Impact of Ocean Circulation." In: *Journal of Climate* 16.17, pp. 2875 –2889. DOI: 10.1175/1520-0442(2003)016<2875:OTCIOO>2.0.CO;2.

Wolff, J.-O., Maier-Reimer, E., and Olbers, D. J. (1991). "Wind-driven flow over topography in a zonal β-plane channel: A quasi-geostrophic model of the Antarctic Circumpolar Current." In: *J. Phys. Oceanogr.* 21.2, pp. 236–264. DOI: 10.1175/1520-0485(1991)021<0236:WDFOTI>2.0.CO;2.

Wu, J., Liu, Y., and Zhao, Z. (2021). "How Should Snowball Earth Deglaciation Start." In: *J. Geophys. Res.-Atmospheres* 126.2. DOI: 10.1029/2020JD033833.

Yang, J., Jansen, M. F., Macdonald, F. A., and Abbot, D. S. (2017). "Persistence of a freshwater surface ocean after a snowball Earth." In: *Geology* 45.7, pp. 615–618. DOI: 10.1130/G38920.1.

Yang, J., Peltier, W. R., and Hu, Y. (2012). "The Initiation of Modern "Soft Snowball" and "Hard Snowball" Climates in CCSM3. Part I: The Influences of Solar Luminosity, CO2 Concentration, and the Sea Ice/Snow Albedo Parameterization." In: *J. Climate* 25.8, pp. 2711 –2736. DOI: 10.1175/JCLI-D-11-00189.1.

Yu, W., Algeo, T. J., Zhou, Q., Du, Y., and Wang, P. (2020). "Cryogenian cap carbonate models: a review and critical assessment." In: *Palaeogeogr. Palaeoclimatol. Palaeoecol.* 552, p. 109727. ISSN: 0031-0182. DOI: 10.1016/j.palaeo.2020.109727.

Yu, W., Algeo, T. J., Zhou, Q., Wei, W., Yang, M., Li, F., Du, Y., Pan, W., and Wang, P. (2022). "Evaluation of alkalinity sources to Cryogenian cap carbonates, and implications for cap carbonate formation models." In: *Global Planet. Change* 217, p. 103949. DOI: 10.1016/j.gloplacha.2022.103949.

Zängl, G., Reinert, D., Rípodas, P., and Baldauf, M. (2015). "The ICON (ICOsahedral Non-hydrostatic) modelling framework of DWD and MPI-M: Description of the non-hydrostatic dynamical core." In: *Q. J. Roy. Meteor. Soc.* 141.687, pp. 563–579. DOI: 10.1002/qj.2378.

Zeebe, R. E. and Westbroek, P. (2003). "A simple model for the CaCO3 saturation state of the ocean: The "Strangelove," the "Neritan," and the "Cretan" Ocean." In: *Geochem. Geophy. Geosy.* 4.12. DOI: 10.1029/2003GC000538.

Zeebe, R. E. and Wolf-Gladrow, D. (2001). *CO2 in seawater: equilibrium, kinetics, isotopes*. 65. Elsevier B.A., Amsterdam, the Netherlands: Elsevier Oceanography Series.

Zhao, Z., Liu, Y., and Dai, H. (2022). "Sea-glacier retreating rate and climate evolution during the marine deglaciation of a snowball Earth." In: *Global Planet. Change* 215, p. 103877. ISSN: 0921-8181. DOI: 10.1016/j.gloplacha.2022.103877.

Ziegler, A. M., Hulver, M. L., Lottes, A. L., and Schmachtenberg, W. F. (1984). *Uniformitarianism and palaeoclimates: inferences from the distribution of carbonate rocks*. 11. New York, NY, USA: John Wiley and Sons, pp. 3–25.

VERSICHERUNG AN EIDES STATT

Hiermit erkläre ich an Eides statt, dass ich die vorliegende Dissertationsschrift selbst verfasst und keine anderen als die angegebenen Quellen und Hilfsmittel benutzt habe.

Hamburg, 28. November 2022

Lennart Ramme